

**A NOVEL USER-CONTROLLED ASSISTED STANDING CONTROL SYSTEM  
FOR A HYBRID NEUROPROSTHESIS**

by

**Albert Edward Dodson IV**

BS in Mechanical and Aerospace Engineering, Cornell University, 2010

Submitted to the Graduate Faculty of  
the Swanson School of Engineering in partial fulfillment  
of the requirements for the degree of  
Master of Science in Mechanical Engineering

University of Pittsburgh

2017

UNIVERSITY OF PITTSBURGH  
SWANSON SCHOOL OF ENGINEERING

This thesis was presented

by

Albert Edward Dodson IV

It was defended on

October 30, 2017

and approved by

Nitin Sharma, PhD, Assistant Professor

William Clark, PhD, Professor

Brad Dicianno, MD, Associate Professor

Thesis Advisor: Nitin Sharma, PhD, Assistant Professor

**A NOVEL USER-CONTROLLED ASSISTED STANDING CONTROL SYSTEM  
FOR A HYBRID NEUROPROSTHESIS**

Albert E. Dodson IV, M.S.

University of Pittsburgh, 2017

Spinal cord injury (SCI) is a serious condition with 17,000 new cases each year and an estimated total of 282,000 people in the United States who have SCI. Some people with SCI who have paraplegia suffer from paralysis, muscle spasticity, bone changes, chronic pain and other problems. Active orthoses such as the ReWalk, EXPOS, and Ekso have improved the quality of life of people with SCI. The hybrid neuroprosthesis is an active orthosis that uses functional electrical stimulation (FES) at the quadriceps and has two main purposes: restoring mobility in people with SCI and providing physical therapy for the user outside of a clinical setting.

To mobilize people with SCI, the neuroprosthesis must provide assisted movement for a sitting to standing motion. A standing control system developed by the Pitt Neuromuscular Control and Robotics Laboratory (NCRL) before this proposed system did not give enough control of the movement to the user and FES alone did not provide enough torque at the knees for standing. The NCRL neuroprosthesis was modified to include a harmonic gearmotor at the knees, a thumb joystick for user control, and a force sensing walker.

A control system using a finite state machine (FSM) was designed to perform hybrid standing in the neuroprosthesis. The FSM is divided into 3 states and uses 5 separate controllers: a tracking controller for forward leaning during sitting, a tracking controller to synchronize the knees, a tracking controller to lock the knees during standing, a hip tracking controller, and open-loop FES.

Four experiments were performed on subjects to analyze control performance, power usage, and energy consumption during motors only and hybrid standing. A subject with SCI successfully performed several trials of hybrid standing. The controllers performed sufficiently accurately, and several minor control problems were fixed. The highest average energy consumption at the knee motors was 88.4 joules during experiment 1. The hybrid standing experiment demonstrated a modest energy reduction of 15% in a subject with SCI. The hybrid standing demonstrated a high energy reduction of 74% in the right knee in experiment 2, through hybrid actuation and a slower standing speed.

## TABLE OF CONTENTS

<b>LIST OF ABBREVIATIONS .....</b>	<b>XII</b>
<b>1.0 INTRODUCTION.....</b>	<b>1</b>
<b>1.1 MOTIVATIONS FOR A NEUROPROSTHESIS .....</b>	<b>2</b>
<b>1.1.1 Rehabilitative Priorities of People with SCI.....</b>	<b>2</b>
<b>1.1.2 Purposes of a Neuroprosthesis.....</b>	<b>3</b>
<b>1.1.3 Potential for Neuroprosthesis Adoption .....</b>	<b>3</b>
<b>1.2 MOTIVATIONS FOR STANDING CONTROL .....</b>	<b>5</b>
<b>1.2.1 Preliminary Standing Control System .....</b>	<b>5</b>
<b>1.2.2 Problems with the Preliminary Standing Control System.....</b>	<b>6</b>
<b>1.3 THESIS CONTRIBUTIONS.....</b>	<b>7</b>
<b>2.0 BACKGROUND INFORMATION AND LITERATURE REVIEW.....</b>	<b>9</b>
<b>2.1 ROBOTIC EXOSKELETON STATE OF THE ART .....</b>	<b>9</b>
<b>2.1.1 Performance-Augmenting Exoskeletons.....</b>	<b>10</b>
<b>2.1.2 Active Orthoses .....</b>	<b>12</b>
<b>2.1.3 The ReWalk Exoskeleton .....</b>	<b>12</b>
<b>2.1.4 The EXPOS Exoskeleton.....</b>	<b>14</b>
<b>2.1.5 The Ekso Bionics Exoskeleton .....</b>	<b>15</b>
<b>2.1.6 The HAL Exoskeleton.....</b>	<b>16</b>
<b>2.1.7 State of the Art Discussion .....</b>	<b>18</b>

2.2	<b>FUNCTIONAL ELECTRICAL STIMULATION .....</b>	<b>19</b>
2.2.1	<b>The History of Electrical Stimulation .....</b>	<b>19</b>
2.2.2	<b>Advantages and Disadvantages of FES in a Neuroprosthesis.....</b>	<b>22</b>
2.3	<b>STANDING CONTROL METHODS.....</b>	<b>23</b>
2.3.1	<b>Donaldson and Yu’s Standing Controller .....</b>	<b>24</b>
2.3.2	<b>Reiner’s Standing Controller.....</b>	<b>27</b>
2.3.3	<b>HAL Sitting to Standing Control System .....</b>	<b>29</b>
3.0	<b>NEUROPROSTHESIS MECHATRONIC DESIGN FOR STANDING .....</b>	<b>32</b>
3.1	<b>PRE-EXISTING NEUROPROSTHESIS DESIGN .....</b>	<b>32</b>
3.2	<b>DESIGN NEEDS FOR STANDING .....</b>	<b>34</b>
3.2.1	<b>Sitting to Standing Knee Motor Requirements.....</b>	<b>35</b>
3.2.2	<b>Assisted Gait Knee Motor Requirements .....</b>	<b>36</b>
3.3	<b>KNEE MOTOR DESIGN .....</b>	<b>37</b>
3.4	<b>FORCE SENSING WALKER DESIGN .....</b>	<b>40</b>
3.5	<b>JOYSTICK DESIGN AND PROGRAMMING LOGIC .....</b>	<b>42</b>
3.6	<b>NEUROPROSTHESIS SAFETY CONSIDERATIONS.....</b>	<b>45</b>
3.7	<b>FUTURE DESIGN CONSIDERATIONS .....</b>	<b>47</b>
4.0	<b>CONTROL SYSTEM DESIGN FOR STANDING .....</b>	<b>50</b>
4.1	<b>CONTROL SYSTEM OVERVIEW .....</b>	<b>50</b>
4.1.1	<b>Expected Advantages and Disadvantages of the Control System .....</b>	<b>52</b>
4.2	<b>FINITE STATE MACHINE.....</b>	<b>53</b>
4.3	<b>STATE 1 – FORWARD LEANING CONTROLLER.....</b>	<b>55</b>
4.4	<b>STATE 2 – KNEE SYNCHRONIZATION CONTROLLER .....</b>	<b>56</b>
4.4.1	<b>Motivation for a Synchronization Controller.....</b>	<b>57</b>
4.4.2	<b>Final Controller Design .....</b>	<b>58</b>

4.5	STATE 3 - KNEE LOCKING CONTROLLER.....	60
4.6	END EFFECTOR TRACKING CONTROL.....	62
5.0	EXPERIMENTAL RESULTS.....	69
5.1	EXPERIMENTAL SETUP.....	69
5.2	EXPERIMENT 1 - DEMONSTRATION OF STANDING WITH MOTORS ONLY IN AN ABLE-BODIED SUBJECT.....	71
5.3	EXPERIMENT 2 - DEMONSTRATION OF HYBRID STANDING IN AN ABLE-BODIED SUBJECT .....	77
5.4	EXPERIMENT 3 - DEMONSTRATION OF STANDING WITH MOTORS ONLY IN A SUBJECT WITH SCI .....	83
5.5	EXPERIMENT 4 - DEMONSTRATION OF HYBRID STANDING IN A SUBJECT WITH SCI .....	89
5.6	CONTROL SYSTEM PERFORMANCE DISCUSSION.....	94
5.7	POWER AND ENERGY ANALYSIS DURING STANDING EXPERIMENTS .....	96
5.7.1	Power and Energy Measurement Methodology.....	97
5.7.2	Power Analysis .....	98
5.7.3	Energy Consumption Analysis.....	102
	APPENDIX A .....	108
	APPENDIX B .....	110
	BIBLIOGRAPHY .....	112

## LIST OF TABLES

Table 1.	Controller gains for states 1-3.....	59
Table 2.	Energy consumption for all trials in experiment 1.....	103
Table 3.	Energy consumption for all trials in experiment 2.....	103
Table 4.	Energy consumption for all trials in experiment 3.....	103
Table 5.	Energy consumption for all trials in experiment 4.....	104
Table 6.	Motors only energy capacity and operational range of several types of potential mobile neuroprosthesis batteries.....	107

## LIST OF FIGURES

Figure 1.	(Left) The Berkeley Lower Extremity Exoskeleton © 2005 IEEE <sup>[13]</sup> and (Right) the ReWalk Exoskeleton © 2012 IEEE <sup>[91]</sup> .....	11
Figure 2.	(Left) The EXPOS Exoskeleton System © 2006 IEEE <sup>[21,51]</sup> , (Center) the Ekso Bionics Exoskeleton © 2017 IEEE <sup>[90]</sup> , and (Right) the Cyberdyne Inc. HAL Exoskeleton © 2005 IEEE <sup>[32]</sup> .....	17
Figure 3.	The torque requirements for slow sitting to standing with forward leaning for the hip (Top Graph), knee (Middle Graph), and ankle (Bottom Graph) in a healthy subject, as recorded by Bajd et al. <sup>[4]</sup> .....	20
Figure 4.	A free-body diagram of the 1-legged standing kinematic model proposed by Donaldson and Yu © 1996 IEEE <sup>[23]</sup> .....	25
Figure 5.	(Left) Sitting to standing motion for the HAL-5B Type C with a mannequin © 2009 IEEE <sup>[83]</sup> and (Right) location of the ZMP in sitting to standing for the HAL-5B Type C with a mannequin © 2009 IEEE <sup>[83]</sup> .....	31
Figure 6.	Preliminary neuroprosthesis design <sup>[20]</sup> .....	33
Figure 7.	Exploded view of the CAD model for the left knee gearmotor assembly .....	37
Figure 8.	(Left) SOLIDWORKS CAD model of the left knee gearmotor assembly with the motor cover omitted for clarity and (Right) a diagram of a harmonic gear from Harmonic Drive LLC <sup>[36]</sup> .....	39
Figure 9.	(Left) The NCRL neuroprosthesis walker showing the approximate FSR locations underneath the walker handles and (Right) right walker handle FSR placement with the walker handle omitted for clarity .....	41
Figure 10.	Walker FSR PCB schematic .....	42
Figure 11.	(Top) Joystick PCB schematic, (Bottom Left) neuroprosthesis walker joystick, and (Bottom Right) neuroprosthesis walker joystick with hand in place .....	43

Figure 12. Controller schematic for the knee synchronization controller and the end effector controller during standing up in state 2 of the FSM .....	52
Figure 13. Finite state machine progression and user intention triggers.....	54
Figure 14. End effector local coordinate frame.....	64
Figure 15. (Left) The end effector start point, at the end of state 1, and end point, at the beginning of state 3, and (Right) a diagram of the desired end effector position algorithm. The algorithm uses the intersection of the desired end effector trajectory and the torso link half circle end effector path to generate desired hip angles.....	66
Figure 16. A sequence of frames from the footage taken during trial 5 of the standing experiment .....	72
Figure 17. Knee angles versus time for trial 5 of the standing experiment.....	73
Figure 18. Left knee motor synchronization error versus time for trial 5 of the standing experiment.....	74
Figure 19. The measured end effector trajectory and the desired end effector trajectory of the subject in X and Y for trial 5 of the standing experiment.....	74
Figure 20. The hip error versus time for trial 5 of the standing experiment .....	75
Figure 21. The walker handle forces versus time for trial 5 of the standing experiment.....	77
Figure 22. Knee angles versus time in trial 2 of the hybrid sitting to standing experiments, with a stimulation amplitude of 25mA .....	78
Figure 23. Left knee motor synchronization error versus time for trial 2 of the hybrid standing experiment.....	79
Figure 24. The measured end effector trajectory and the desired end effector trajectory of the subject in X and Y for trial 2 of the hybrid standing experiment .....	80
Figure 25. The hip error versus time for trial 2 of the hybrid standing experiment.....	81
Figure 26. The walker handle forces versus time for trial 2 of the hybrid standing experiment .	82
Figure 27. A sequence of frames from the footage taken during trial 2 of the standing experiment .....	83
Figure 28. Knee angles versus time or trial 2 of the standing experiment.....	84
Figure 29. Left knee motor synchronization error versus time in state 2 for trial 2 of the standing experiment.....	85

Figure 30. The measured end effector trajectory and the desired end effector trajectory of the subject in X and Y for trial 2 of the standing experiment.....	86
Figure 31. The hip error versus time for sitting to standing for trial 2 of the standing experiment .....	87
Figure 32. The walker handle forces versus time for trial 2 of the standing experiment.....	88
Figure 33. Knee angles versus time for trial 3 of the hybrid standing experiment .....	90
Figure 34. Left knee motor synchronization error versus time in state 2 for trial 3 of the hybrid standing experiment .....	91
Figure 35. The measured end effector trajectory and the desired end effector trajectory of the subject in X and Y for trial 3 of the hybrid standing experiment .....	92
Figure 36. The hip error versus time for trial 3 of the hybrid standing experiment.....	93
Figure 37. The walker handle forces versus time for trial 3 of the hybrid standing experiment .	93
Figure 38. The right knee motor power for trial 5 of experiment 1 .....	99
Figure 39. The absolute values of the right knee motor power for trial 2 of experiment 2 .....	100
Figure 40. The absolute values of the right knee motor power for trial 2 of experiment 3 .....	101
Figure 41. The absolute values of the right knee motor power for trial 3 of experiment 4 .....	102
Figure 42. Luigi Galvani’s experimental setup in his work “The Effect of Electricity on Muscular Motion” <sup>[29]</sup> .....	109

## LIST OF ABBREVIATIONS

BMI	Brain-Machine Interface
BWSTT	Bodyweight Supported Treadmill Training
CAD	Computer-Aided Design
CHRELMS	Control by Handle Reactions of Leg Muscle Stimulation
CNP	Chronic Neuropathic Pain
COG	Center of Gravity
DOF	Degree of Freedom
EE	End Effector
EST	Estimate / Estimated
FES	Functional Electrical Stimulation
FSM	Finite State Machine
FSR	Force Sensing Resistor
FSW	Force Sensing Walker
HAL	Hybrid Assistive Limb
HMI	Human-Machine Interaction
HMIC	Human Machine Interface Crutches
I/O	Input / Output
NCRL	Neuromuscular Control and Robotics Laboratory (Pitt)
OPR	Operational

PAE	Performance Augmenting Exoskeleton
PCA	Personal Care Assistant
PCB	Printed Circuit Board
PD	Proportional Derivative
PDMR	Patient Driven Motion Enforcement
PID	Proportional Integral Derivative
PID-DC	Proportional Integral Derivative - Delay Compensating
QOL	Quality of Life
RISE	Robust Integral of the Sign of the Error
SCI	Spinal Cord Injury
SYNCH	Synchronization
THEOR	Theoretical
VC	Virtual Clutch
WSC	Wrap Spring Clutch
ZMP	Zero Moment Point

## 1.0 INTRODUCTION

The main motivation for the hybrid neuroprosthesis research at the Pitt Neuromuscular Control and Robotics Laboratory (NCRL) is to improve the quality of life (QOL) in individuals with spinal cord injury (SCI). A hybrid neuroprosthesis is a type of powered orthosis that uses a combination of electric motor actuation and functional electrical stimulation (FES) to restore mobility in users with disabilities. SCI is a serious condition which can significantly detract from a person's QOL, especially when SCI leads to complete paraplegia or quadriplegia. There are around 17,000 new SCI cases each year, with an estimated total of 282,000 people (0.09% of the population) in the United States who have SCI<sup>[87]</sup>. The types of accidents that cause SCI are not exceptionally rare, with 38% of SCI caused by vehicular accidents and another 30.5% of SCI caused by falls in the United States since 2010<sup>[87]</sup>. Since 2010 in the US, 20% of spinal cord injuries cause complete paraplegia, wherein the injured person does not have control of their legs and lower body, and another 13.3% of spinal cord injuries cause complete quadriplegia, wherein the injured person does not have control of any of their 4 limbs<sup>[87]</sup>. Lifetime costs of SCI can be astronomical, with an average lifetime costs for a 25-year-old individual with paraplegia exceeding 2 million dollars in 2015<sup>[87]</sup>. The total cost of all SCI treatment in the US is over 7 billion dollars annually<sup>[60]</sup>.

In addition to paralysis, SCI can cause a variety of other negative physical conditions including bladder dysfunction, sexual dysfunction, autonomic dysreflexia, muscle spasticity,

bone changes, respiratory problems, and chronic pain, among other conditions<sup>[16,76]</sup>. Furthermore, there are negative psychosocial effects of SCI<sup>[16]</sup>. People with SCI often experience a loss of independence in daily life and rely on personal care assistants (PCA's) to help them function in day-to-day activities<sup>[16]</sup>. However, many people with SCI do not have the resources to hire top PCA's and must rely on low skilled PCA's<sup>[16]</sup>. There have been many documented instances of PCA's abusing or neglecting people with SCI<sup>[16]</sup>. Another negative psychosocial aspect of SCI is that it degrades a person's mobility. Despite US legislation such as the Americans with Disabilities Act (ADA), not all public buildings are fully wheelchair accessible and many private buildings have no wheelchair accessibility<sup>[16]</sup>. These physical and psychosocial effects can combine to detract from QOL of a person with SCI, especially immediately after the injury when the person is adapting to these life changes. Nevertheless, despite all the negative effects of SCI, people in their 20's with SCI who survive more than 1 year after their injury have average life expectancies of about 46 years, as compared to 53 years in a healthy individual without SCI<sup>[87]</sup>.

## **1.1 MOTIVATIONS FOR A NEUROPROSTHESIS**

This section describes the applicability of a neuroprosthetic device in treating people with SCI.

### **1.1.1 Rehabilitative Priorities of People with SCI**

Several studies have been performed to identify the life priorities of persons with SCI. One systematic review of SCI life priority surveys performed by the Spinal Cord Injury

Rehabilitation Evidence Research Team (SCIRE) identified four major life priorities among people with SCI and paraplegia: restoring bowel function, bladder function, sexual function, and motor function<sup>[80]</sup>. Among the studies reviewed addressing persons with SCI and paraplegia, recovering the ability to walk was the third highest life priority, and was chosen as the most important or second-most important QOL improvement by about 38% of the sample<sup>[80]</sup>. In a study by Brown and Triolo, restoring walking functionality was selected as the most important mobility functionality among four total mobility functionalities<sup>[10,80]</sup>.

### **1.1.2 Purposes of a Neuroprosthesis**

The University of Pittsburgh Neuromuscular Control and Robotics Laboratory (NCRL) hybrid neuroprosthesis is a type of powered orthosis that has two main purposes: restoring mobility in people with SCI and providing physical therapy for the user outside of a clinical setting. By providing sitting to standing and assisted gait movements, the neuroprosthesis can decrease the dependency on PCA's and expand access to areas that do not have wheelchair accessibility<sup>[56]</sup>. Overground walking training for patients with lower body disabilities commonly requires three technicians to assist the patient to walk<sup>[56]</sup>. This therapy can be very exhausting for the therapists and is unsafe if the therapists are fatigued<sup>[56]</sup>. With a neuroprosthesis, the user can reduce the number of therapists needed and perform walking outside of a clinical setting<sup>[56]</sup>.

### **1.1.3 Potential for Neuroprosthesis Adoption**

Although restoring mobility is valuable for people with SCI, it is important to identify that not all people with SCI will be able to benefit from the NCRL neuroprosthesis. The 13.3% of people

with SCI that have complete quadriplegia<sup>[87]</sup> will most likely not be able to use the NCRL hybrid neuroprosthesis. Quadriplegia presents a unique set of challenges that are not present with paraplegia, since the user is not able to use their arms or upper body during standing or an assisted gait. Additionally, a full body neuroprosthesis would be required to accommodate for quadriplegia. Further complicating the issue is the fact that user input into the neuroprosthesis must not use the arms or legs for a person with quadriplegia. Most likely, user input for a person with quadriplegia would also require advanced user intention technologies, such as a brain-machine interface (BMI)<sup>[15]</sup>. Thus, restoring mobility in people with quadriplegia is beyond the present scope of the NCRL capabilities.

In addition to people with complete quadriplegia, the 41% of people with SCI diagnosed with incomplete quadriplegia<sup>[87]</sup> may not be able to benefit from use of the neuroprosthesis, depending on the nature of their upper-body functionality. Additionally, spinal cord injuries can be accompanied by other serious medical problems including traumatic head injury and other serious physical injuries<sup>[76,82]</sup> which may limit their ability to use a neuroprosthesis. Some people with SCI with damaged peripheral nervous system may not respond well enough to FES to restore their mobility with a hybrid neuroprosthesis. The statistics on SCI since 2010 suggest that a substantial proportion of the 41% of people with SCI that have either complete or incomplete paraplegia<sup>[87]</sup> could benefit from hybrid neuroprosthesis mobility therapy.

## 1.2 MOTIVATIONS FOR STANDING CONTROL

The main goal of a standing control model is to transition to user into a standing position where they can begin an assisted gait control model and thereby increase their mobility. Standing control also provides physical therapy to the user.

### 1.2.1 Preliminary Standing Control System

Much of the direction for the controls and hardware design was motivated by a preliminary standing experiment performed on a subject with SCI before the research for this thesis was started.

In a preliminary experiment, a simple finite state machine (FSM) was created with the end goal of moving the subject with SCI from sitting to standing. The SIMULINK model used a pushbutton to transition between FSM states, where state 0 was sitting, state 1 was sitting to standing, and state 2 was full standing. This FSM relied only on functional electrical stimulation (FES) to move the subject's leg shanks, and there were no powered motors at the knees. There was very little user control in this system, with all standing movement was automatically initiated by the program. The hip and knees were controlled to track predefined trajectories to move them from sitting to standing using Robust Integral of the Sign of the Error (RISE) controllers at the hip and PID-DC controllers for FES at the knees. The FSM moved between a start sitting position and a set end position, but there was insufficient consideration for the user trajectory. The subject with SCI used the walker and harness system during the experiment.

Although this preliminary experiment was ultimately safe, the experiment failed to move the user from sitting to standing in a way that as satisfactory to the user. In the experiment, once

the Subject with SCI moved into state 1 they slouched down and forward onto the walker handles and were unable to stand effectively. As a result, the safety stop button was pressed to end standing. The SCI user did not feel confident with this preliminary standing model.

### **1.2.2 Problems with the Preliminary Standing Control System**

The four major problems with the preliminary standing control system are listed below:

1. FES did not supply enough power at the knee: The control system primarily failed because FES alone could not produce enough torque at the knees for sitting to standing. Previous research has shown that many subjects with SCI only had sufficient knee muscle power to perform standing with FES after months of training using FES<sup>[4]</sup>, which our Subject did not have. Furthermore, it is impractical for every subject with SCI to have completed extensive FES training, and it can take months for a subject with SCI to sufficiently develop their muscles using FES<sup>[4]</sup>. Therefore, FES alone cannot be relied upon for subjects with SCI, and external mechanical power needs to be provided using an electric motor or some other type of actuation.
2. Poor user control and human-machine interaction (HMI) – The user did not feel like they were in control of the standing motion because the movement was completely automated. As a result, they did not feel confident in the control system. Thus, the control system should allow the user to have greater control of the standing movement so that they want to use the control system. An improved

user-machine interface is needed that incorporated a user control input into the controls.

3. Insufficient torso control of the standing trajectory – This problem was not directly observed in the experiment because the experiment was unable to perform standing, however it was inferred from the control structure. The torso trajectory was not considered in the control. The user's torso must be controlled so that it moves through a safe and natural trajectory from sitting to standing.

These problems, along with the research done on existing standing control methods, helped define the design direction for the standing control system described in this thesis.

### **1.3 THESIS CONTRIBUTIONS**

This thesis presents a novel control system to achieve standing in a user who has SCI. The research contributions developed in this thesis are listed below:

- Mechatronic re-design and fabrication of a hybrid neuroprosthesis with knee motors and a user-controlled joystick to perform standing in subjects with SCI. This hardware is designed for both standing and assisted walking functionalities (see Section 3).

- Design of a novel control system used to perform standing in subjects with SCI, which combines user control and automated control. This control system tracks the end effector of the user in a defined trajectory to enable balanced standing (see Section 4).
- Experimental validation of the standing control system in an able-bodied subject and a subject with SCI. Experiments were performed with and without FES power for both subjects and control system performance was analyzed across all experiments (see Section 5).
- Collection of energy consumption data in the knee motors during the standing experiments to compare energy consumption for standing without FES to standing with FES. This data is used to analyze the energy efficiency of the hybrid standing control system (see Section 5).
- Analysis of power usage and energy consumption in the knee motors to select a mobile power source for a future mobile neuroprosthesis design (see Section 5).

## **2.0 BACKGROUND INFORMATION AND LITERATURE REVIEW**

This chapter introduces the background knowledge that was used to develop the novel standing control system proposed in this thesis. Section 2.1 discusses the current state of the art for robotic exoskeletons, including the history and evolution of the technology. Section 2.2 discusses the use of FES as it has been applied to rehabilitation and its potential for use in active orthoses. Section 2.3 discusses active orthosis design and control methods used to perform sitting to standing.

### **2.1 ROBOTIC EXOSKELETON STATE OF THE ART**

As a formal definition of the technology used, the hybrid neuroprosthesis is a class of wearable robotics known as robotic exoskeletons. An exoskeleton is defined as any wearable robotics which closely fits to the user's body in an anthropomorphic design and works in coordination with the user's movements or intention<sup>[21]</sup>. Robotic exoskeletons are typically classified into two distinct categories based on intended use: performance-augmenting exoskeletons (PAE) and active orthoses<sup>[21]</sup>. Active orthoses can be further subdivided into two categories based on intended use: assistive orthoses, which expand a disabled subject's physical capabilities, and therapeutic orthoses, which provide therapeutic benefits to the subject<sup>[90]</sup>. The NCRL hybrid neuroprosthesis is an active orthosis which can be classified as both an assistive and a therapeutic orthosis. The neuroprosthesis is assistive in the sense that it restores a disabled user's

ability to stand up and walk, and it is therapeutic in the sense that the FES stimulation can provide therapeutic health benefits to users.

### **2.1.1 Performance-Augmenting Exoskeletons**

A PAE seeks to expand the capabilities of a user beyond their natural capabilities or decrease the metabolic requirements for performing a task<sup>[21,90]</sup>. Many of the design challenges faced in developing a PAE are similar to the challenges faced in developing an active orthosis, and therefore it is of benefit to study both types of exoskeletons. One of the first, and perhaps the most ambitious, PAE designs was the Hardiman prototype developed by General Electric, in cooperation with Cornell University, in the early 1960's<sup>[9,21]</sup>. One of the design goals for this exoskeleton was to allow a user to lift up to 1,500 lbs<sup>[9,27,58]</sup>. Testing verified that one arm of the device was capable of lifting over 750 lbs, however the arm weighed a massive 1,500 lbs itself<sup>[9,27,58]</sup>. Although the arm showed satisfactory performance, the project suffered setbacks in the operation of the exoskeleton lower limbs. It was alleged that the Hardiman exoskeleton was never tested with a user<sup>[21]</sup>.

Another example of a PAE is the Berkeley Lower Extremity Exoskeleton (BLEEX), shown in Figure 1, which is an exoskeleton designed to increase the load carrying capabilities of soldiers over long distances<sup>[9,21,63,90]</sup>. This exoskeleton transmits the user load into the ground and implements a control structure designed to use kinematic sensors to detect user intent<sup>[44]</sup>. Early prototypes of this exoskeleton used hydraulic actuators to move a total of 7 DOF's at each leg<sup>[92]</sup>. The PAE consumed 1143W of hydraulic power during level walking as compared to a 75 kg human who consumes about 165W of power during a level gait<sup>[13,21,92]</sup>. The performance of PAE exoskeleton is typically measured in two ways: the ability of the exoskeleton in expanding the

user's capabilities and the ability of the exoskeleton to decrease the metabolic cost of performing specified tasks<sup>[21]</sup>. Contrary to design intention, several PAE's, including an MIT exoskeleton using passive assistance at the joints, have been shown to increase the metabolic cost of walking<sup>[21,86]</sup>. This increase in metabolic costs in these exoskeletons has been attributed to inefficiencies in human-robot interaction, specifically relating to a misalignment of the exoskeleton with the user's body, and an alteration in combined system dynamics, as the PAE add weight to the user and alters the movement dynamics<sup>[21]</sup>. Although PAE exoskeletons fundamentally differ in their purposes as compared to active orthoses, they highlight that human-robot interaction is critical in any exoskeleton and that energy costs are an important design consideration. Excessively heavy exoskeleton designs can fundamentally alter the systems dynamics and create energy inefficient systems.

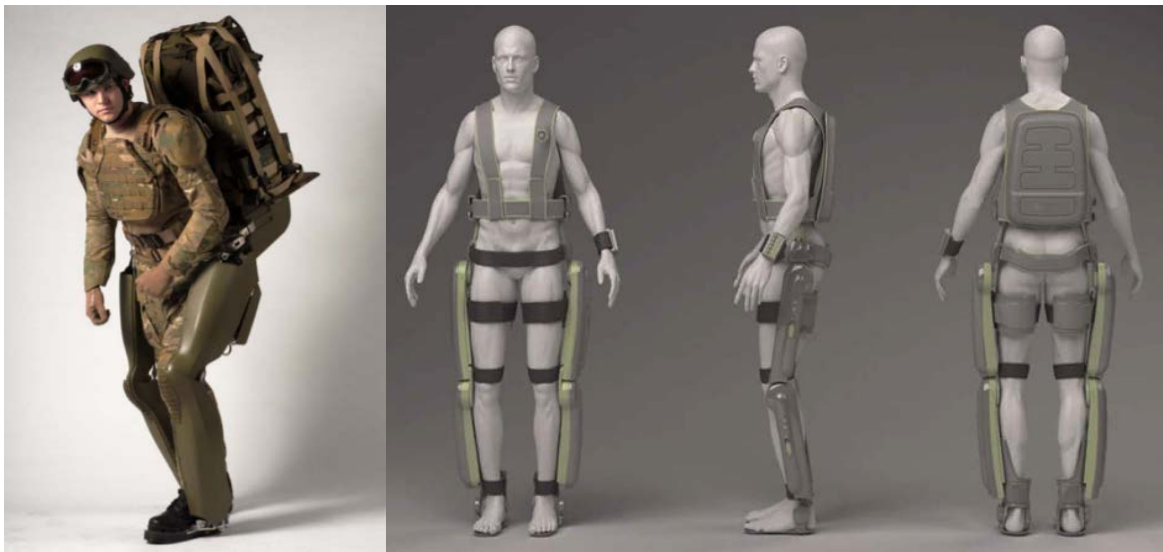


**Figure 1.** (Left) The Berkeley Lower Extremity Exoskeleton © 2005 IEEE<sup>[13]</sup> and (Right) the ReWalk Exoskeleton

© 2012 IEEE <sup>[9]</sup>

### **2.1.2 Active Orthoses**

Active orthoses are robotic exoskeletons that are designed to re-enable movement abilities in a user with disabilities<sup>[21]</sup>. The NCRL hybrid neuroprosthesis is an active orthosis designed to enable sitting to standing and assisted walking in users who have paralysis caused by SCI. This technology evolved from adding active elements to passive orthoses. One of the earliest active orthosis braces was developed by Miomir Vukobratovic at the Mihailo Pupin Institute in the late 1960's<sup>[21,38,40,63]</sup>. This early orthosis was surprisingly complex with pneumatic actuation at the hip in flexion/extension and abduction/adduction, flexion/extension actuation at the knee, and flexion/extension actuation at the ankle, and a light total weight of 12 kg<sup>[21]</sup>. This device used an electric diode function generator to produce reciprocating motion at these joints to create assisted walking for users with several types of paralysis<sup>[21]</sup>.

Some treadmill-based exoskeletons, such as Lokomat, also provide therapy to the user, however this device and other similar devices are often categorized in a separate class of non-mobile exoskeletons<sup>[21,24]</sup>. Although these devices have been shown to provide realizable therapy to the user, one of the main advantages of active orthoses is their ability to provide therapy outside of a clinical setting. A mobile active orthosis allows the user to realize increased mobility and therapy in their day-to-day life<sup>[56]</sup>, thereby allowing for a substantial increase in their QOL<sup>[17,26,71]</sup>.

### **2.1.3 The ReWalk Exoskeleton**

To date, one of the most well established active orthoses has been the ReWalk, shown in Figure 1, which was approved by the FDA to be used with patients with SCI<sup>[90,91]</sup>. This device can

provide sitting to standing, standing to sitting, and assisted walking functionalities<sup>[90]</sup>. It uses a remote control that allows the user to control the orthosis' high-level functionality<sup>[90]</sup>. The ReWalk incorporates an inclination sensor at the torso to generate step trajectories<sup>[26]</sup>. A manual mode is also available to bypass the torso initiated gait<sup>[26]</sup>. The walking characteristics of the user can be optimized with ReWalk using an external computer<sup>[26]</sup>. Controlled actuation is provided at the hip and knees<sup>[90]</sup>. The ankle does not incorporate closed loop control, but it uses a spring to assist dorsiflexion over a limited range of motion<sup>[26]</sup>. The ReWalk requires the use of crutches in coordination with the exoskeleton to maintain user balance<sup>[26]</sup>.

One study performed by Esquenazi et al. investigated the use of the ReWalk orthosis on 12 subjects with SCI to analyze the safety and performance of the device<sup>[26]</sup>. The subjects were trained in up to 24 sessions, lasting 60 to 90 minutes for each session, over 8-week training periods<sup>[26]</sup>. Performance results showed that all subjects were capable of walking 6 minutes without direct assistance and walking speeds ranging from 0.03 to 0.5 meters per second<sup>[26]</sup>, as compared to mean pedestrian walking speeds ranging from about 1.3 meter per second to about 1.5 meters per second<sup>[11]</sup>. In addition to achieving assisted walking, the ReWalk showed a positive influence on the bowel function of 5 out of 12 subjects and some of the subjects reported a positive influence of their emotional wellbeing<sup>[26]</sup>. No falls or major injuries were reported in the walking sessions<sup>[26]</sup>. Only minor adverse effects were documented, including skin abrasions, lightheadedness, and edema<sup>[26]</sup>, and these effects were easily prevented with adjustments to setup. A noticeable increase in blood pressure and heart rates were documented in the tests<sup>[26]</sup>. However, clear limitations of the ReWalk were documented in the tests, including the dependent nature of the ReWalk operation. It was observed that although falls did not occur, the subjects occasionally lost their balance and either caught their balance or required the assistance of the

therapist to regain their balance<sup>[26]</sup>. The authors of this study did not believe that the ReWalk is developed to the point that it could be used by subjects completely independently<sup>[26]</sup>. The ReWalk also requires a modest level of trunk control to initiate the next step in the assisted gait<sup>[26]</sup>.

An individual case study by Raab et al. produced positive results with the ReWalk, wherein the subject's bowel function improved<sup>[71]</sup>. A third study on the ReWalk performed by Zeilig et al. on 6 subjects with SCI allowed the subjects to attain 100m of assisted walking in an average of 13 to 14 walking sessions<sup>[91]</sup>. This study also didn't experience any major safety issues with the ReWalk, however it noted that the ReWalk requires a relatively long 10 to 20 minutes to equip and unequip<sup>[91]</sup>. Although the ReWalk can be a vital tool for therapy of patients with SCI, functional implementation of the device in daily use required high energy demands, and about 58% of SCI a moderately large 74 user sample ended up abandoning the commercial version of the ReWalk in an Italian survey<sup>[28,91]</sup>. These studies produced evidence that active orthoses can improve the QOL of subjects with SCI.

#### **2.1.4 The EXPOS Exoskeleton**

EXPOS, a novel active orthosis shown in Figure 2, has been developed by researchers at Sogang University in South Korea<sup>[51,85]</sup>. This orthosis houses most of its heavy components, including the battery, dc motors, and computer, in a mobile walker unit used for stability to decrease the amount of weight attached to the user<sup>[51,85]</sup>. This exoskeleton is designed primarily to aid elderly users to replace the physical aid of younger PCA's<sup>[51]</sup>, but the underlying technology of moving exoskeleton components into a walker unit could be developed for people with physical

disabilities as well. The wearable exoskeleton in this system weights less than 3 kg<sup>[51]</sup>, which is among the lightest active orthoses in existence.

The EXPOS orthosis provides sitting to standing and assisted gait functionalities. The orthosis transmits the DC motor power from the walker to the hip and knee joints using a pulley system<sup>[51]</sup>. The knee and hip joints both have 1-DOF<sup>[51]</sup>. The ankle joints have 2-DOF and are unactuated but use shock absorbers to aid in walking<sup>[51]</sup>. The wheels of the walker are also actuated to decrease weight resistance<sup>[51]</sup>. The control system uses potentiometers to measure joint angles and has pneumatic pressure sensors at the thighs and feet to measure HMI torques<sup>[51]</sup>. A fuzzy controller is used with the pressure sensor readings and joint velocities to determine the motor inputs during movement<sup>[51,85]</sup>. The study compared electromyography (EMG) signals for unassisted standing to standing with EXPOS, and it found that the average of the EMG peak values was 32% lower using EXPOS<sup>[51]</sup>. Moving the heavy components of an exoskeleton into the walker device is a unique method which could have potential to decrease the high energy demands found in exoskeletons such as ReWalk, since the overall weight of the wearable exoskeleton can be drastically reduced.

### **2.1.5 The Ekso Bionics Exoskeleton**

The Ekso Bionics exoskeleton, shown in Figure 2, is an active orthosis which provides bilateral actuation at the hip and knee joints to enable assisted walking in patients with lower limb disabilities<sup>[14,90]</sup>. This device is unique, as compared to other exoskeletons in this review, in that it allows the therapist to control the movement of the exoskeleton in two walking modes and allows the user to control the walking in two other walking modes by changing the movement of the user's hips<sup>[14]</sup>. Ekso uses two crutches for user stability that have force sensors in them<sup>[14]</sup>.

Both crutches must be on the ground to trigger the next step in the control finite state machine (FSM)<sup>[14]</sup>. Ekso also features a partial assist mode which adapts to the force generation of the user<sup>[14]</sup>.

A study performed by Kolakowski et al. on the safety and feasibility of the Ekso was performed on eight individuals with complete SCI and concluded, from the assisted walking sessions performed, that the Ekso was safe to use in the presence of trained assistants<sup>[50]</sup>. A training effect was observed in this device, where the subjects became more proficient and capable in using the device over time<sup>[50]</sup>. However, this study also reported several subject falls related to programming errors in a prototype human machine interface crutches (HMIC) control program and one fall using the original control program due to user error<sup>[50]</sup>.

### **2.1.6 The HAL Exoskeleton**

The Hybrid Assistive Limb (HAL) exoskeleton produced by Cyberdyne Inc. in Japan, shown in Figure 2, provides assisted walking and assisted standing functionalities for users with SCI, stroke, and other disabilities, and it provides PAE functionalities for able-bodied users<sup>[21,43,83,90]</sup>. HAL comes in multiple models, allowing for different modular body coverage and functionalities<sup>[14]</sup>. HAL is the only easily purchasable exoskeleton on the market today which uses EMG signals as a control input<sup>[90]</sup>. The components of the HAL include: computer controller, a battery, a power unit, EMG sensors, accelerometers, inclinometers, and floor reaction force sensors<sup>[14]</sup>. HAL is used with a walker or a cane, which is a regular safety feature for active orthoses<sup>[14]</sup>.

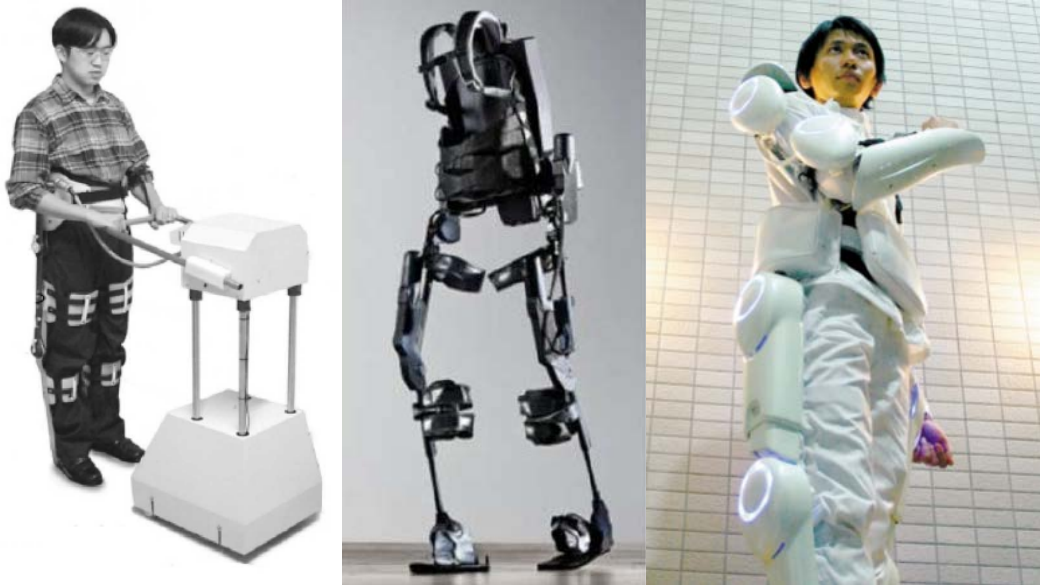


**Figure 2.** (Left) The EXPOS Exoskeleton System © 2006 IEEE<sup>[21,51]</sup>, (Center) the Ekso Bionics Exoskeleton © 2017 IEEE<sup>[90]</sup>, and (Right) the Cyberdyne Inc. HAL Exoskeleton © 2005 IEEE<sup>[32]</sup>

A study done by Cruciger et al. was performed with bodyweight supported treadmill training (BWSTT) using the HAL to observe changes in chronic neuropathic pain (CNP) and QOL in patients with SCI<sup>[17]</sup>. Two patients with moderate CNP used the HAL for BWSTT 5 times a week for 12 weeks<sup>[17]</sup>. At the start of the program both patients used several pain reduction drugs, and these drugs were reduced 4 weeks into the program<sup>[17]</sup>. The program utilized the Short Form-36 (SF-36) questionnaire<sup>[61]</sup> to assess changes in the subjects' QOL during training and it also utilized the numerical pain rating scale (NRS-11)<sup>[37]</sup> to assess the level of CNP present during training<sup>[17]</sup>. The results of the study showed that the overall pain severity caused by CNP decreased significantly by the end of the trial as compared with the first session<sup>[17]</sup>. Both patients also reported a positive impact on QOL throughout every domain measured in the SF-36<sup>[17]</sup>. This study suggested that HAL has the potential to alleviate CNP in SCI patients, which in turn improves their QOL.

### **2.1.7 State of the Art Discussion**

This review of robotic exoskeleton state of the art is not comprehensive, including all exoskeleton technology in existence, and it only includes exoskeleton examples which are similar in nature to the NCRL neuroprosthesis. In fact, there is sufficient difficulty in covering all exoskeleton technologies, since new exoskeleton technologies emerge at a lightning fast pace and some technological information is inaccessible due to the proprietary nature of robotics in the private sector<sup>[90]</sup>. Nevertheless, exoskeleton state of the art can serve as a useful research reference to observe the technical details of recent technologies and their effectiveness. Studies on the exoskeleton technologies highlighted in this section have demonstrated that existing exoskeletons have produced improvements in the QOL of some subjects with SCI<sup>[17,26,71]</sup>. This suggests that it is also possible for the NCRL exoskeleton to achieve improvement in the QOL of people with SCI.

## 2.2 FUNCTIONAL ELECTRICAL STIMULATION

The NCRL neuroprosthesis employs hybrid knee actuation, combining motor actuation and FES actuation of the knee joint. Robotic exoskeletons that combine robotic actuation with FES applied to some part of the user's body are known as hybrid exoskeletons<sup>[33]</sup>. Both robotic actuation and FES have advantages and disadvantages in use for gait rehabilitation. The main objective of hybrid exoskeletons is to combine both actuation methods to maximize their advantages and minimize their disadvantages<sup>[19]</sup>. The overall goal of lower extremity FES is to enable ambulation in people with paraplegia<sup>[66]</sup>. This section gives a brief introduction to the history of FES, how FES works on skeletal muscles, and the advantages and disadvantages of using FES in a rehabilitative exoskeleton. See Appendix A for a brief description of the early history of electrical stimulation. See Appendix B for a brief description of how FES functions in skeletal muscles.

### 2.2.1 The History of Electrical Stimulation

The first FES stimulator was developed by Liberson et al. in 1962 to rehabilitate drop foot in subjects with hemiplegia<sup>[54]</sup>. Liberson's work was inspired by pre-existing "classical electrotherapy," which was designed to prevent muscle atrophy and increase muscle strength, but he modified this electrotherapy so that it provided a functional benefit to the user<sup>[54]</sup>. One main problem with FES that Liberson discovered was the pain associated with stimulation, and he identified that this pain was a result of synchronous contraction of the muscle, as compared to

natural asynchronous muscle contraction<sup>[54]</sup>. There was no observed reduction in pain when the stimulation pulse time was reduced from 20ms to 0.3ms<sup>[54]</sup>. Liberson also noted difficulty in applying transcutaneous stimulation to the peroneal nerve, and designed a custom stimulator pad to achieve this<sup>[54]</sup>. He implemented a novel foot sensor approach, where the FES would only actuate when the foot sensor detected that the disabled foot had left the ground<sup>[54]</sup>. This system was successful in correcting drop foot in subjects with hemiplegia and reported positive physiological benefits<sup>[54]</sup>.

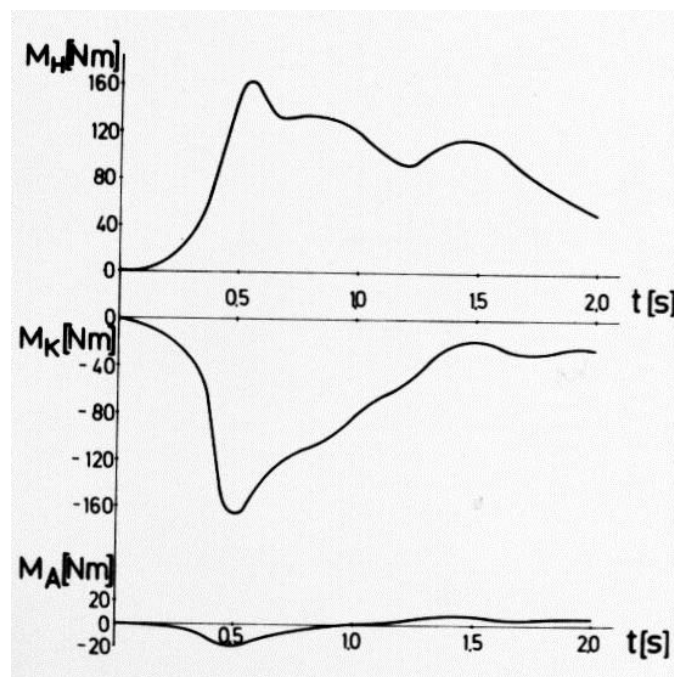


**Figure 3.** The torque requirements for slow sitting to standing with forward leaning for the hip (Top Graph), knee (Middle Graph), and ankle (Bottom Graph) in a healthy subject, as recorded by Bajd et al.<sup>[4]</sup>

FES later enabled people with paraplegia to stand up using their own muscles. Experiments were performed by Kantrowitz in 1963 where FES was used to stimulate the subject's glutes and quadriceps muscle to achieve standing and an FES actuated gait<sup>[42,46]</sup>.

Further work by Bajd and Kralj in the 70's and 80's involved the stimulation of the peroneal nerve to produce movement in the hip knee and ankle to provide complete movement for an FES gait cycle<sup>[5,46]</sup>. In 1973 Kralj and Grobelnik demonstrated that standing up could be achieved in subjects with paraplegia by applying FES to the hip, knee, and ankle extensors<sup>[31]</sup>.

In 1982 Bajd and Kralj performed a study on standing up in both healthy subjects and subjects with paraplegia<sup>[4]</sup>. The study first analyzed the joint torques and joint angles in a healthy subject performing normal sitting to standing and slow sitting to standing with the subject leaning forward<sup>[4]</sup>. The study found that, in the case of a healthy subject with leaning forward, that the torque requirements at the knee joint were reduced by 37% in the same subject<sup>[4]</sup>. The 82 kg subject required 160 Nm of total torque at the knees to perform slow sitting to standing with leaning forward<sup>[4]</sup>, and a graph of the joint torques is shown in Figure 3. Bajd and Kralj assumed, based on research done by Ellis et al.<sup>[25]</sup>, that knee torque requirements for standing are halved when the subject has access to arm support and that subjects with paraplegia, of roughly the same weight, would require at least 40 Nm of torque per knee for standing<sup>[4]</sup>. The study then analyzed the muscular performance of 19 subjects with paraplegia and upper SCI lesions after externally applied FES<sup>[4]</sup>. They found that nine of the original subjects could produce nearly 20 Nm of torque without prior FES training and determined that these subjects could stand with FES and arm support only<sup>[4]</sup>. The subjects were then given an FES stimulator and performed an FES training program over several weeks<sup>[4]</sup>.

After training, four of subjects could only stand for a few minutes and the other five subjects could stand for over an hour<sup>[4]</sup>. The study showed that some people with paraplegia could stand with FES only, but that none of the subjects with paraplegia could do this right away. The subject with SCI could only perform standing after a relatively long FES training program.

## 2.2.2 Advantages and Disadvantages of FES in a Neuroprosthesis

There are two primary potential advantages to using FES in a rehabilitative lower-extremity robotic exoskeleton: therapeutic health benefits to the user<sup>[7,12,52,53,66,81]</sup> and decreased exoskeleton power requirements<sup>[33,34,70]</sup>. FES can create an energy reduction in a neuroprosthesis because some of the power requirements for movement can be fulfilled with FES. In this way, a hybrid actuation at the knee recruits some of the energy from the user's metabolic system, thereby decreasing the power requirements and energy consumption experienced by the power supply. This power reduction has been shown experimentally by Goldfarb et al. with a hybrid control method to produce assisted walking in subjects with paraplegia with the Vanderbilt exoskeleton<sup>[33]</sup>. The power contributed by FES at the knees was shown to be an average of 20% across all subjects<sup>[33]</sup>. In an earlier study completed with the Vanderbilt exoskeleton performed in 2012 for level assisted walking, FES was shown to yield a 34% reduction of electrical power requirements at the hip joint<sup>[34]</sup>. Yet another study with the exoskeleton showed that the FES provided 55% of the energy for weighted leg lift experiments<sup>[70]</sup>. Thus, it has been shown that FES can provide a modest to substantial power reduction in hybrid control systems as compared to a non-hybrid exoskeleton. FES has been shown to bolster muscle strength, the cardiovascular system, and bone density, while ameliorating muscle spasticity<sup>[7,12,53,70]</sup>.

The main disadvantage to combining FES and powered actuation into a hybrid system is that it increases system complexity. If the hybrid control system is improperly implemented, it could result in undesirable or dangerous HMI. Furthermore, FES could fatigue the user's muscles after a period determined by the user's muscular development<sup>[57]</sup>. Eventually muscles could fail due to fatigue, potentially causing injury. Thus, to combat fatigue, the operational time

must be limited or the fatigue must be monitored, thereby adding more complexity to an already complex hybrid system.

## 2.3 STANDING CONTROL METHODS

The sitting to standing movement is paramount to restoring movement in users with a lower extremity exoskeleton. Many people with SCI who have complete or partial paraplegia are unable to stand and require assistance for this motion to get in an upright position, where an assisted gait cycle can be initiated.

A large wealth of research has been published detailing assisted gait control methods, however relatively less work has been published detailing control methods to achieve standing<sup>[41]</sup>. Several standing methods have been successfully implemented for use with FES only<sup>[4,22,31,42,52,59]</sup>. This section details control methods used for sitting to standing in FES only systems and robotic exoskeletons.

An exoskeleton has several advantages in performing hybrid sitting to standing as compared to FES only standing. While FES stimulation has been used to achieve standing in subjects with SCI, such as in the experiments performed by Katrowicz, Kralj, and Bajd<sup>[4,31,42]</sup>, none of the subjects with SCI tested in Bajd's 1982 standing experiment had the muscular strength to stand using FES at the beginning of their training<sup>[4]</sup>. The subjects with SCI required extensive FES training to perform FES-only standing<sup>[4]</sup>. This presents a significant barrier to entry for subjects with SCI to restore their ambulation. In the case of a hybrid exoskeleton, standing can be achieved immediately. Users can achieve sitting to standing with a low FES muscle output and scale up FES output as their muscular development increases. Furthermore, a

hybrid exoskeleton using FES has the possible advantage of providing therapeutic benefit to the user<sup>[7,12,33,52,53,66,81]</sup> as compared to an exoskeleton that does not use FES. There is evidence to suggest that hybrid actuated sitting to standing could provide an energy reduction as compared to motor actuation only<sup>[49]</sup>.

### 2.3.1 Donaldson and Yu's Standing Controller

In 1996, Donaldson and Yu performed a kinematic analysis of sitting to standing and created a control structure, but did not translate their work into simulations or experiments<sup>[23]</sup>. Their main goal was to create an FES control that modulated the stimulation based on standing position<sup>[23]</sup>. Their initial observation was that since most FES based sitting to standing used arm supports, force reactions from the arm handles could be used to drive the FES control for standing<sup>[23]</sup>.

Donaldson and Yu reached the observation based on standing kinematics, that a subject who had control of their upper body behaved like a two-bar linkage and a subject without control of their upper body behaved like a three-bar linkage, with the shank, thigh, and torso each representing a linkage<sup>[23]</sup>. In a 3-bar linkage, if only the position of the end effector (EE) is known then the exact angles of the linkages are indeterminate<sup>[23]</sup>. It was determined that subjects with high spinal cord lesions could not be controlled easily without imposing complex restraints<sup>[23]</sup>.

They then analyzed the case of a one-legged standing model, where a person has one central leg that represents the set of both legs to simplify the kinematics shown in Figure 4<sup>[23]</sup>. In the case of static equilibrium of the one-legged model the leg joint moments can be represented by the following equation:

$$M = LF + wPW$$

where  $M$  is a matrix of leg joint moments,  $L$  is a matrix of hand leverage distances,  $F$  is a vector of hand reaction forces and moments,  $w$  is the scalar body weight,  $P$  is a matrix of the positions of the centers of masses of the linkages, and  $W$  is a vector of the body weights of the 3 linkages<sup>[23]</sup>. In this model, the mathematical relationship between the joint moments and the handle reactions is linear<sup>[23]</sup>. However, in the kinematic analysis of a more realistic two-leg kinematic model there are twice as many unknown joint moments<sup>[23]</sup>. As a result, the model becomes indeterminate and the joint moments cannot be directly determined based on the handle reaction forces<sup>[23]</sup>. For this reason, a one-leg kinematic model is used for the analysis<sup>[23]</sup>.

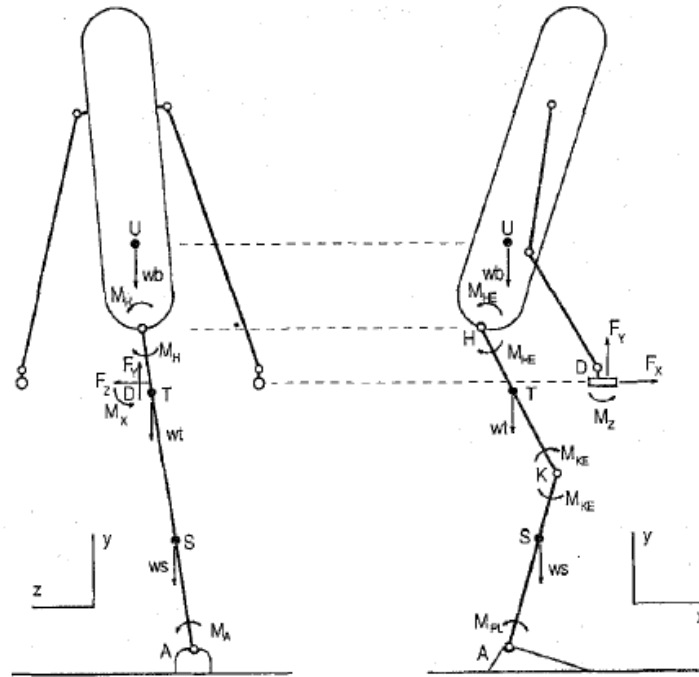


**Figure 4.** A free-body diagram of the 1-legged standing kinematic model proposed by Donaldson and Yu © 1996

IEEE<sup>[23]</sup>

The controller proposed by Donaldson and Yu, called “Control by Handle Reactions of Leg Muscle Stimulation” (CHRELMS), was designed to minimize the hand reaction forces because high hand reaction forces were correlated with fatigue in prolonged standing found by

Bajd et. al<sup>[3,23]</sup>. The following control law for the knee moments was established for the kinematics<sup>[23]</sup>:

$$M = H(z)LF$$

where  $H(z)$  is a discrete time transfer function defined as:

$$H(z) = \left( \frac{K_I}{1 - z^{-1}} + K_P \right)$$

where  $K_I$  and  $K_P$  are control gains and  $z$  is the discrete time transfer function variable. This controller discrete-time transfer function combines integral and proportional terms for stability<sup>[23]</sup>. In the specific case, where only the knee extensors are stimulated, the control law for the knee torque takes the following form:

$$M_{KE} = H(z) \begin{bmatrix} 1 & -y_{KD} & x_{KD} \end{bmatrix} \begin{bmatrix} M_z \\ F_x \\ F_y \end{bmatrix}$$

where  $M_z$  is the combined z-direction moment for both handles,  $F_x$  is the combined x-direction force for both handles,  $F_y$  is the combined y-direction force for both handles,  $y_{KD}$  is the y-direction distance between the handle and the knee, and  $x_{KD}$  is the x-direction distance between the handle and the knee<sup>[23]</sup>. It is important to note, however, that Donaldson and Yu did not yet determine how to modulate FES stimulation to produce the moments required for this control law<sup>[23]</sup>. Although this controller is designed to minimize the hand reaction forces it assumes that both the left and right legs behave nearly identically<sup>[23]</sup>, which may not be the case for people with incomplete paraplegia or hemiplegia.

### 2.3.2 Reiner's Standing Controller

In 1998, Reiner et al. designed a similar controller, called “Patient Driven Motion Enforcement” (PDMR) for sitting to standing, inspired by the CHRELMS design, to decrease the arm reaction forces in standing<sup>[72,73]</sup>. They performed a simulation study where they compared their control model to the CHRELMS control model, and they also performed experiments on subjects with SCI<sup>[72,73]</sup>. The main idea behind PDMR is that patient-driven control and a reduction in arm forces can be achieved by changing the control effort based on the voluntary arm support of the subject<sup>[73]</sup>. However, in this model, hand reaction forces are not directly measured, but they are predicted based on measurements of the shoulder position and trunk inclination<sup>[73]</sup>. Three separate fuzzy rule sets were created to relate the horizontal shoulder position, vertical shoulder position, and trunk inclination, and the first derivative of these variables, to the horizontal shoulder force, vertical shoulder force, and shoulder moment, respectively<sup>[73]</sup>. The control model uses this estimate arm effort in addition to an inverse kinematic model to determine the joint torques required for sitting to standing<sup>[73]</sup>. As a part of the inverse kinematic model, the torque response of the muscle in the presence of FES was modeled<sup>[73]</sup>. In this model, the active knee moment is computed by the following equation:

$$M_k^{act} = \sum M_k - M_k^{ela} - M_k^{visc}$$

where  $\sum M_k$  is the total moment at the knee,  $M_k^{ela}$  is the elastic moment at the knee, and  $M_k^{visc}$  is the viscous moment at the knee, which is linearly proportional to a damping coefficient  $d$ <sup>[73]</sup>. The elastic moment at the knee can be determined by the following equation:

$$M_k^{ela} = \exp(c_1 + c_2 q_k)$$

where  $c_1$  and  $c_2$  are shape constants and  $q_k$  is the angle of the knee<sup>[73]</sup>. Furthermore, the quadriceps activation can be determined by the following equation:

$$a_k = \frac{M_k^{act}}{M_k^{max} f_q f_{\dot{q}}}$$

where  $a_k$  is the normalized quadriceps activation,  $M_k^{max}$  is the maximum isometric knee moment,  $f_q$  is the knee angle factor, and  $f_{\dot{q}}$  is the knee velocity factor<sup>[73]</sup>. The researchers did not include the time delay associated with FES stimulation in the control model, which could be a significant omission affecting controller performance<sup>[73]</sup>.

One main issue with CHRELMS, found in the simulation, was that the hand reaction force data was insufficient to drive the subject into a fully standing position, whereas PDMR did not have this problem<sup>[73]</sup>. The PDMR control method was found to create synchronous standing and significantly decreased arm reaction forces in the simulation<sup>[73]</sup>. However, simulation showed that the CHRELMS controller produced buckling of the knee joint by nearly 25 degrees just after the knees approached full extension<sup>[73]</sup>. It was hypothesized that this buckling was caused by insufficient leg forces and a reduction of arm forces in the arm force simulation<sup>[73]</sup>. Simulation showed that the reduction in the arm forces using the PDMR strategy is significantly higher than the reduction in arm forces found in CHRELMS<sup>[73]</sup>. As a secondary benefit, the PDMR was found to have superior disturbance rejection for the arm forces<sup>[73]</sup>.

The arm based sitting to standing controllers designed in CHRELMS<sup>[23]</sup> and PDMR<sup>[72,73]</sup> reveal several design ambiguities. Reiner states that a patient with paraplegia can “control the SU and SD movement by their voluntary upper body effort.” However, since subjects with paraplegia do not have control of their legs and are using their arms to support a portion of their body weight, it is unclear how much voluntary “control” of the standing up motion is provided to

the user. It is unclear if users are capable of precisely controlling arm effort or if they are simply reacting to the amount of force necessary to elevate their center of mass. Secondly, there is no explanation included about what would happen if the arm handle force sensor readings were minimized due to sensor malfunction or muscle failure<sup>[73]</sup>, since this would represent an optimal loading of zero. The quality of user-control and control safety are somewhat ambiguous for an arm effort based standing control.

### **2.3.3 HAL Sitting to Standing Control System**

The robotic exoskeleton HAL enables sitting to standing in people with SCI and other disabilities, and it is one of the only exoskeletons to provide actuation at the hip, knee, and ankle, although it does not use FES<sup>[83]</sup>. Specifically, in Tsukahara et al., the HAL-5B Type C exoskeleton uses a balance based control method, with the human-robot zero moment point (ZMP) at the foot as a control input, to perform sitting to standing<sup>[83]</sup>. The HAL-5B Type C exoskeleton includes a frame, potentiometers to measure joint angles, an accelerometer attached to the user's trunk to measure the absolute trunk angle, and force sensors at the feet<sup>[83]</sup>. The sitting to standing motion is divided into 3 sections in the controls: sitting (phase 0), transition from sitting to standing (phase 1), and upright standing (phase 2)<sup>[83]</sup>. The controls program transitions from phase 0 to phase 1 based on the trunk angle and the ZMP, and it transitions from phase 1 to phase 2 based on the knee joint angle of the exoskeleton<sup>[83]</sup>. The system uses intention estimation initiates when the user, who has some control over their upper body, will lean forward before standing<sup>[83]</sup>. Thus, the intention estimation algorithm works by beginning the standing up motion once a torso angle threshold and a ZMP location threshold have been exceeded<sup>[83]</sup>.

In the HAL controls, the knee joints are solely recruited to move the user's center of gravity (COG) upwards<sup>[83]</sup>. The hip joints and the ankle are recruited to control the location of the ZMP and balance the user<sup>[83]</sup>. HAL uses two control algorithms to determine the torque being applied to the joints: a balance control algorithm and a gravity assist algorithm<sup>[83]</sup>. Three force sensors are in the heel, ball, and toe of the foot, where the location of the ZMP in the x-direction (sagittal plane) is calculated by the following equation:

$$x_{ZMP} = \frac{\sum f_i x_i}{\sum f_i}$$

where  $x_{ZMP}$  is the location of the ZMP,  $f_i$  are the force sensor outputs, and  $x_i$  are the x-locations of the 3 force sensors<sup>[83]</sup>. In this model, a normal ZMP is defined as 30mm to 50mm in front of the ankle joint, although the researchers do not specify if this range is dependent on the size of the user's foot<sup>[83]</sup>. In the balance control, the ankle joint control is computed directly from the error of the ZMP, whereas the knee joint control is computed based on a ZMP which is calculated by the direct kinematics of the exoskeleton<sup>[83]</sup>. An additional gravity compensation torque is calculated for each joint, with the purpose of increasing the controls performance<sup>[83]</sup>. By compensating for the gravity term, the stiffness at the joints for HAL can be decreased and the overall flexibility can be increased<sup>[83]</sup>. The overall torque applied to each joint is a summation of the torque computed in the balance control algorithm and the gravity control algorithm<sup>[83]</sup>. Thus, the HAL control model combines elements of balance control, kinematics based trajectory generation, and gravity compensation to move from sitting to standing.

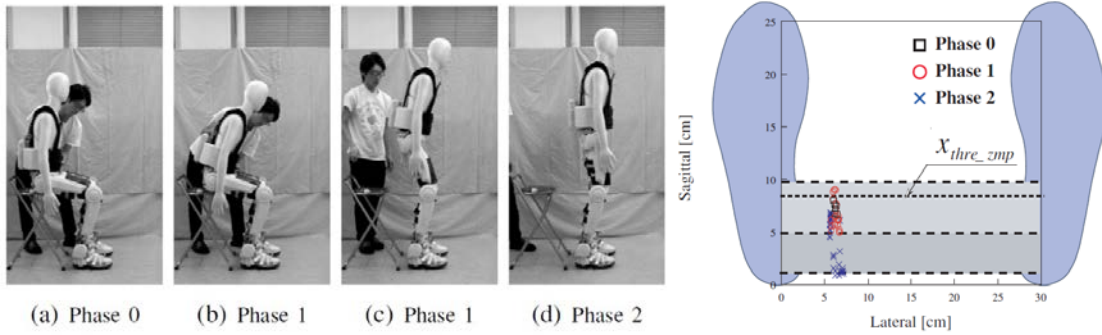


**Figure 5.** (Left) Sitting to standing motion for the HAL-5B Type C with a mannequin © 2009 IEEE<sup>[83]</sup> and (Right) location of the ZMP in sitting to standing for the HAL-5B Type C with a mannequin © 2009 IEEE<sup>[83]</sup>

Sitting to standing tests were performed in 3 stages for the HAL exoskeleton. Testing was performed on a mannequin, an able-bodied subject, and a subject with paraplegia<sup>[83]</sup>. Figure 5 shows both the standing-up motion and the path of the ZMP at the feet for the mannequin<sup>[83]</sup>. One of the attractive aspects of the HAL standing control is that it can achieve standing without external supports. However, horizontal bars were provided for balance in the case of the test on the subject with paraplegia<sup>[83]</sup>. The testing showed minimal arm support of less than 8 kgf for the subject with paraplegia<sup>[83]</sup>. HAL successfully achieved sitting to standing for all 3 tests safely with sufficient balance<sup>[83]</sup>.

### **3.0 NEUROPROSTHESIS MECHATRONIC DESIGN FOR STANDING**

This section describes in detail the mechatronic design directions taken to modify the NCRL hybrid neuroprosthesis so that a subject with SCI could achieve hybrid sitting to standing.

#### **3.1 PRE-EXISTING NEUROPROSTHESIS DESIGN**

Before the NCRL neuroprosthesis was modified for standing control, the knee joints were actuated using only FES stimulation. The knee joints each featured a wrap spring clutch (WSC) locking mechanism [Warner Electric, USA]. Each WSC used an analog controlled linear actuator [Actuonix Motion Devices Inc., Canada] to lock the knee during stimulation. The main purpose of the WSC was to lock the knee during standing, since stimulation is required to keep users with SCI in an upright standing position<sup>[46,49]</sup>. The knee joints also featured one attached external incremental optical encoder per knee [Automation Direct, USA], which measured the angle of each knee for closed loop FES control using a delay compensating controller<sup>[20]</sup>. The pre-existing NCRL neuroprosthesis design is shown in Figure 6.

The neuroprosthesis has two LPA-17-100 harmonic gearmotors [Harmonic Drive LLC, USA] attached to the hip joints. These motors can produce a maximum repeated peak torque, or a maximum long-term cyclical torque, of 54 Nm and have a maximum rotational speed of 30

RPM. These gearmotors each feature one embedded incremental optical encoder with 4000 counts per revolution. Each gearmotor weighs 4.3 lbs.

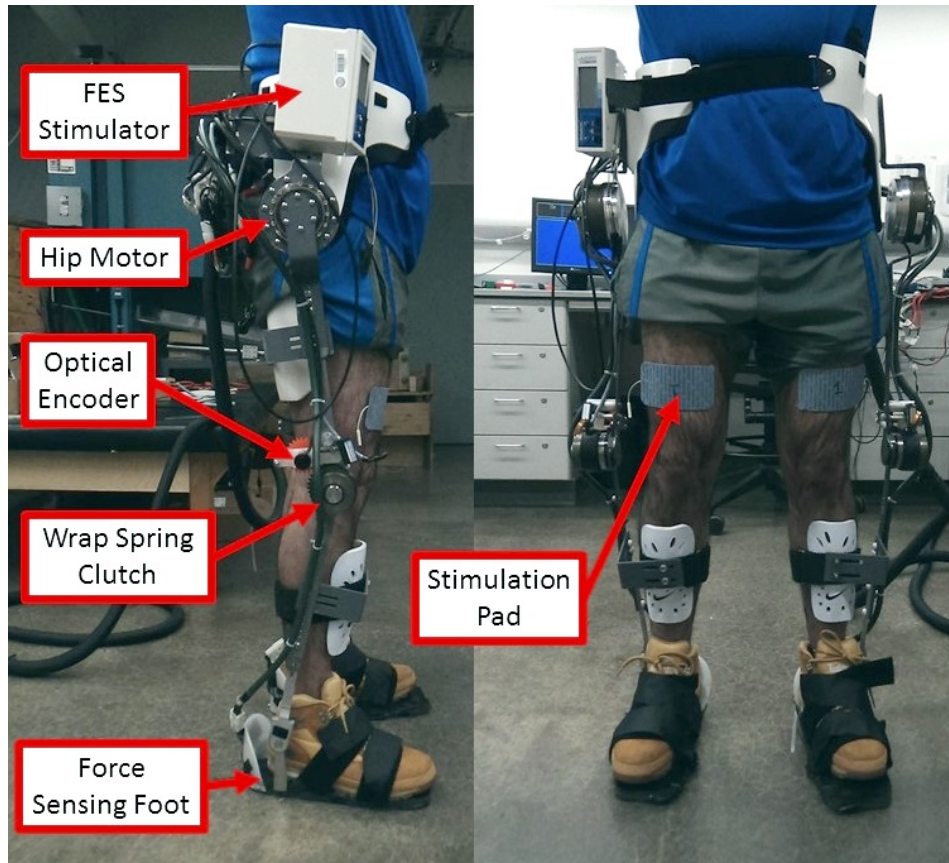


**Figure 6.** Preliminary neuroprosthesis design<sup>[20]</sup>

Additionally, the hip attachment interface and the neuroprosthesis feet were obtained from a walking orthosis and retrofitted onto the frame. Two thigh attachment pads with leg straps are attached to the neuroprosthesis frame to transmit force into the user's thighs. Two shin attachment pads with leg straps are attached to the neuroprosthesis frame to transmit force into the user's shins. The FES stimulator is mounted to the neuroprosthesis hip frame.

The FES stimulator is a RehaStim model [Hasomed GmbH, Germany] that features 2 modules with 4 stimulation channels per module. The stimulator can produce stimulation amplitudes ranging from 20mA to 130mA in amplitude steps of 5mA with a pulse width ranging from 20 microseconds to 500 microseconds. A custom program was created in Python to convert SIMULINK control signals into stimulation patterns in the FES stimulator.

An XPC target [Speedgoat GmbH, Switzerland] is used to run the SIMULINK control program and collect data in real time. The XPC target is attached to two I/O boards [Speedgoat GmbH, Switzerland] which have digital and analog inputs and outputs. The hip motor drivers [Harmonic Drive LLC, USA], knee motor drivers [Maxon Precision Motors Inc., USA], I/O boards, walker handle PCB's, and additional electronics are attached to a custom-built electronics panel that is affixed to the lab table.

A powered gait trainer [Rifton Equipment, USA] is used to move disabled individuals for safe donning and doffing of the neuroprosthesis.

### **3.2 DESIGN NEEDS FOR STANDING**

One of the major disadvantages of FES is that it can quickly fatigue a user's muscles. The use of motors in addition to FES can lessen the development of muscle fatigue in persons using neuroprosthetic devices<sup>[46]</sup>. Also, the use of knee motors in addition to FES can lessen the user's overall strength requirements and the power requirements for the sitting to standing motion. In the preliminary standing experiments, it was found that the untrained subject with SCI was incapable of standing with FES only. Therefore, a new knee motor assembly was designed and installed into the pre-existing NCRL hybrid neuroprosthesis. The knee motors were designed so

that they would be able to match an able-bodied subject's performance in sitting to standing as closely as possible. Furthermore, the knee motors were designed with a functional assisted walking gait cycle in mind, since new assisted gait control methods have been designed for the NCRL hybrid neuroprosthesis<sup>[1,47,77,78]</sup>.

### **3.2.1 Sitting to Standing Knee Motor Requirements**

The knee motor torque is the most important design requirement, since insufficient torque could lead to a failure to stand. A relatively high amount of torque is required at the knee for the sitting to standing motion in an able-bodied subject<sup>[4]</sup>. The standing study performed by Bajd et. al. in 1982 showed that an 82 kg able-bodied subject required a maximum torque of 80 Nm at each knee to stand up<sup>[4]</sup>. The results of this study were used to estimate the required torque for the knee motor assembly and the assembly was designed to match this performance. Since a person with SCI can use hand supports to support some of their bodyweight during sitting to standing, Bajd et. al. approximated that at least 50 percent of the patient's bodyweight would be supported by the hand supports during sitting to standing<sup>[4,25]</sup>. This assumption was used for the knee assembly selection, and it indicates that the knee motor assemblies need to produce at least 40 Nm of torque at each knee<sup>[4]</sup>.

A secondary design requirement for the knee is the ability to perform the standing up at the same speed as an able-bodied user. The knee assembly was designed so that it would be able to move from sitting to standing, or over a 90-degree range of motion, in 1 second using a sinusoidal tracking trajectory. This requirement stipulates that the knee motor assembly must be able to rotate at an angular speed of at least 15 RPM at the output.

### 3.2.2 Assisted Gait Knee Motor Requirements

With future assisted gait control techniques in mind, the knee motor assembly was also designed to closely match the performance of an able-bodied subject during walking. The walking trials performed by Winter were used as an approximation for the assisted gait torque and speed requirements<sup>[88]</sup>. The subject walking in these trials was about 57 kg, which is lighter than the subject in the sitting and standing experiments performed by Bajd et. al<sup>[4,88]</sup>. The speed requirement was not treated as a critical requirement, since there are currently no known neuroprostheses capable of creating full-speed assisted gait cycles in people with SCI. Furthermore, attempting to reach a full speed gait cycle is realistically beyond the near-term design goals of the NCRL. In the walking trials performed by Winter, there was a maximum absolute angular velocity of 7.2 radians per second or about 69 RPM during the walking cycle<sup>[88]</sup>. Additionally, there was a maximum absolute knee moment of about 38 Nm during the walking cycle<sup>[88]</sup>.

Combining the knee assembly requirements for both sitting to standing and an assisted walking gait, the knee motors must produce at least 40 Nm of torque at the knee for standing. The knee motor must also be able to rotate at 15 RPM at the output. Ideally, the knee motor assembly will simultaneously be able to rotate at an output speed of 69 RPM at the maximum continuous torque of 40 Nm.

Finally, the knee motor assembly needs to be as small and as light weight as possible. If the knee assembly is too heavy, it could decrease the capability of the hip motor and negatively affect the dynamics of an assisted gait cycle. The knee assembly also needs to be kept to a reasonable overall cost so that it fits within the budget of the NCRL.

### 3.3 KNEE MOTOR DESIGN

A variety of possible knee motor assembly configurations were considered for the design. As a preliminary design, the knee motor was determined to consist of an electric knee motor, a gear connected to the motor, a knee encoder, and a knee braking system. Additionally, power supply units were selected to provide sufficient power to the knee motors. An analysis was performed for several combinations of these components to design an assembly that sufficiently meets the engineering needs outlined in the previous section. Figure 7 shows an exploded view of the knee motor assembly.

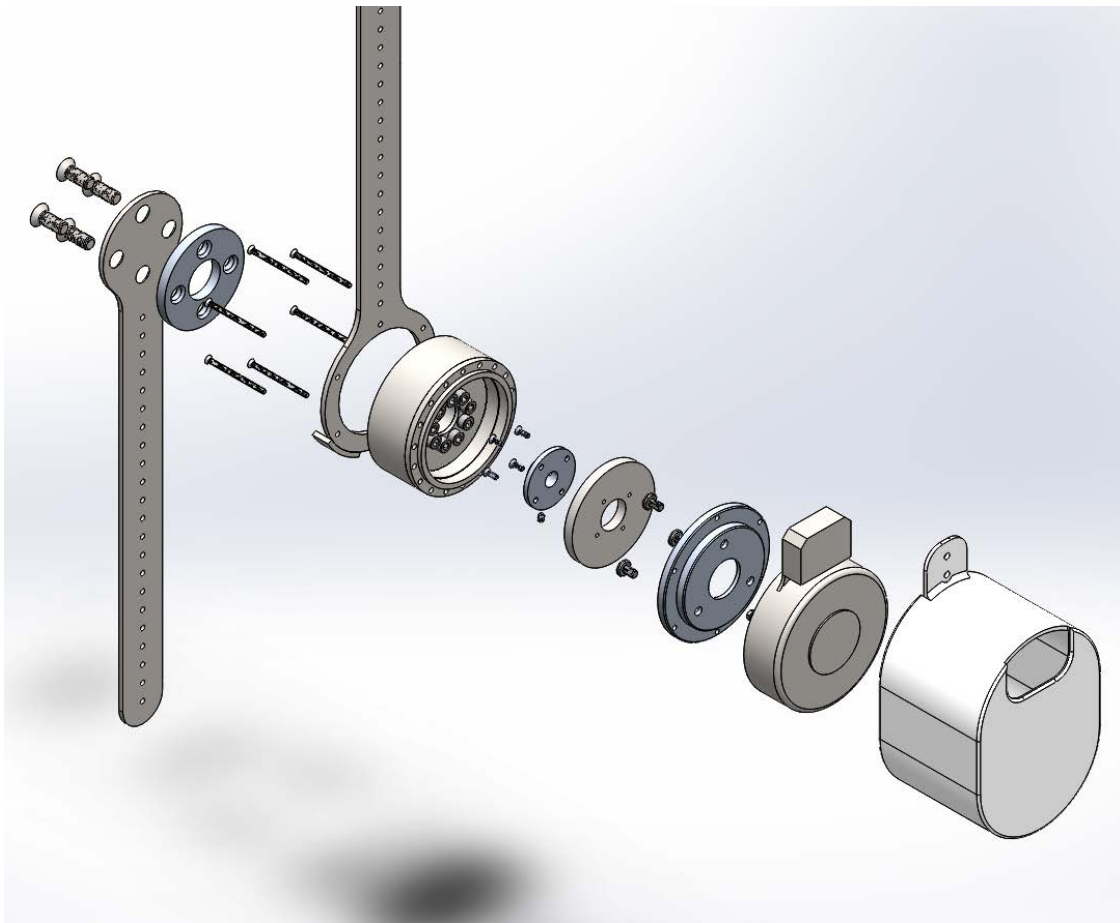


**Figure 7.** Exploded view of the CAD model for the left knee gearmotor assembly

For the knee motor, a 90W EC Flat motor [Maxon Precision Motors Inc., USA] was chosen. Each EC90 motor includes an imbedded optical MILE encoder [Maxon Motor AG, Switzerland] with 4096 counts per turn. Several aspects of this motor are ideal for the knee assembly. The Maxon motor can produce a torque of about 550 mNm at the output of the motor, which is relatively high in comparison to other electric motors considered. This exceeds the 40 Nm torque requirement stated previously after a 100:1 gear ratio is applied. Additionally, this motor has a maximum speed of 5000 RPM, which is reduced to 50 RPM after the same gear ratio is applied. Although the 50 RPM is lower than the ideal goal of 69 RPM at the knee for a full speed assisted gait, this speed is more than sufficient for the sitting to standing functionality required. Another motor considered claimed to exceed the EC90's performance, but the motor driver required to control it was still in the prototyping phase and this motor was deemed too risky. The EC90 motor offered the best performance specifications out of all motors considered and was chosen for the final knee design.

A harmonic gear was determined to be the most suitable gear drive system to transmit power to the knee joint. Figure 8 shows the inner components of a harmonic gear. In the harmonic gear, an inner wave generator rotates inside of a flex spline attached to the output, which causes the flex spline to rotate inside of a fixed circular spline<sup>[39,48]</sup>. As a result, the flex spline rotates in the opposite direction of the wave generator and this creates a mechanical advantage. The harmonic gear is ideal because it can create very high reduction ratios in a smaller profile than a traditional gear design. The harmonic gear chosen for this design [Harmonic Drive LLC, USA] has a gear ratio of 100:1.

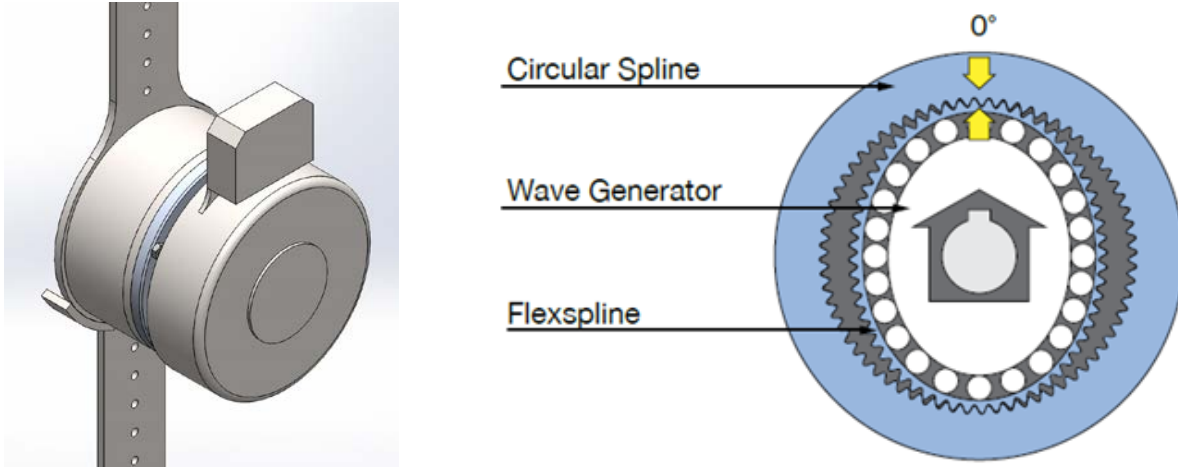


**Figure 8.** (Left) SOLIDWORKS CAD model of the left knee gearmotor assembly with the motor cover omitted for clarity and (Right) a diagram of a harmonic gear from Harmonic Drive LLC<sup>[36]</sup>

### **3.4 FORCE SENSING WALKER DESIGN**

A walker is used so that the neuroprosthesis user can push themselves upwards and stabilize their balance. The walker used was originally purchased from a medical supply company and retrofitted with force sensors, a joystick, and a safety stop button. The walker features adjustable length legs that can be custom set to adjust the walker height for each user. A lower walker height is used for sitting to standing, as compared to assisted gait cycles, because it is easier for the user to support their weight from a lower height during sitting to standing. The neuroprosthesis force sensing walker (FSW) is shown in Figure 9.

Force sensors are used on the FSW to provide human intent detection for the control system and to collect data for the user's force distribution patterns during sitting to standing. This FSW force distribution can show how much of the user's weight is distributed on the walker during standing and this data is collected during all neuroprosthesis operation.

The walker is retrofitted to include four total force sensing resistors (FSR) [Tekscan Inc., USA], with two FSR's in each walker handle. On each walker handle, one FSR is located at the top of the handle (forward with respect to the user) and one FSR is located at the back of the handle. By using two FSR's in each handle the walker can detect the location that the handle reaction force is being applied as well as the resultant reaction force magnitude. Two FSR's are used in each FSW handle to determine if the user's weight is distributed forwards or backward on the handle. A top down view of the right walker handle with the 3D printed handle cover removed is shown below in Figure 9.

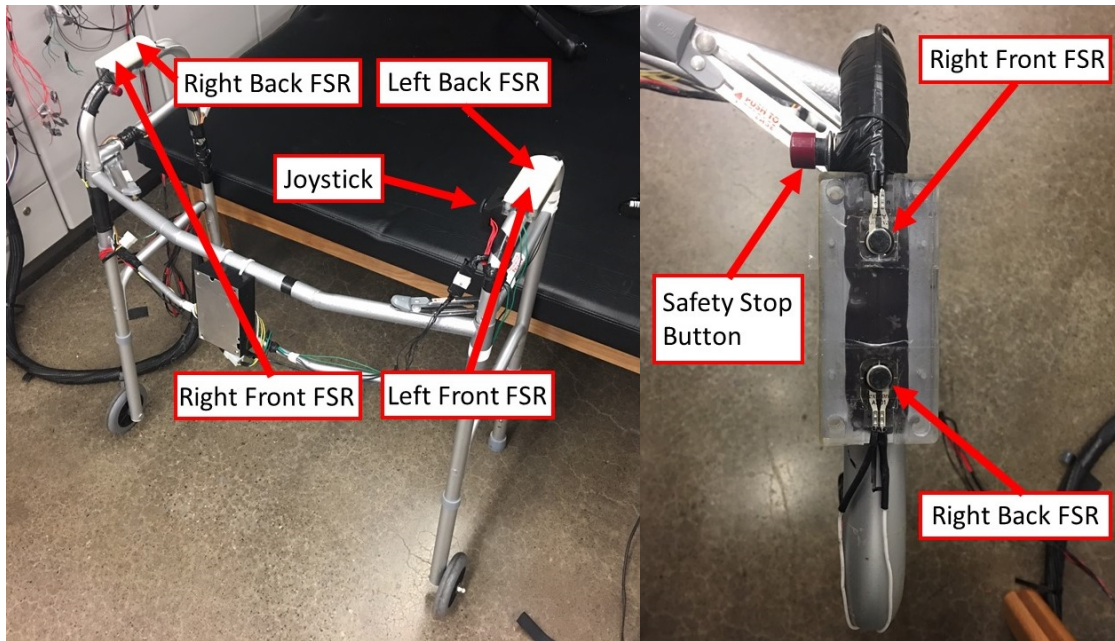


**Figure 9.** (Left) The NCRL neuroprosthesis walker showing the approximate FSR locations underneath the walker handles and (Right) right walker handle FSR placement with the walker handle omitted for clarity

The FSR's transduce applied force into a voltage signal because the electrical resistance of each FSR varies with the amount of force being applied to it<sup>[89]</sup>. A signal processing circuit is used to convert all four FSR resistance values into voltages. The feedback resistors in the circuit were selected to have resistance values of 27 kOhms so that each FSR could have a maximum force measurement of approximately 150 lbf. Since the neuroprosthesis is only designed for a maximum 200 lbm (90.7 kg) user, the force measurement range is designed to cover the user's total support weight, equal to half of their total weight, at each FSR. Figure 10 shows a schematic of the FSR PCB's.

Furthermore, FSR's need to be calibrated to provide accurate measurements for force. A calibration was performed for each of the 4 FSR's by applying 5 different loadings on each FSR with 8 trials per loading, for a total of 40 loading trials per FSR, wherein the voltage output of the FSR circuit is recorded for each loading trial. A correlation between the voltage output and

the FSR loading is obtained for each FSR. The FSR's have an accuracy of  $\pm 5\%$  of the full-scale loading, according to Tekscan Inc., equal to  $\pm 7.5$  lbf for the FSR configuration.

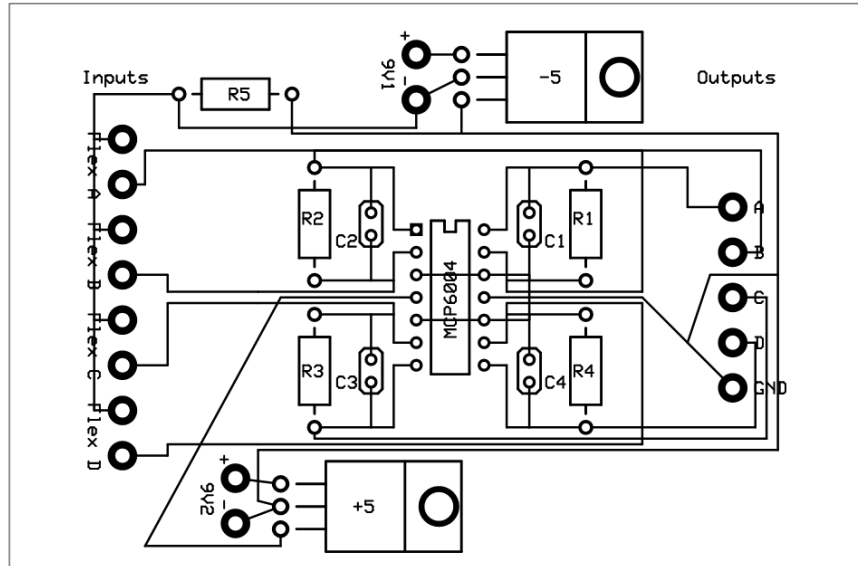


**Figure 10.** Walker FSR PCB schematic

### 3.5 JOYSTICK DESIGN AND PROGRAMMING LOGIC

The neuroprosthesis joystick is attached to the left handle of the walker, as shown in Figure 11. This joystick allows the user to control a desired effort, or input torque, into the knee motors during sitting to standing. A thumb joystick and joystick breakout PCB board [Adafruit Industries, USA] were used for this design. The joystick can measure movement in the X and Y directions simultaneously and pressing in the joystick will activate a select button functionality. See Figure 11 below for the joystick PCB circuit diagram. Only the forward direction of the

joystick, or the Y Axis, is used for the controls. A 3D printed plastic enclosure was created to protect the joystick assembly from damage.

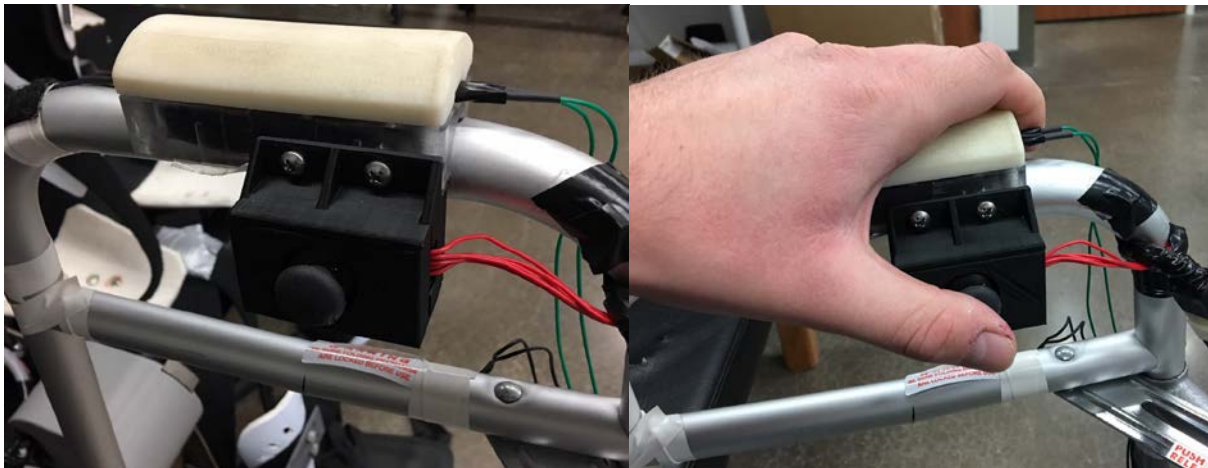
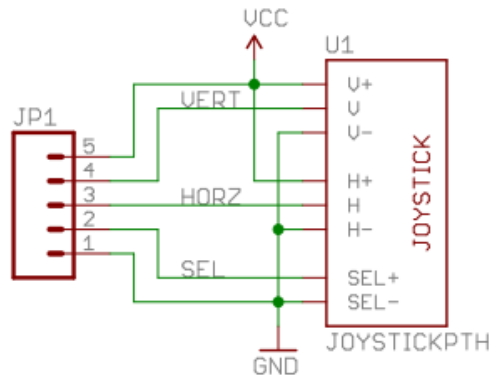


**Figure 11.** (Top) Joystick PCB schematic, (Bottom Left) neuroprosthesis walker joystick, and (Bottom Right) neuroprosthesis walker joystick with hand in place

A custom joystick logic was created in SIMULINK to convert the joystick signal into a torque signal into the right knee motor. This logic works by adjusting the torque setpoints of the knee motors based on the joystick input. For example, the user will start at a torque setpoint of 0 at the beginning of state 2 and then push forward on the joystick (away from the user) for some amount of time to linearly increase the torque setpoint to T1. Once the user lets go of the joystick

the joystick logic will stay at the torque setpoint of T1 indefinitely. If the user then pulls backwards on the joystick for an equal amount of time as they pushed forward, the torque setpoint will be reduced back down to zero. The user can then retroactively change the torque input by pushing forward or pulling back on the joystick. The user input is also constrained between zero and  $T_{\max}$ , where  $T_{\max}$  corresponds to a 5 amp torque setpoint. The user can see the torque setpoint on the XPC target display in real time during experimentation, if needed. The sensitivity of the joystick can be adjusted to move from zero to  $T_{\max}$  faster or slower.

An alternate joystick logic was also considered that had a full range joystick input instead of a setpoint adjustment. In this logic, each absolute joystick position would correspond with a discrete torque value. For instance, the torque input would be 0 at the joystick middle position and would be  $T_{\max}$  at the fully forward joystick position, and the torque values would vary linearly between the middle and fully forward positions. However, this logic was determined to be poorly suited for controlling the torque into the knees for the sitting to standing motion. If the user accidentally let go of the joystick in the middle of the motion the knee actuation will give out and they will fall back down into the seat. For a subject with both SCI and paraplegia, this could be an unsafe outcome. Additionally, the thumb joystick selected for the design does not have high resolution between the middle position and the fully forward positions and it would be very challenging for the user to maintain a specific torque value between 0 and  $T_{\max}$ . Thus, the setpoint logic was used instead.

### 3.6 NEUROPROSTHESIS SAFETY CONSIDERATIONS

Since this control model is applied to human subjects, it is of highest importance that the neuroprosthesis operation is safe and does not injure users. Some possible control designs which might be acceptable for a robotic system are ultimately unsafe for a living subject due to dangerous human-robot interaction. The neuroprosthesis incorporates several powered motors, which, if run unsafely, can cause severe injury to the user. Additionally, even if motor operation is demonstrated as being safe, incorrect system dynamics can cause the user to fall from standing. This section outlines the safety designs incorporated into the neuroprosthesis hardware and control system to protect the user from injury.

Establishing safe sitting to standing operation first begins with communicating with the experimental subjects and strictly following the Institutional Review Board (IRB) safety procedures<sup>[2]</sup>. Before experimentation, an IRB approval from the University of Pittsburgh was acquired for all subjects using the neuroprosthesis. Each subject receives a detailed explanation on how to safely operate the neuroprosthesis and what to do in case of an emergency. All human controlled interfaces available to the user were explained before experimentation. Furthermore, the control design for sitting to standing was first tested on the empty exoskeleton to demonstrate the safety of the controls methods.

The robustness of safety design is important for neuroprosthesis operation. If the neuroprosthesis only used a safety stop button, and the user did not press the safety stop button in time, an unsafe event could still occur. Therefore, the neuroprosthesis features four layers of safety:

- Safety Stop Buttons - There are two safety stop buttons that can be pressed at any time during operation to turn off all outputs from the FSM. The user has access to

a safety stop button on the right walker handle and the experiment operator also has access to an external safety stop button. If either safety stop button is pressed the safety state will be turned on and the program will disable all electric motors and the FES until the SIMULINK control program is completely restarted.

- Joint Angle Safety Stops - The FSM SIMULINK control program features programmed joint angle safety limits that only allow the motors to operate within preset angular ranges. The SIMULINK program monitors will turn on the safety state if any of the joint angle safety limits are exceeded, thereby shutting off the powered motors and FES. The hip and the knee joints are constrained so that the user can flex each joint by 30 degrees and extend each joint by 90 degrees. It is also important to ensure that right and left side knee joints do no drift apart. Therefore, an additional knee synchronization safety limit is imposed that will turn on the safety state if the knee synch error, or the angular difference between the right and left knees, exceeds 15 degrees. A detailed explanation of knee synchronization control is described in Section 4.
- A Knee Hyperextension Stop - A mechanical hyperextension stop at the knee is fabricated out of steel and physically prevents the knee from hyperextending. Calculations and testing were performed to ensure that the knee stop will not fail.
- A Body Harness - Since the neuroprosthesis will no longer be held upright by the motors once the motors are turned off, the safety stop button must be used in

coordination with the body harness. The body harness includes a fitted body harness, similar to a climbing harness, which is tethered to the ceiling along a sliding track. The sliding track is approximately 5 yards long and is rated to support the weight of the user and the exoskeleton. The safety harness is not always necessary in the case of able-bodied subjects and is typically only used for subjects with SCI.

Also note that the joint safety limits are only relative to the starting position of the user as the FSM initiates, since the neuroprosthesis motors use incremental encoders that initialize at zero degrees. Therefore, it is important for the user to begin the sitting to standing movement in the upright sitting position with their knees at 90 degree angles and with their back approximately normal to the plane of the floor. An unsafe event could still occur if the user starts in an incorrect position. Additionally, the correct user body segment length parameters must be updated in the FSM for each user. By implementing these safety features at the hardware and software levels, there is a sufficient level of redundancy in the design to keep the user safe during the sitting to standing motion.

### **3.7 FUTURE DESIGN CONSIDERATIONS**

Future design changes will need to be made to the NCRL neuroprosthesis to provide improved utility to people with SCI. Firstly, the neuroprosthesis hip brace will need to be redesigned to improve ergonomics and HMI<sup>[75]</sup>. At present, the hip brace only attaches to the user's waist using a belt strap and the brace regularly slips down on the user's waist. The hip can become disjointed

with the user's body and this causes encoder reading inaccuracies. The hip brace also shows deflection due to torsion in the brace, which adds a deflectional angular inaccuracy during an assisted gait. An improved hip brace is currently being designed by the NCRL and fabricated for enhanced structural rigidity and a better attachment to the user.

A second possible improvement in the neuroprosthesis design is to provide actuation at the ankle joint. Ankle actuation allow the implementation of a 3-link model in the controls. Adding actuation to the ankle joint would allow the neuroprosthesis to follow a more natural movement for an assisted gait cycle. All assisted gait experiments performed by the NCRL thus far have featured an exaggerated gait step to clear the user's foot above the ground and counteract the inability to actuate the ankle joint<sup>[20]</sup>. Also, previous research has been done with the addition of ankle actuation to combat drop step caused by stroke<sup>[8,21]</sup>, and there is a potential for expansion of the NCRL neuroprosthesis functionality so that it can also rehabilitate stroke patients.

However, several major challenges exist in adding actuation to the ankle joint. Most current ankle actuation methods fall into 3 categories, based on current technology: FES actuation, electric motor actuation, and hydraulic actuation. Each of these 3 actuation methods has significant disadvantages. Hydraulic actuators at the ankle are incredibly heavy and take up an impractical amount of space. An electric knee motor at the ankle is typically less bulky than an actuator, but is still heavy and typically produces less torque than hydraulics.

One long term goal of the NCRL is to have a mobile neuroprosthesis that is detached from a computer station. All active orthoses analyzed in Chapter 2 are detached from a workstation. A mobile neuroprosthesis is advantageous because it makes it much easier the user to perform therapy at a home setting<sup>[56]</sup> and it could allow for outdoor mobility. A new compact

computer to run the controller and the motor drivers would need to be mounted to the exoskeleton. These components could be mounted in configuration similar to the HAL orthosis<sup>[14]</sup>. A second, more ideal option, would be to mount these components to the walker in configuration like the EXPOS orthosis to reduce the weight of the neuroprosthesis<sup>[51]</sup>. Any mounting configuration would need to be sufficiently protected from the environment and from falls. Perhaps the most challenging aspect of neuroprosthesis mobilization is that the system design would need to be finalized before mobilization, making new research design impractical.

## **4.0 CONTROL SYSTEM DESIGN FOR STANDING**

This section describes in detail the control system designed to perform hybrid sitting to standing and how it was developed.

### **4.1 CONTROL SYSTEM OVERVIEW**

The hybrid standing control system combines multiple controllers into an FSM. From the dynamical analyses of the standing up motion in able-bodied subjects, the knees are primarily used to move the user's center of mass at the torso upwards in the vertical direction<sup>[4]</sup>. Therefore, the knee control is used to move the person upwards. The ankles and the hip are both used to manipulate the subject's ZMP at the feet. This control model does not actuate the ankle joints and the ankle joints are locked during the movement. The hip control is used to actively guide the user's torso so that they can stabilize themselves during sitting to standing.

First, the user is leaned forward in the sitting position so that more of their center of mass is moved closer to the feet in the horizontal direction of the user's sagittal plane. This has been shown to decrease the overall torque requirement from the knees during sitting to standing by a small amount<sup>[4]</sup> and is in concordance with the movement observed in natural sitting to standing. This movement uses a tracking controller to move the user's torso into a forward leaning position while they are still sitting, and it is described in Section 4.3.

When the user wants to stand up they control the torque input going into the right knee motor using the joystick. The same user command cannot be sent to both the left and right knee motors because this would cause a drift error between the left and right legs, due to slight differences in motor impedances and any asymmetry of the human body. A customized feedback controller is designed to synchronize the left leg with the right leg during the movement.

Simultaneously during standing up, the FES stimulator is applying an open loop constant transcutaneous stimulation to the user's quadriceps muscles, based on the status of the user input. This stimulation is stopped when full standing has been achieved. This stimulation is meant to decrease the torque requirements of the knee motors, in addition to actualizing the physical benefits of FES.

During standing up, end effector tracking is employed so that the user's end effector, defined as a point at approximately at the top of the sternum, is guided along a predefined linear trajectory from a point at sitting to the final position at standing. By controlling the movement of the hip motors and thereby guiding the position of the torso, the user can properly balance themselves using the walker handles and they are guided into a standing-up motion. The desired hip angles are generated using a predefined EE linear trajectory.

Finally, once the full standing position has been achieved, the control program keeps the user standing for an arbitrarily long duration of time. A locking "virtual clutch" (VC) feedback controller was designed to lock the knees at the top of the standing movement. This controller is designed to emulate a WSC mechanical lock at the knees. This eliminates bulky hardware at the neuroprosthesis knee.

The neuroprosthesis ties all 4 controllers together using the FSM: the forward leaning controller, the left leg synchronization controller, the hip EE controller, and the knee locking VC

controller. The FSM determines the activation sequencing between the controllers based on the user intention. A control diagram showing the user knee control and the EE control, enacted in the standing up state of the FSM, is shown below in Figure 12.

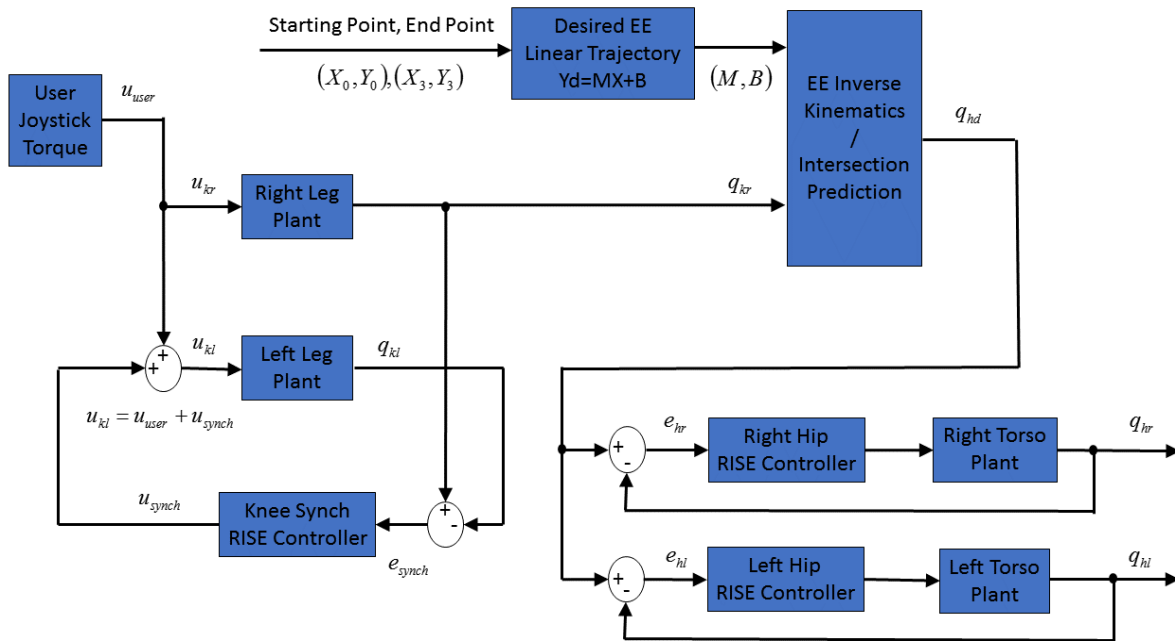


**Figure 12.** Controller schematic for the knee synchronization controller and the end effector controller during standing up in state 2 of the FSM

#### 4.1.1 Expected Advantages and Disadvantages of the Control System

This sitting to standing control system has been designed to have several expected advantages. Firstly, the control system is designed to perform sitting to standing with virtually any subject using only visually obtained user data with no integration of the underlying user dynamics or muscle parameters, thus providing simplicity in design and universality in application. Secondly,

the control system is expected to allow the user to directly control the sitting to standing motion by using a joystick, while also employing intent detection. Lastly, the control system is expected to provide the physical benefits and energy reduction of FES.

The control system is also expected to have several disadvantages. Firstly, the relative simplicity of the model means that the controls cannot adapt to the user's muscular capabilities and the performance is limited to the feedback control system. Additionally, the application of FES can fatigue the user's muscles<sup>[57]</sup>.

## 4.2 FINITE STATE MACHINE

The sitting to standing SIMULINK program uses an FSM to transition between movement events. Rather than having an FSM where the next state is triggered by a pushbutton, transition between states is completely automated based on user intention. Automated FSM state transitions are designed to reduce the amount of multitasking that the user needs to perform to achieve standing. Figure 13 below shows a diagram of the FSM state progression.

In state 0, the neuroprosthesis is in a sitting position without any inputs being sent to the motors. This state is a transitional state where the user can take as much time as they need to prepare for the standing up motion. Once the user is ready to stand up they will place both of their hands on each of the FSW handles. If both walker handles have a resultant force that exceeds the force threshold of 5 lbf vertically applied downward, this will trigger state 1 initiation and move the FSM into state 1.

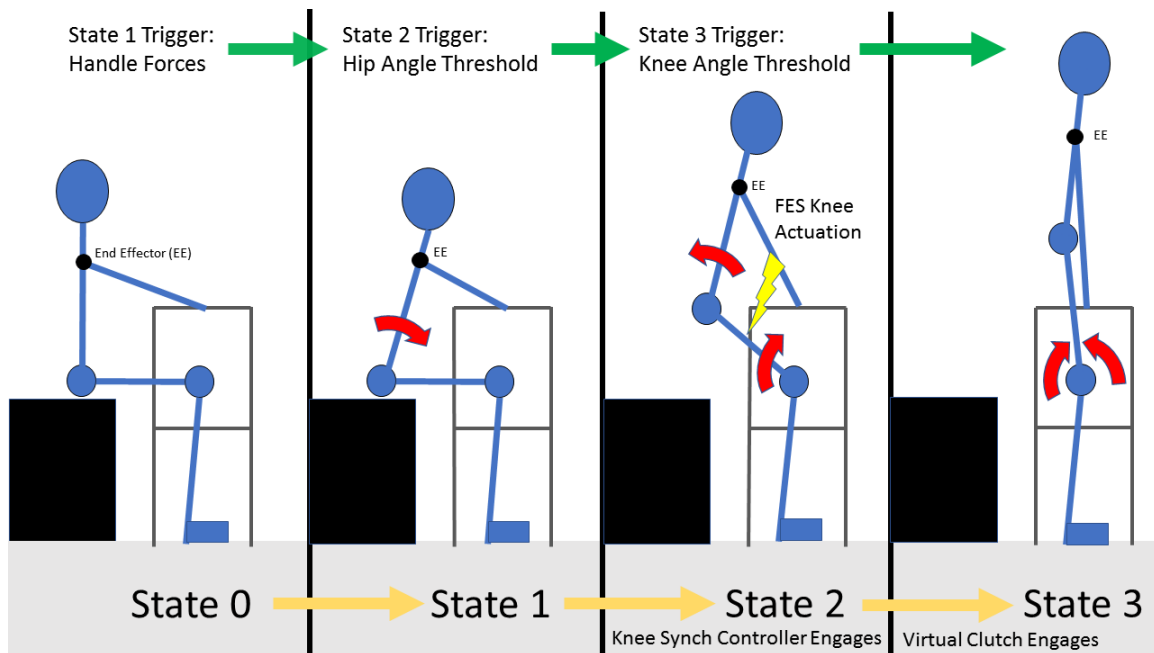


**Figure 13.** Finite state machine progression and user intention triggers

In state 1 the neuroprosthesis guides the user into a leaning forward position. In this state, only the hip motors are actuated and there is no input into the knee motors. The user is guided into a forward leaning position so that the subject's center of mass is closer to the knees and they can support their weight using the walker handles. The hip motors lean the torso forward 15 degrees in 2 seconds. Once both hip motors have reached the set value, within a preset margin of error, this will trigger state 2 initiation and move the FSM into state 2.

In state 2, the standing-up movement is performed based on the user input at the joystick. The right knee motor torque will increase or decrease based on the user input and the left knee will synchronize to the angular position of the left knee by using the synchronization (synch) controller, detailed in Section 4.4. The hip motors will adjust position to control the trajectory of the EE. Once the user stands up and the right knee has reached a predefined setpoint, equal to 75

degrees in extension for this program, initiation event 3 is triggered and the FSM will move into state 3.

In state 3 the FSM will indefinitely hold the user in the upright standing position. Once state 3 begins, the VC, or a controller used to lock the knee detailed in Section 4.5, is engaged. The VC will keep each knee locked at their angular positions at the beginning of state 3. Once the user wants to end the standing experiment, the safety stop button is pressed and the user is then lowered back onto their seat.

One possible pitfall of this automated FSM interface is that there is nothing constraining the neuroprosthesis to move from state 0 to state 3 in a consecutive order, since the FSM does not have built in state memory. This situation is unlikely, but it could occur during improper use of the control system or during sensor malfunction. To address this, an auxiliary safety signal was created to detect if the FSM moves between states in the correct order. If the states transition incorrectly the auxiliary safety switch will turn on the safety stop.

### **4.3 STATE 1 – FORWARD LEANING CONTROLLER**

Immediately after the FSM is initiated the controller transitions into state 0, a null sitting state. Once the user activates the FSW user intention and the FSM shifts into state 1, two RISE tracking controllers<sup>[20,45,79]</sup> are used to track the hip motors and torso into the forward leaning position. These RISE controllers are also used in the hip controller described in section 4.6. A single smooth trajectory is used to track the hip motors and the torso from upright sitting at a torso angle of 0 degrees to forward leaning at an angle of 15 degrees.

One problem encountered with the application of this controller was observed in testing, where the knee motors would rapidly jerk at the start of state 1. This problem was attributed to the operation of the optical encoders at the hip. Since the optical encoders initialize at 0 degrees at the beginning of the program, the user will inevitably move the hip motors into some position slightly in front of or behind zero degrees. Thus, as the forward leaning controller starts to track the hip angles it will detect a starting error and rapidly jerk the hips into the tracking trajectory. This was found to cause user discomfort and a loss of user confidence in the control methods.

To solve this problem, the tracking curve was adjusted to adapt to the user's initial movement. Rather than tracking from 0 degrees to the forward lean angle, the angle at the beginning of state 1 was saved and the controller generated a smooth tracking curve from this angle to the forward lean angle. This adjustment improved the controller jerking. Additionally, the maximum controller input was decreased so that the hip motors did not have enough torque output to produce a powerful hip jerking motion.

#### **4.4 STATE 2 – KNEE SYNCHRONIZATION CONTROLLER**

The user is instructed to generate a control input by using the thumb joystick on the FSW during state 2 of the FSM. This will directly determine the input going into the right knee motor and the right knee torque output. This knee motor input is constrained between zero and a maximum allowable input, set at 5 amps, for the right knee motor. The user control only allows the right knee in the direction of extension. A controller is required so that both legs move synchronously in standing.

#### 4.4.1 Motivation for a Synchronization Controller

An identical input sent to both motors will produce slightly different gearmotor responses. This inconsistency is partly due to innate EC motor performance variance and mechanical resistance in the harmonic gears. This effect was also verified beforehand in the NCRL; it was observed that maintaining the same angular velocity limit in both motors required a larger input into the left knee motor. In practice, these mechanical resistances can be reduced but not eliminated.

Secondly, the standing dynamics of the user are not always consistent. The position and orientation of the user's center of mass in 3-dimensional space will influence the movement of the legs during sitting to standing. For instance, if the user's weight is shifted to the right side of the body then the right knee motor will require a higher torque.

Lastly, in the case of perfectly symmetrical user positioning, the weigh distribution of the user and the neuroprosthesis are not necessarily symmetrical about the sagittal plane. Partial SCI can cause the user's body to develop asymmetrical lower-limb bone mineral density (BMD) loss<sup>[55]</sup>. Regardless of this fact, the internal organs of the human body are not symmetrical about the sagittal plane. Thus, an identical motor input into both legs will not always produce identical movement for sitting to standing.

Asymmetrical movement in the right and left legs during sitting to standing can create unsafe situations, and therefore it is important to maintain this symmetry. The right knee input, as described earlier, is controlled directly by the user. Therefore, a left knee tracking controller, or synch controller, is employed to ensure that the left leg moves synchronously with the user-controlled right leg during the sitting to standing motion.

#### 4.4.2 Final Controller Design

In the controller, the joint angle of the left knee tracks the joint angle of the right knee. The error for the tracking controller is defined as the difference between the right knee angle and the left knee angle. It follows that the control input will be calculated from the knee error, with a control input of zero corresponding to an error of zero.

During standing the maximum torque requirement occurs at the beginning of standing in state 2, when the user's torso is about to leave the seat<sup>[4]</sup>. What this means is that the controller error could be zero at the beginning of sitting to standing when the torque requirements are at their maximum. This creates an undesirable situation where the user generated input is being sent to the right knee with zero input into the left knee. The neuroprosthesis is not designed to perform standing with only one motor. Therefore, the synch controller needs to generate the maximum torque in the right and left knee motors at the beginning of standing in state 2.

The synch controller uses a linear variable offset to the left knee input that is set equal to the user-generated input torque. In other words, the user generated torque is sent to both knees and the controller generates a compensation term used to track, or synchronize, the left knee angle to the same angle as the right knee angle. The intended advantage of this tracking control method is that it actualizes the maximum knee torque capacity at a tracking error of zero. The same RISE controller model used in the forward leaning control and the hip motor control<sup>[20,45,79]</sup> is used for synchronization. An equation for the left knee input is shown below:

$$U_{KL} = U_{user} + U_{synch}$$
$$U_{synch} = K \left( \dot{e}_{synch} + \alpha_1 e_{synch} + \alpha_2 \int_0^t e_{synch} d\tau + \beta \operatorname{sgn}(\dot{e}_{synch} + \alpha_1 e_{synch}) \right)$$

where  $U_{KL}$  is the total control input into the left knee motor in amps,  $U_{user}$  is the user generated input into the right knee motor in amps,  $U_{synch}$  is the controller synchronization term used to track the left knee angle in amps,  $e_{synch}$  is the synchronization error, defined as the difference between the right knee angle and the left knee angle,  $K$  is a derivative controller gain,  $\alpha_1$  is a proportional controller gain,  $\alpha_2$  is an integral controller gain, and  $\beta$  is a sign controller gain. The gains for all state controllers, including state 2, is shown in Table 1.

**Table 1.** Controller gains for states 1-3

Controller	Alpha 1	Alpha 2	Beta	K	Kp	Kd
State 1 - Hip Leaning	175	200	0.01	0.01		
State 2 - Left Knee Synch	350	400	0.01	0.01		
State 3 - Knee Locking			0.0001		100	0.3
State 2/3 - Hip EE Tracking	175	200	0.01	0.01		

Additionally, following safety limitations are established within SIMULINK:

$$-15^\circ < e_{synch} < 15^\circ, \quad -30^\circ < q_k < 75^\circ$$

where  $q_k$  is the angle of the knees. As mentioned earlier, the right knee motor can be driven in the direction of extension by the user input, but not in the direction of flexion. The left knee motor can be driven in both extension and flexion by the synch control and is set to run at a faster maximum angular speed than the right leg so that it can stabilize the movement.

The thumb logic constrains the user generated control input to the following linear piecewise function:

$$U_{user}(t) = Kt + A \quad \text{when the thumb joystick is pressed forward}$$

$$U_{user}(t) = C \quad \text{when the thumb joystick is not pressed}$$

$$U_{user}(t) = -Kt + B \quad \text{when the thumb joystick is pressed backwards}$$

$$\text{with } 0 \leq U_{user}(t) \leq 5 \text{ for all } T_{S2} \leq t \leq T_{S3}$$

where K is an adjustable joystick sensitivity constant manually set in in the SIMULINK FSM, A is the user U-intercept of the linear function when the joystick is pressed forward, B is the user U-intercept of the linear function when the joystick is pressed backwards, C is a constant input value when the thumb joystick is not pressed,  $T_{S2}$  is the time at the start of state 2 of the FSM, and  $T_{S3}$  is the time at the start of state 3 of the FSM. The linear constants A, B, and C will change with each forward press of the joystick. This function is continuous over all time values in state 2 of the FSM. A synch controller safety limit of 15 degrees is implemented to prevent any problems in the controller from creating an unsafe event in experimentation.

#### **4.5 STATE 3 - KNEE LOCKING CONTROLLER**

In the knee assembly mechanical design, it was determined that a mechanical locking mechanism at the knee would be physically burdensome. All practical configurations of such a mechanism would make the knee assembly excessively complex and large when combined with the selected motor and harmonic gear. However, the FSM functionality in state 3 still requires the knee to be locked at the end of standing. To address this issue the VC locking controller logic was integrated into the control program. The VC is designed to perform as if it were a mechanical locking mechanism at the knee.

The VC uses a simple PD controller, with a term to compensate for the sign of the error, to lock the angular position of the knee. A binary signal is used to turn on and off the VC and

this can be done at any time. Once the VC is turned on the logic stores the values of the knee angles at the discrete time that the clutch is turned on. These values are used as the desired angular position for the knees in the PD controller. The equation for the control input for the PD controller is shown below:

$$U_{VC} = K_p e_k + K_d \dot{e}_k + \beta \text{sgn}(e_k)$$

where  $U_{VC}$  is the control input into the knee motors,  $e_k$  is the knee motor error, defined as the difference between the measured knee angle and the desired knee angle,  $K_p$  is the proportional control gain,  $K_d$  is the derivative control gain, and  $\beta$  is the sign gain. The gains for state 3 are listed in Table 1. A PD controller was determined to be more appropriate than a PID controller for this application because the integral term adds an unnecessary level of complexity to the controller for the relatively simple task of locking the knees. This locking controller does not need to compensate for the time memory component of the error and preliminary testing using a PID controller was prone to error in situations with an accumulated integral error.

Higher gains were used for this controller in comparison to other FSM controllers to create a stiff locking mechanism. To test this controller, the motors were run at full speed (7.5 RPM at the gearmotor output) in an empty neuroprosthesis and the VC was then engaged. The controller gains were tuned such that the knees locked with less than a 3-degree overshoot error in the knees for full speed locking.

## 4.6 END EFFECTOR TRACKING CONTROL

During the state 2 control in the FSM, the hip motors track the user's end effector (EE) along a predefined trajectory. The user's EE is chosen as the point at the top of the user's sternum between the shoulder sockets. This point is chosen for the EE because it is a point directly between the glenohumeral joints, and the user's arms are used to manipulate and stabilize their upper body with the FSW. Tracking the trajectory of the user's EE along a predefined trajectory assures that the sitting to standing movement is natural and moves the user in such a way that they can stabilize themselves with the FSW. The EE tracking is based completely on spatial kinematics and does not require the physical dynamics of the system.

It is important to note that the end effector tracking used in this controller is different than classical end effector control. In classical end effector tracking control, the Euler-Lagrange dynamics of the system are established and are written in the following form:

$$M(q)\ddot{q} + C(q, \dot{q})\dot{q} + Dq + G(q) = \tau$$

where  $M(q)$  is the inertial matrix,  $C(q, \dot{q})$  is the Coriolis matrix,  $D$  is the joint friction matrix,  $G(q)$  is the gravitational matrix,  $\tau$  is the joint torque matrix, and  $q$  is the joint variable<sup>[84]</sup>. In this model, the joint trajectories are also typically determined by either a cubic or quartic polynomial, where starting and ending conditions for the position, velocity, and higher polynomial derivatives are used to define the exact equation for the polynomial<sup>[84]</sup>. A cost function also typically defines an optimal trajectory and velocity profile<sup>[84]</sup>. The reason that this more common end effector control is not employed is because it could conflict with the user's control input. With classical end effector control the final speed of the motion would need to be pre-determined, whereas this final speed must be controlled by the user so that they have full

control of the motion. Additionally, the exact EE trajectory determined by the cost function may not produce a comfortable or stable standing up motion for the user. Since user control and natural motion were top priorities for the control, a trajectory-based end effector tracking control was employed over traditional end effector control. The method used ensures that the hip motors track the end effector along a predefined trajectory that is comfortable and stable for the user.

The forward kinematics of the system are determined to establish tracking. The kinematics are analyzed from a 2D cartesian coordinate reference frame, where the neuroprosthesis sagittal plane represents the XY plane and the origin is located at the center of the knee motor, with the positive x-direction being oriented towards the front of the neuroprosthesis and the positive Y direction being oriented towards the ceiling. The dynamics are analyzed from a 2-dimensional perspective, similar to the 1 leg model proposed by Donaldson and Yu<sup>[23]</sup>, where both legs are assumed to behave synchronously as one link. The neuroprosthesis is designed as a 2-link robotic manipulator, shown in Figure 14, where the thigh is the first link and the torso is the second link. The system can be modeled as a 2-link manipulator rather than a 3-link manipulator because the origin, or the point of the knee, is held relatively stationary during the movement, since the ankles are locked.

For this 2-link kinematic model, the location of the EE can be uniquely determined based on the angles of the knee and hip angles. Inversely, each point in the robotic workspace corresponds to a unique set of joint angles in the exoskeleton. The robotic workspace is defined as an annulus with the following dimensions:

$$R_o = L_1 + L_2, \quad R_i = \begin{cases} L_1 - L_2, & L_1 < L_2 \\ 0, & L_2 \geq L_1 \end{cases}$$

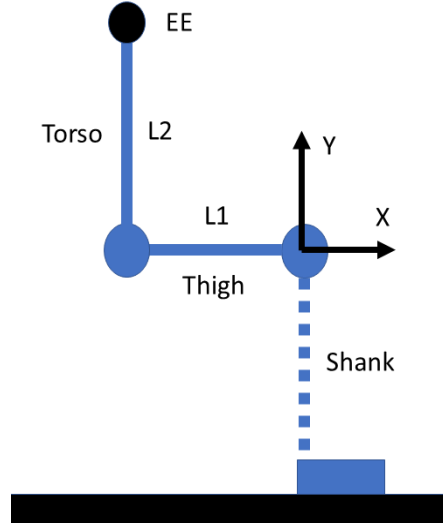


**Figure 14.** End effector local coordinate frame

where  $R_o$  is the outer annulus radius and  $R_i$  is the inner annulus radius. Thus, the predefined EE trajectory must fall completely within the robotic workspace, or a logic error will be created in the controls. The forward kinematics of a 2-link manipulator are given by the following equations:

$$X_{EE} = L_1 C_1 + L_2 C_{12}$$

$$Y_{EE} = L_1 S_1 + L_2 S_{12}$$

$$C_{12} = \cos(q_1 + q_2), S_{12} = \sin(q_1 + q_2)$$

with initial position at sitting  $(-L_1, L_2)$ , where  $X_{EE}$  and  $Y_{EE}$  are the x and y positions of the EE, respectively<sup>[65]</sup>. The predefined EE trajectory is chosen as a linear trajectory. The equation for the desired EE can be expressed in the following simple algebraic form:

$$X_{EE,d} = \frac{1}{M}(Y_{EE} - \beta)$$

where  $X_{EE,d}$  is the desired x-position of the EE,  $Y_{EE}$  is the current y-position of the EE,  $M$  is the line slope, and  $\beta$  is the y-intercept. A linear trajectory was selected versus a curve trajectory based on the results of EE tracking experiments performed by the NCRL. In these experiments, one able-bodied user was instructed to stand up with a configuration of the NCRL hybrid neuroprosthesis attached to them, which was used to measure the angles of the joints and the location of the EE during sitting to standing. These experiments showed that the trajectory of the EE was roughly a linear. This result does not show conclusive statistic evidence of a linear EE relationship for standing, however a linear trajectory was deemed to be a starting point for the controls model. This linear trajectory is calculated based on the initial and final positions of the user's EE. The initial position is defined as the EE position at the end of the state 1 forward leaning control. The final position is defined as the position where the knees reach the state 3 knee angle threshold, with the final x-position always held at zero above the knees. Additionally, a SIMULINK script within the control system was created to update this linear trajectory equation based on the user's body measurements. The SIMULINK control system generates desired hip angle  $q_{h,d}$  from the predefined EE trajectory and the EE kinematics.

A custom algorithm, using discrete mathematics, was used to calculate the inverse kinematics and desired hip angles. A predicted hip angle is calculated based on where the hip angle needs to be. In this algorithm, the knee angle is assumed to be controlled by the user input. The position of the hip joint is then calculated using basic trigonometry. The desired position of the EE is calculated by the intersection of the circular EE path of the torso link and the predefined EE trajectory, and an illustration of this kinematic model is shown in Figure 15.

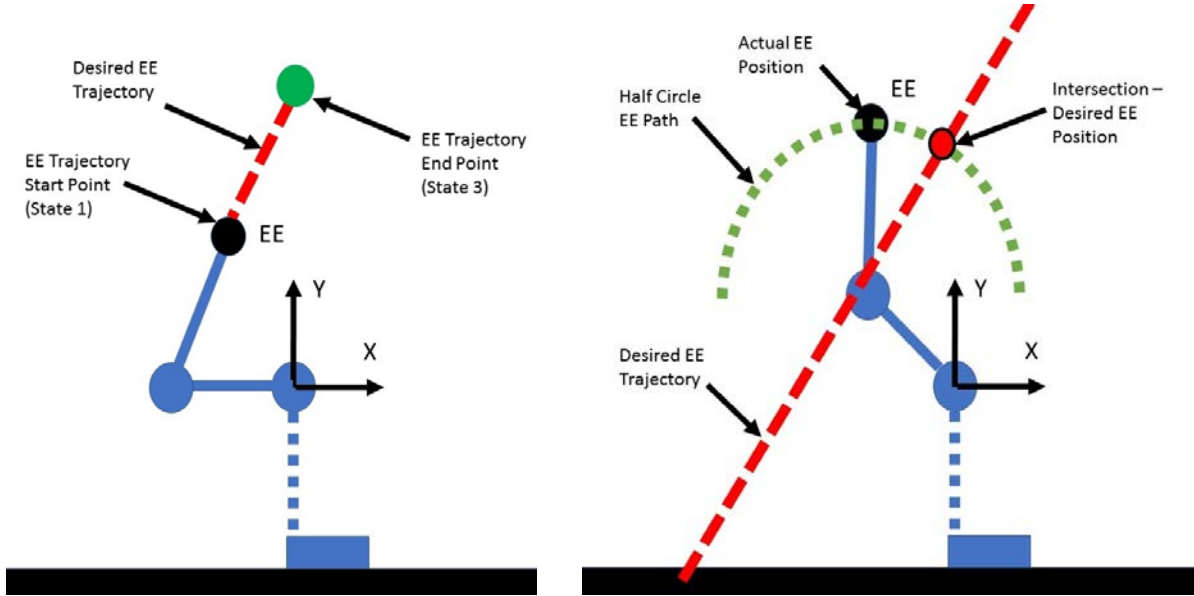


**Figure 15.** (Left) The end effector start point, at the end of state 1, and end point, at the beginning of state 3, and (Right) a diagram of the desired end effector position algorithm. The algorithm uses the intersection of the desired end effector trajectory and the torso link half circle end effector path to generate desired hip angles.

The equation of the torso link path is given by the half-circle implicit equation:

$$(X_{EE} - X_h)^2 + (Y_{EE} - Y_h)^2 = L_2^2$$

where  $X_h$  is the x-position of the hip joint and  $Y_h$  is the y-position of the hip joint. The linear desired EE trajectory can then be inserted into the equation above for  $Y_{EE}$  in terms of  $X_{EE}$  and grouped into the following quadratic form:

$$AX_{EE,d}^2 + BX_{EE,d} + C = 0$$

Solving the quadratic equation for  $X_{EE,d}$  yields:

$$X_{EE,d} = \frac{-B \pm \sqrt{B^2 - 4AC}}{2A}$$

$$\text{where } A = [M^2 + 1],$$

$$B = [2M\beta - 2X_h - 2MY_h],$$

$$C = [X_h^2 + Y_h^2 - 2\beta Y_h + \beta^2 - L_2^2]$$

Since there are two intersection points between the desired EE trajectory and the circular torso EE path, only the most positive x solution is used, and the other solution is discarded. The location of  $X_{EE,d}$  is used to compute  $Y_{EE,d}$  and  $q_{h,d}$  in real time and track the hip motors along the desired linear EE trajectory. This method was found to smoothly control the position of the torso in the controls. This method is not foolproof and has several requirements: the desired EE trajectory must be a straight line, and it must always be within the range of the torso link. If these conditions are not met it could cause a dangerous malfunction in the controls.

All EE kinematic calculations for this algorithm are based on the angular position of the right knee. Only the right knee angle is used, as opposed to an average of both knee angles, to add resiliency to the performance. If the left knee synch controller were to fail, and the EE kinematics were reliant on the left knee angle, this failure would propagate to the hip control as well. By calculating the desired hip angles with only the right knee angle signals, the hip controller works independently to all other automated controllers in the neuroprosthesis.

Once the desired hip angles are generated, two RISE controllers are used to track the angles of the hip joints<sup>[20,45,79]</sup>. A RISE controller is essentially a PID controller with an additional term added that is based on the integral of the signum of the error. The hip error is defined as the difference between the measured hip angles and the desired hip angles. The same desired hip angle and control input is sent to both motors, however there are two separate controllers for both hip motors in the SIMULINK programming. The control input into the hip motor can be represented by the following equation:

$$U_h = K \left( \dot{e}_h + \alpha_1 e_h + \alpha_2 \int_0^t e_h d\tau + \beta \operatorname{sgn}(\dot{e}_h + \alpha_1 e_h) \right)$$

where  $U_h$  is the control input into the hip motor,  $e_h$  is the hip joint angular error, defined as the difference between the measured hip joint angle and the desired hip joint angle,  $K$  is a derivative controller gain,  $\alpha_1$  is a proportional controller gain,  $\alpha_2$  is an integral controller gain, and  $\beta$  is a signum controller gain. The gains for the EE RISE controllers are listed in Table 1. These gain values for the hip control were chosen based on previous experiments demonstrating a delay compensating controller for assisted walking<sup>[20]</sup>. It was later observed that the hip control had the potential to be too powerful for EE guidance. The assisted walking hip controller was designed to fully manipulate the weight of the legs in this previous hip control method, whereas in this control the maximum hip torque requirement is lower. The gains  $\alpha_1$  and  $\alpha_2$  were chosen to be half of their values for the assisted walking experiments to lessen the response of the overall controller. Additionally, an output saturation threshold was applied to the hip motors to reduce their torque capacity, for safety reasons.

## **5.0 EXPERIMENTAL RESULTS**

This section reviews and analyzes the experiments performed to test neuroprosthesis standing on able-bodied subjects and subjects with SCI. The performance of the mechatronic design detailed in Section 3 and the performance of the control system design detailed in Section 4 are both evaluated in this section.

### **5.1 EXPERIMENTAL SETUP**

Experiments were performed with human subjects to test the functionality and performance of the sitting to standing control system. Able-bodied subject B1 is a 25-year-old male weighing about 185 lbs with no previous history of SCI. Subject with SCI A4 is a 44-year-old male weighing roughly 190 lbs with partial SCI at the T10 level.

Three separate experiments were performed on three separate days. In the first experiment, able-bodied subject B1 performed sitting to standing without FES stimulation. For the second experiment, able-bodied subject B1 performed sitting to standing with FES stimulation. For the third and fourth experiments, subject with SCI A4 performed sitting to standing with and without FES stimulation. Additionally, the power and energy consumption data for the knee motors was collected during experimentation and is analyzed at the end of this section.

During the experimentation, the proper Internal Review Board (IRB) documentation was completed for all subjects<sup>[2]</sup>. Subjects completed IRB consent forms before experimentation. IRB experiment documentation was completed during each experiment to document the user condition and FES safety, along with other data. Additionally, before any experiments were performed on human beings, the controls system was tested on the empty neuroprosthesis to perform sitting to standing. No unsafe conditions or malfunctions were observed in the control system.

For the first experiment, the able-bodied subject B1 was first educated on how to control standing. The subject donned the exoskeleton and the exoskeleton was adjusted to fit them. The subject's thigh (L1 equal to 16.5 in) and torso (L2 equal to 21 in) lengths were measured while they were in the sitting position. The subject was instructed to begin the experiment in the upright sitting position with their knees at 90-degree angles and their leg shanks normal to the plane of the floor. No FES was used during sitting to standing. The maximum right knee motor speed was set at 750 RPM and the maximum left knee motor speed was set at 1000 RPM in the driver configurations. The FSW was supported at the base to firmly secure it to the ground. The subject performed the sitting standing for 5 successful trials and data was recorded in SIMULINK during experimentation.

For the second experiment, subject B1 again donned the neuroprosthesis. Previous values recorded for L1 and L2 were used. FES was used, and two stimulator pads were attached to the skin above each of the user's quadriceps. The subject was instructed to begin the experiment in the upright sitting position with their knees at 90-degree angles and their leg shanks normal to the plane of the floor. The maximum right knee motor speed was set at 500 RPM and the maximum left knee motor speed was set at 750 RPM in the driver configurations. The subject's

skin condition at the thighs was documented before and after the experiment. A total of 3 trials at each of two stimulation intensities were performed, for a total of six trials.

For the third and fourth experiments, subject with SCI A4 was first educated on how to control standing. The subject donned the exoskeleton and the exoskeleton was adjusted to fit them. The subject's thigh (L1 equal to 17 in) and torso (L2 equal to 21 in) lengths were measured while they were in the sitting position. The subject was told when the control program was started and performed the sitting standing for 5 trials without FES and 4 trials with FES. Six FES trials were planned, but the experiment was reduced to 4 trials due to bending in the neuroprosthesis frame. This bending was caused by unexpectedly high torsional loads on the shank frames.

## **5.2 EXPERIMENT 1 - DEMONSTRATION OF STANDING WITH MOTORS ONLY IN AN ABLE-BODIED SUBJECT**

Able-bodied subject B1 successfully performed 5 trials of standing with motors only. For analysis, the data from trial 5 of the experiment will be used in the discussion of control system performance. Since the control system continued to collect data after standing had been achieved, the data discussed in this section has been abridged to only include all data up until 2 seconds after full standing in state 3 has been achieved by the FSM. Figure 16 shows screen captures of the user as they transition between FSM states in trial 5 of the experiment. The EE tracking smoothly guided the user's torso above the walker during standing. No discomfort was reported by the user. The largest problem observed was that the state 1 controller had a jerky start, but this problem was addressed for all subsequent experiments.

Figure 17 shows the knee angles versus time in trial 5 during standing. The graph shows that the left knee joint angle closely follows the right knee joint angle and that the synch controller in state 2 of the FSM works successfully. Both knees lock at nearly 75 degrees, the knee angle set to trigger the transition into state 3 of the FSM. There is a small overshoot of about 1 degree in both knees at the beginning of state 3 after the knees are locked. Also, the right and left knees are seen to lock at slightly different angles. This occurs because the state 3 progression is triggered by the both knee angles and the VC is set to track the knee angle to the angle of the knee at the beginning of the VC engagement.

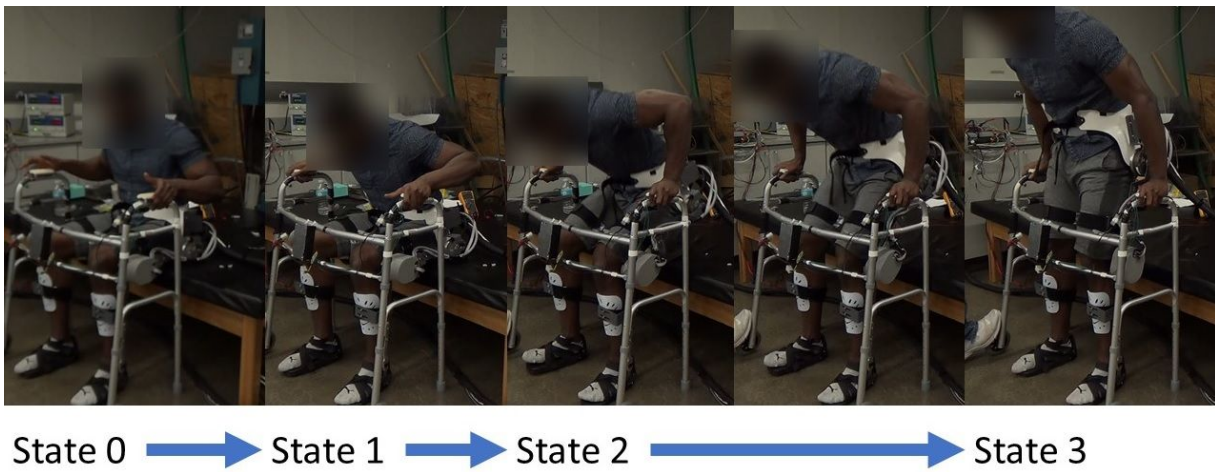


**Figure 16.** A sequence of frames from the footage taken during trial 5 of the standing experiment

To standardize the analysis, the synch error is only evaluated in the period of state 2 after the user has initiated the knee torque using the thumb joystick. If state 2 is delayed due to user hesitation, this will artificially decrease the overall RMS error measured in state 2 because the synch error will be zero for all sampling times before the movement begins. The graph of the synch error versus time in Figure 18 shows that the synch error, calculated during the user initiated section of state 2, is held below an absolute maximum of 0.89 degrees during sitting to

standing with an RMS error of 0.44 degrees. This indicated better than satisfactory controller performance and it is not expected that a human user would be able to detect any synch error.

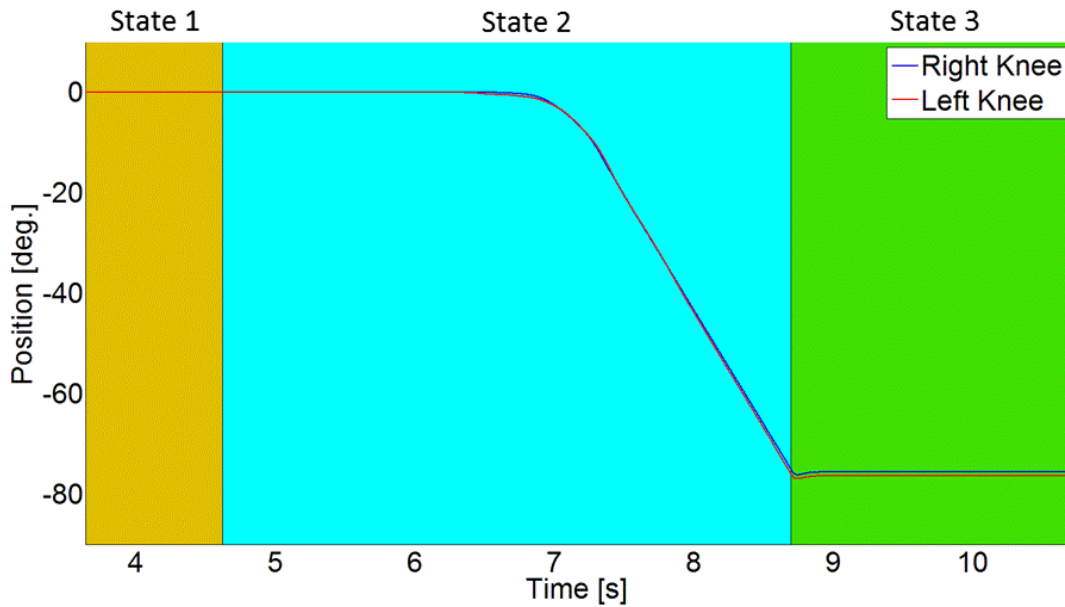


**Figure 17.** Knee angles versus time for trial 5 of the standing experiment

A graph of the calculated EE trajectory during the experiment is shown in Figure 19. The EE tracking successfully guides the position of the EE along the predefined linear trajectory specified in the controls. The hips first lean the torso forward by 15 degrees and then adjust to keep the EE along the path of the linear trajectory. The main discrepancy in the EE trajectory is that the EE position is lower than desired at the beginning of standing. The cause for this error is unknown, but it may indicate the presence of undesirable HMI or an imperfect tracking trajectory.

Furthermore, the graph of the hip error, shown in Figure 20, shows relatively small state 1 absolute maximum hip errors of 0.52 degrees and 0.44 degrees for the right hip and the left hip,

respectively. The RMS error for state 1 is 0.27 degrees and 0.25 degrees for the right hip and the left hip, respectively.

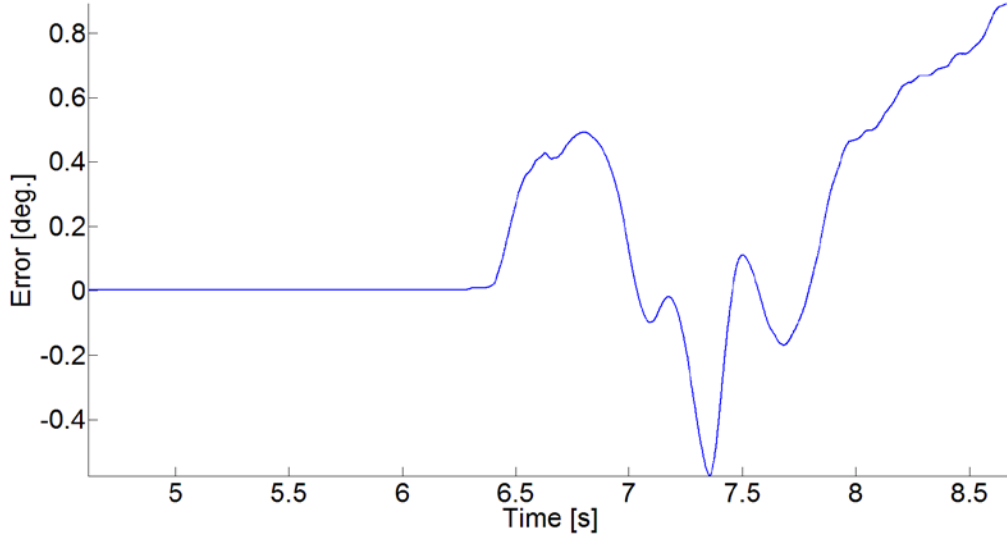


**Figure 18.** Left knee motor synchronization error versus time for trial 5 of the standing experiment

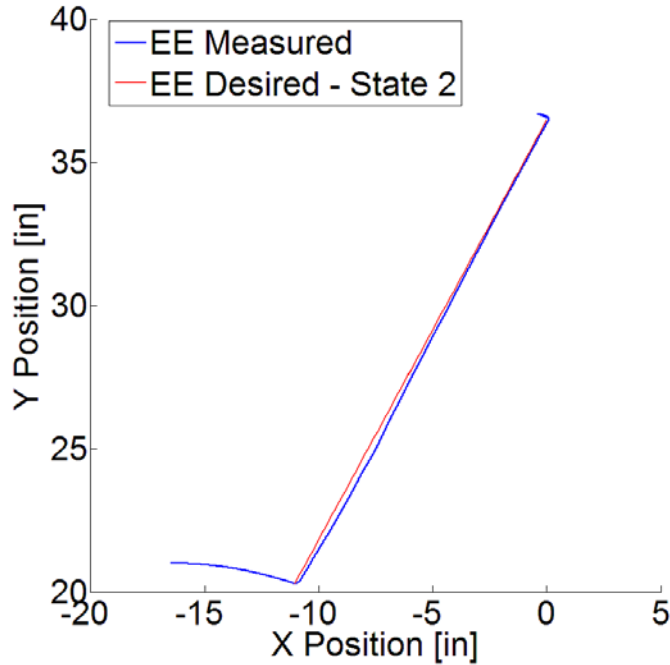


**Figure 19.** The measured end effector trajectory and the desired end effector trajectory of the subject in X and Y for trial 5 of the standing experiment

For state 2 there are absolute maximum hip errors of 0.82 degrees and 0.99 degrees for the right hip and the left hip, respectively. The RMS error for state 1 is 0.43 degrees and 0.51 degrees for the right hip and the left hip, respectively.

For state 3 there are relatively large hip error spikes at the initiation of the VC. There are absolute maximum hip errors of 1.36 degrees and 1.52 degrees for the right hip and the left hip, respectively. The RMS error for state 1 is 0.31 degrees and 0.36 degrees for the right hip and the left hip, respectively, indicating that the controller performance improves after the VC engages. None of the RMS errors for the hips during sitting to standing exceed 1 degree and the controller tracks the trajectory stably and sufficiently accurately.

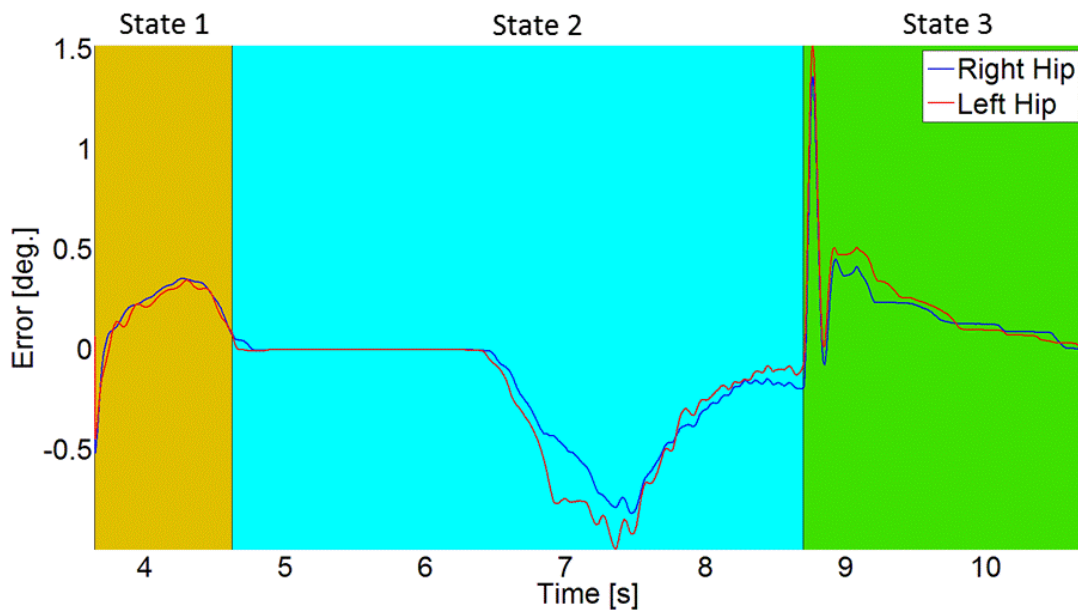


**Figure 20.** The hip error versus time for trial 5 of the standing experiment

The walker handle forces are analyzed to determine weight distribution of the subject's body during sitting to standing. The graph of the walker handle forces versus time is shown in Figure 21. The graph shows the that user's hand weight distribution is towards the back FSR's of

the walker handles and that the total loading of both handles peaks at approximately 100 lbf (54% of the user's weight) after the user begins controlled standing in state 2. The user leans more to the right-side walker handle in state 2 and this may be due to the user's right-handed bias. The support forces drastically decrease in state 3 during full standing and do not exceed 10 lbf per FSR. This indicates that the final EE position is adequately upright that does not have an overdependence of support in the FSW.

The results from trial 5 of the sitting to standing experiment with motors only successfully achieved standing with minor undesirable operation. No instabilities were observed in the controls. The user reported satisfactory performance for sitting to standing but were concerned with the large jerk at the beginning of the state 1 forward leaning control. This jerk was found to be caused by incidental drift of the user's torso which causes the leaning control, and the solution to this problem is detailed in Section 4.3.

One minor incongruence with the control system is the small hip error spike at the beginning of state 3. This hip error is caused by the rapid engagement of the VC in state 3, which in turn propagates to the EE position and the hip control. It is unlikely that this error could be eliminated, since the controller must rapidly compensate for the user's upward momentum to stop at the upright standing position in a short amount of time. The most successful solution to this problem might be to add intelligent braking, to slow the knee and hip motors slightly before full standing. However, the locking error was not found to cause discomfort or a noticeably undesirable standing motion.

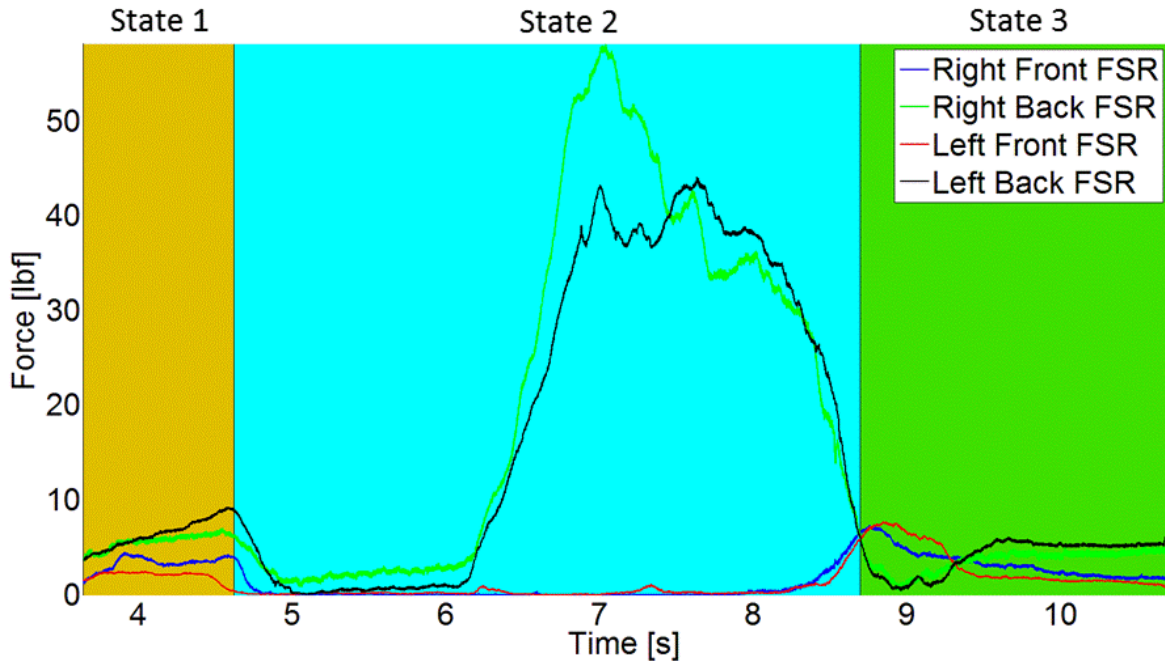


**Figure 21.** The walker handle forces versus time for trial 5 of the standing experiment

### **5.3 EXPERIMENT 2 - DEMONSTRATION OF HYBRID STANDING IN AN ABLE-BODIED SUBJECT**

Able-bodied subject B1 successfully performed 6 trials of sitting to standing with hybrid knee actuation: 3 trials with an FES amplitude of 25mA and 3 trials with an FES amplitude of 30mA. For analysis, the data from trial 2 of the hybrid sitting to standing experiments, with a stimulation amplitude of 25mA, will be used in the discussion of control system performance. From observation during the experiment, the EE tracking smoothly guided the user's torso above the walker during standing. No discomfort was reported by the user during standing, however an FES amplitude of 35mA was attempted and was too high for the subject.

Figure 22 shows the knee angles versus time in trial 2 during standing. The graph shows that the left knee joint angle closely follows the right knee joint angle, however there is some waviness in the knee angle due to FES. The left knee locks at nearly 75 degrees, but the right knee overshoots by approximately 3 degrees. There is a small overshoot in the left knee of about 1 degree in both knees at the beginning of state 3 after the knees are locked. The right and left knees are seen to lock at significantly different angles. This disparity in locking angles is seen consistently in the hybrid standing experiments but is only minimally present in the motor-only trials. This could indicate that there is a delay in the VC engagement or a knee overshoot due to FES.

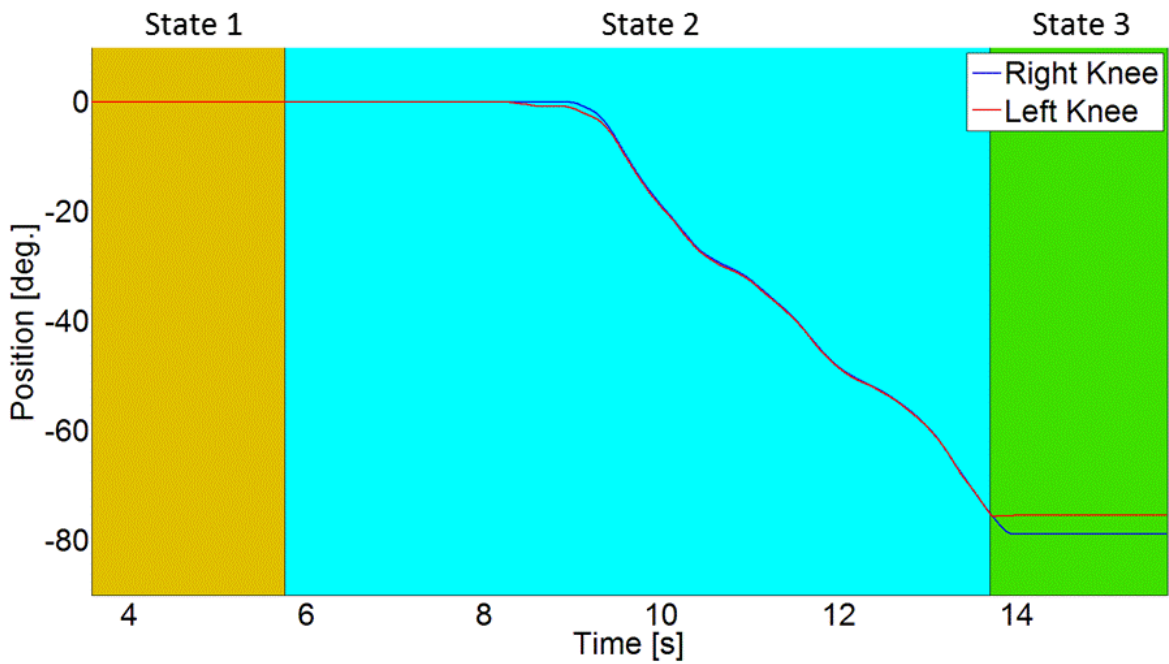


**Figure 22.** Knee angles versus time in trial 2 of the hybrid sitting to standing experiments, with a stimulation amplitude of 25mA

The graph of the synch error versus time in Figure 23 shows that the error, calculated during the user initiated section of state 2, is held below an absolute maximum of 1.21 degrees during sitting to standing with an RMS error of 0.42 degrees. The synch controller RMS error decreased slightly in this trial as compared to trial 2 of the sitting to standing experiment with motors only, even in the presence of added FES. This error decrease can be attributed to the slower rate of standing set at the motor drivers. Overall, the synch controller quickly reduces the synch error to a low value and transitions into state 3 with a very small final error.

A graph of the calculated EE trajectory during the experiment is shown in Figure 24. The hips first lean the torso forward by 15 degrees and then adjust to keep the EE along the path of the linear trajectory. There is a minor discrepancy with the continuity of the EE trajectory at the end of forward leaning, and this is most likely due to the change in the FSM that allows the FSM to move into state 2 when only one hip motor exceeds 15 degrees, as opposed to both hip motors exceeding 15 degrees. However, the measured EE follows the desired EE trajectory with minimal discrepancies in the tracking.

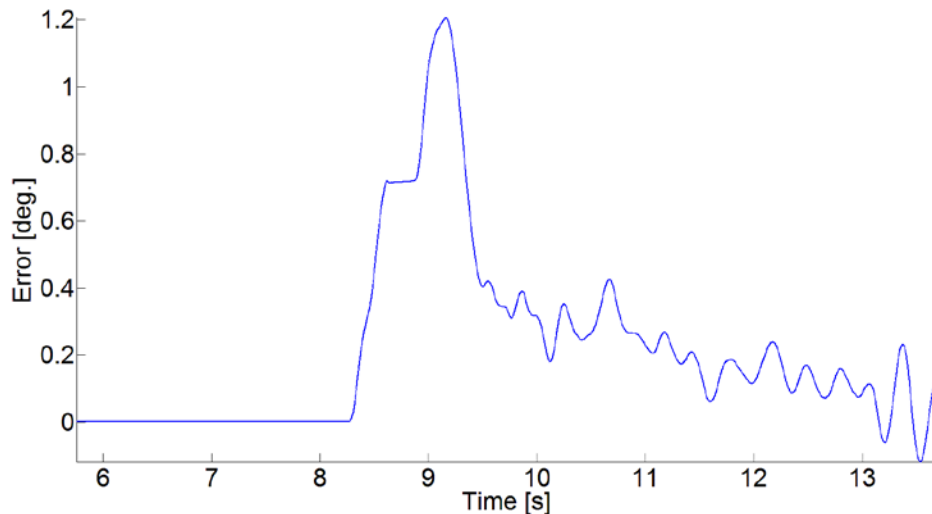


**Figure 23.** Left knee motor synchronization error versus time for trial 2 of the hybrid standing experiment

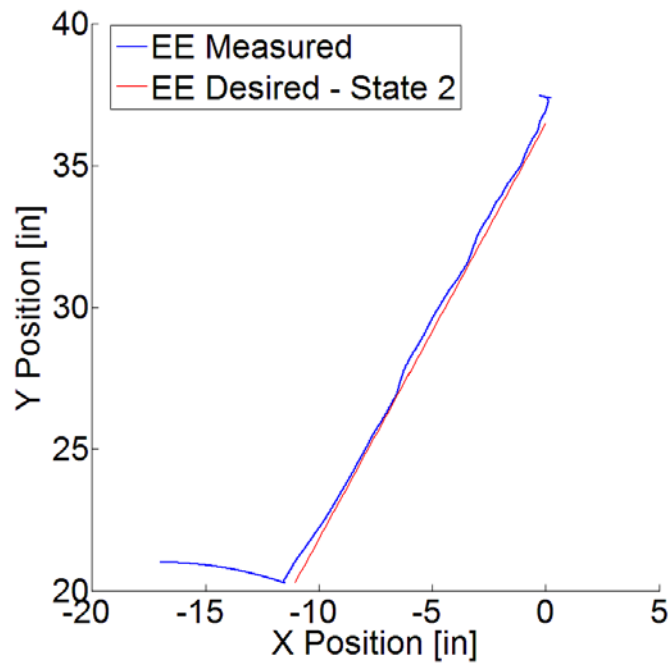


**Figure 24.** The measured end effector trajectory and the desired end effector trajectory of the subject in X and Y for trial 2 of the hybrid standing experiment

Furthermore, the graph of the hip error, shown in Figure 25, shows relatively small state 1 absolute maximum hip errors of 0.31 degrees and 0.60 degrees for the right hip and the left hip, respectively. The RMS error for state 1 is 0.19 degrees and 0.35 degrees for the right hip and the left hip, respectively.

For state 2 there are absolute maximum hip errors of 0.87 degrees and 0.76 degrees for the right hip and the left hip, respectively. The RMS error for state 1 is 0.42 degrees and 0.35 degrees for the right hip and the left hip, respectively.

For state 3 there are relatively large hip error spikes at the initiation of the VC. There are absolute maximum hip errors of 1.58 degrees and 1.31 degrees for the right hip and the left hip, respectively. The RMS error for state 1 is 0.68 degrees and 0.56 degrees for the right hip and the

left hip. Overall, none of the RMS errors for the hips during sitting to standing exceed 1 degree and the controller tracks the trajectory stably and sufficiently accurately.

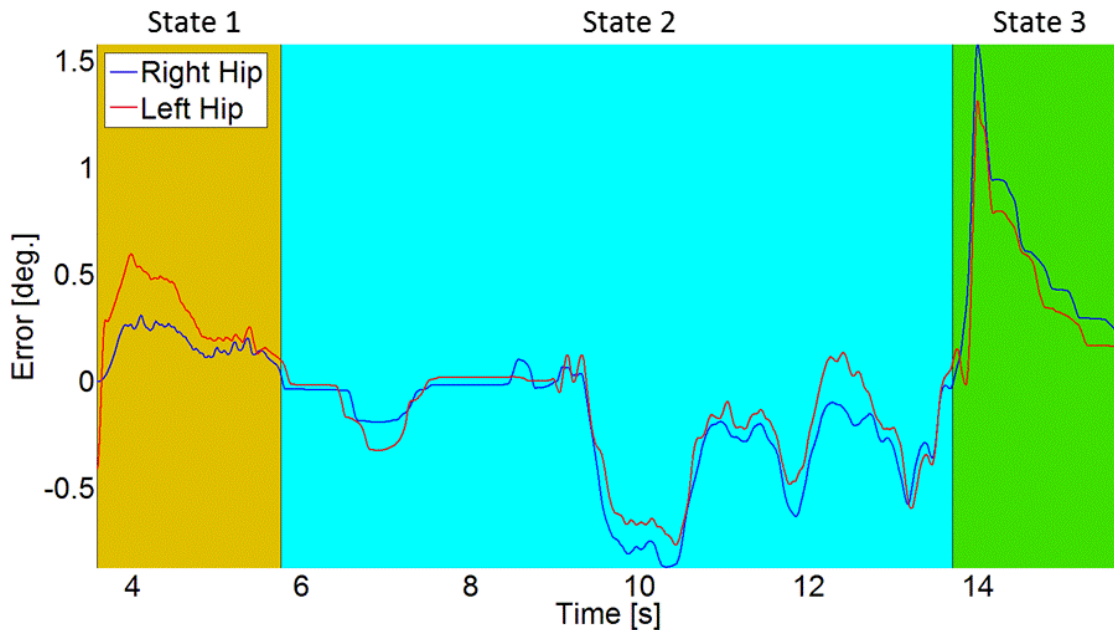


**Figure 25.** The hip error versus time for trial 2 of the hybrid standing experiment

The graph of the walker handle forces versus time are shown in Figure 26. The graph shows that the user's hand weight distribution is towards the back FSR's of the walker handles and that the total loading of both handles peaks at approximately 80 lbf (43% of the user's weight) after the user begins controlled standing in state 2. The user leans nearly equally on both walker handles in state 2. The support forces decrease in state 3 during full standing and do not exceed 10 lbf per FSR.

The results from Trial 2 of the hybrid sitting to standing experiments, with a stimulation amplitude of 25mA, successfully achieved standing with minor undesirable operation. No instabilities were observed in the controls. The user reported satisfactory performance for sitting

to standing. The jerking error experienced by the user in the first experiment was no longer noticeable, although it is questionable if the overall torque limiter imposed in the hip motors is functionally necessary.

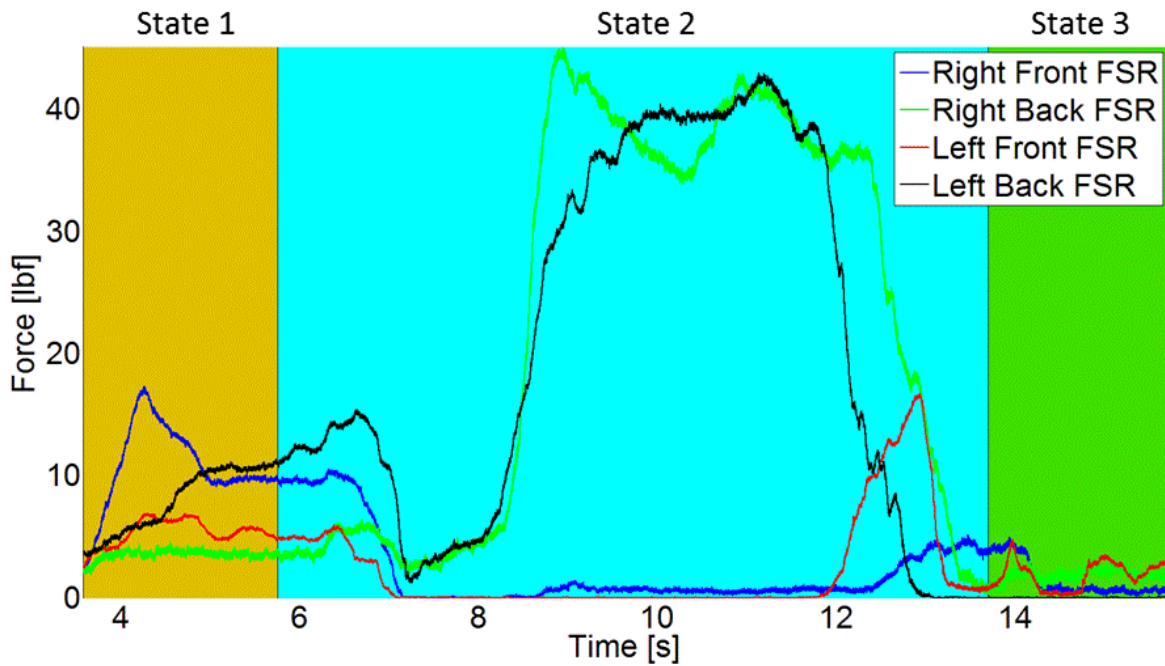


**Figure 26.** The walker handle forces versus time for trial 2 of the hybrid standing experiment

The control system performed more accurately in this trial as compared with trial 5 of experiment 1. The EE tracking performed as well or better than the tracking in the first experiment. Also, the RMS hip error decreased in the left leg as compared with trial 5 of the first experiment. The decrease in user arm support could suggest a lessening of walker loading with a larger proportion of support coming from the neuroprosthesis and FES actuation, as compared with the first experiment.

Therefore, the largest problem with the control system performance is the right knee offset in state 3. This problem was observed to be worse in hybrid standing. Thus, this problem is

expected to be caused by the presence of FES. Since the error is caused during state 3, it is possible that some residual muscle activation is occurring in state 3, either due to controls or physical discrepancies. To fix this error, FES could be stopped within a margin of time before the end of state 2.

#### 5.4 EXPERIMENT 3 - DEMONSTRATION OF STANDING WITH MOTORS ONLY IN A SUBJECT WITH SCI

Subject with SCI A4 successfully performed 4 trials of standing with motors only. Figure 27 below shows a screen capture of the user as they transition between FSM states in trial 2 of experiment 3. The EE tracking appeared smoothly guided the user's torso above the walker during standing. For analysis, the data from trial 2 of the experiment will be used in the discussion of control system performance. The user specifically said during the experiment that they believed that the standing control system performed well, and they thought that it could benefit other SCI users.

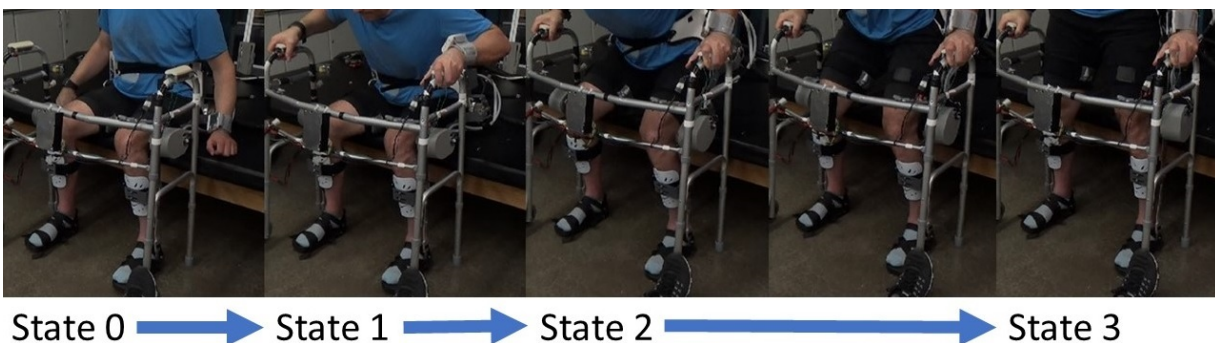


**Figure 27.** A sequence of frames from the footage taken during trial 2 of the standing experiment

Figure 28 shows the knee angles versus time in trial 2 during standing. The graph shows that the left knee joint angle closely follows the right knee joint angle and that the synch controller in state 2 of the FSM appears to work successfully. Both knees lock at nearly 75 degrees, the knee angle set to trigger the transition into state 3 of the FSM, when the VC engages. There is a small overshoot of about 1 degree in both knees at the beginning of state 3 after the knees are locked, which is to be expected. The knee angle progression is seen to perform as well or better than the able-bodied motors only sitting to standing in experiment 1.

The graph of the knee synch error versus time in Figure 29 shows that the overall knee synch error is held below an absolute maximum of 1.67 degrees during sitting to standing with an RMS error of 0.71 degrees.

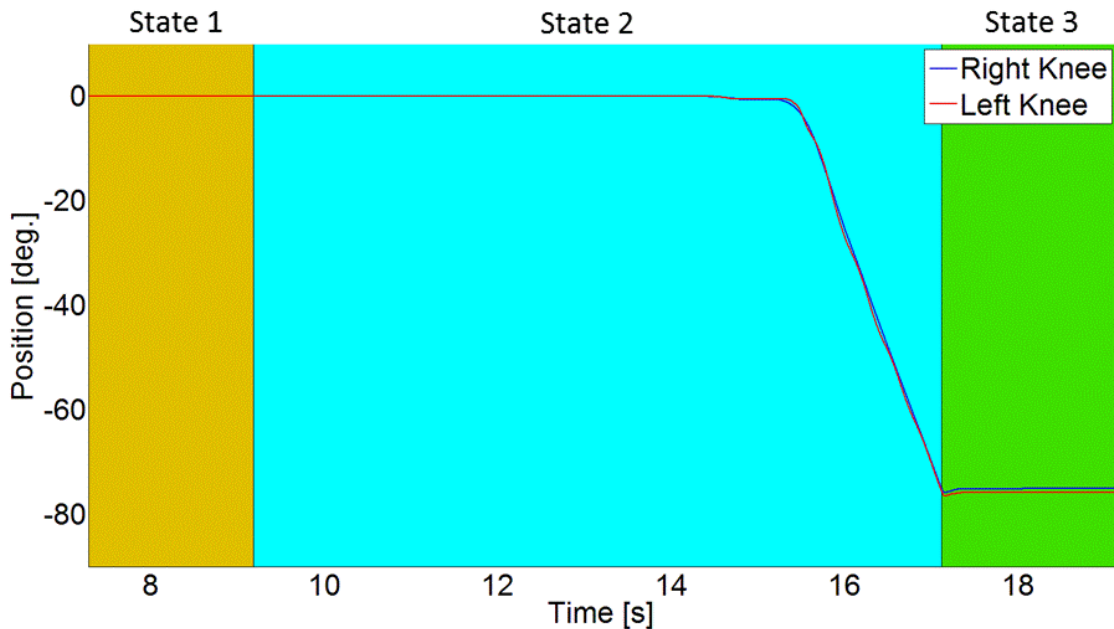


**Figure 28.** Knee angles versus time or trial 2 of the standing experiment

A graph of the calculated EE trajectory during the experiment is shown in Figure 30. The EE tracking accurately guides the position of the EE along the predefined linear trajectory specified in the controls. The hips first lean the torso forward by 15 degrees and then adjust to keep the EE along the path of the linear trajectory. This trial showed the best EE tracking along the desired trajectory, with very little deviation away from the desired EE trajectory in all 3 controller states.

Furthermore, the graph of the hip error, shown in Figure 31, shows relatively small state 1 absolute maximum hip errors of 0.26 degrees and 0.33 degrees for the right hip and the left hip, respectively. The RMS error for state 1 is 0.14 degrees and 0.20 degrees for the right hip and the left hip, respectively.

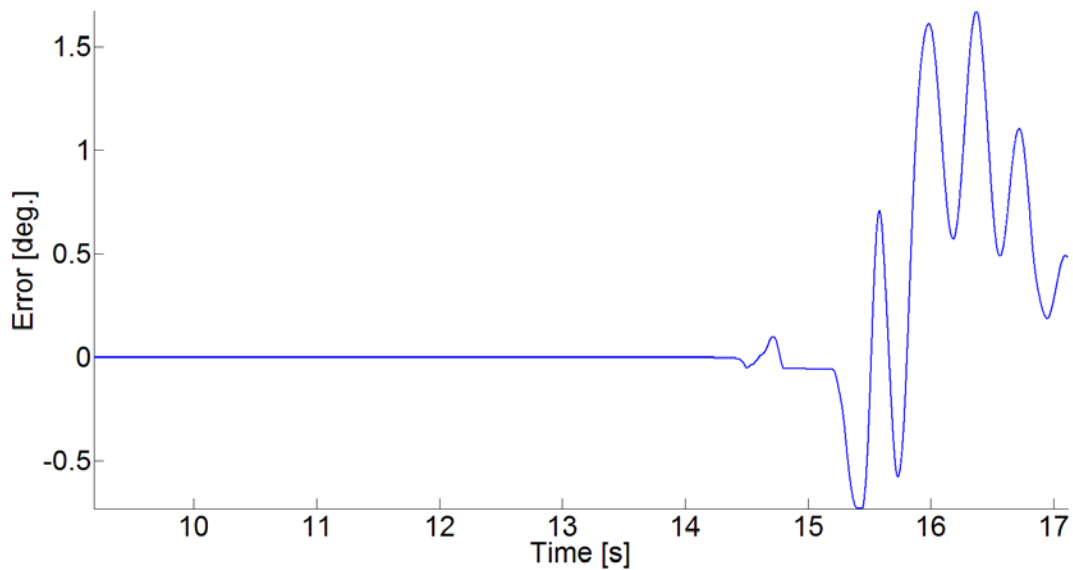


**Figure 29.** Left knee motor synchronization error versus time in state 2 for trial 2 of the standing experiment

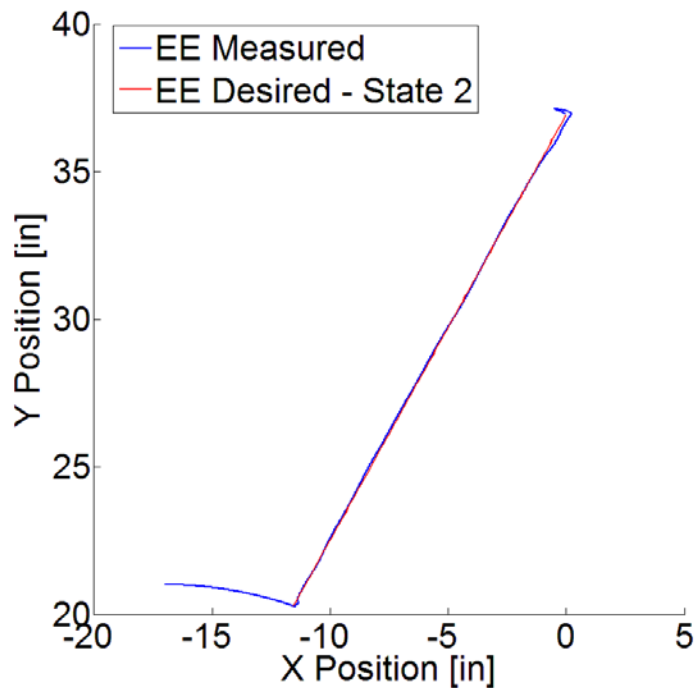


**Figure 30.** The measured end effector trajectory and the desired end effector trajectory of the subject in X and Y for trial 2 of the standing experiment

For state 2 there are absolute maximum hip errors of 0.51 degrees and 0.75 degrees for the right hip and the left hip, respectively. The RMS error for state 1 is 0.22 degrees and 0.42 degrees for the right hip and the left hip, respectively.

For state 3 there are relatively large hip error spikes at the initiation of the VC. There are absolute maximum hip errors of 1.58 degrees and 2.05 degrees for the right hip and the left hip, respectively. The RMS error for state 3 is 0.37 degrees and 0.64 degrees for the right hip and the left hip, respectively, indicating that the controller performance improves after the VC engages. Overall, none of the RMS errors for the hips during sitting to standing exceed 1 degree and the controller tracks the trajectory stably and sufficiently accurately. This trial shows a high maximum state 3 left hip error of 2.05 degrees.

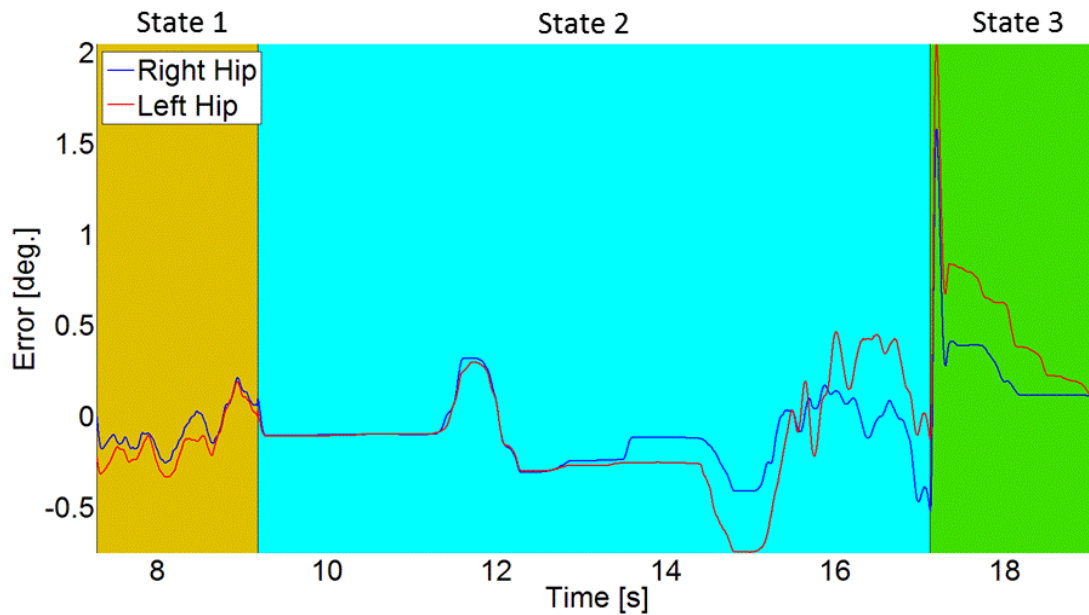


**Figure 31.** The hip error versus time for sitting to standing for trial 2 of the standing experiment

Lastly, the walker handle forces are analyzed to determine weight distribution of the subject's body during sitting to standing. The graph of the walker handle forces versus time are shown in Figure 32. The graph shows that the user's hand weight distribution is towards the back FSR's of the walker handles and that the total loading of both handles peaks at approximately 170 lbf after the user begins controlled standing in state 2. The user leans more to the right-side walker handle in state 2 and this may be due to the user's right-handed bias. Unlike subject B1, subject A4 does not shift their weight towards the front of the walker handles in state 3. However, one pronounced difference in the standing is that the subject with SCI relies much more heavily on the walker to support their weight. The subject with SCI applies approximately 80 lbf of combined walker handle support forces during upright standing in state 3. This weight distribution is expected since the subject with SCI has less control over their lower body than the able-bodied subject.

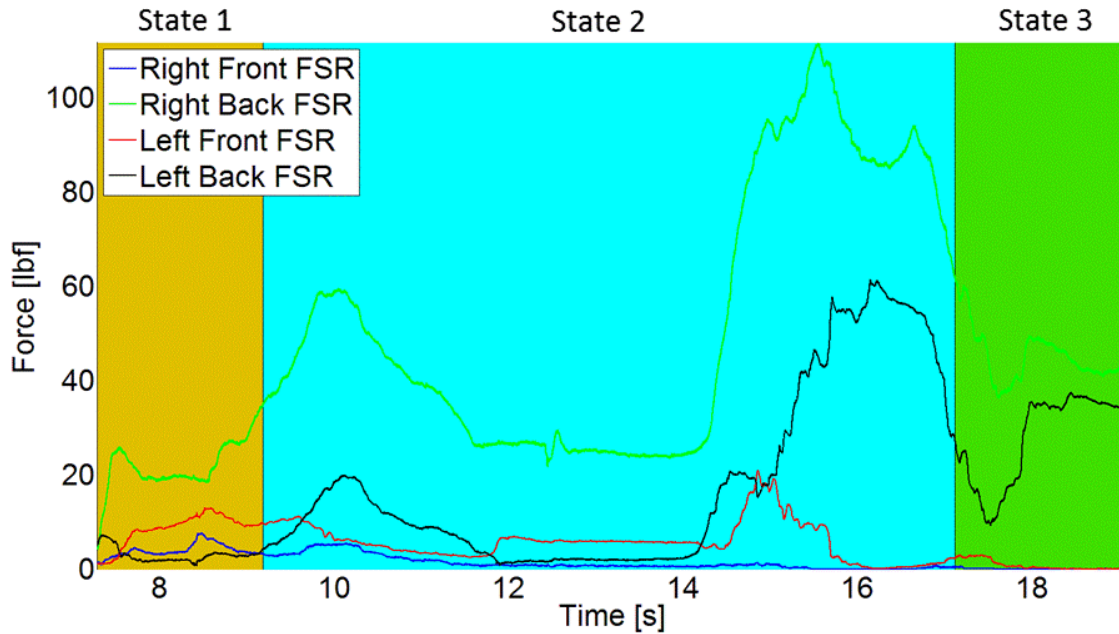


**Figure 32.** The walker handle forces versus time for trial 2 of the standing experiment

The results from trial 2 of the experiment show that the subject successfully achieved standing with minor undesirable operation. No instabilities were observed in the controls. The user willfully commented that the standing control worked well and did not experience any jerky movements in the state 1.

The synch controller performed noticeably worse than in experiments 1 and 2 with the able-bodied subject, with nearly twice as high of an RMS error. This increase in error could be partially attributed to the heavier user weight, since a heavier weight would need to be manipulated by the controls. Nevertheless, the error values in the synch controller were not noticed by the subject with SCI and did not cause problems with standing.

Trial 2 of this experiment yielded one of the most accurate tracking trajectories for the user's EE, as there was virtually no discrepancy between the measured and desired EE trajectories. The hip error was not significantly higher than in experiment 1. However, the

maximum hip error in state 3 was slightly higher than in subject B1, which may again be attributed to the increased user weight. Most importantly, the user felt confident in the control system and had a positive outlook on the usefulness of the sitting to standing functionality in daily life.

## **5.5 EXPERIMENT 4 - DEMONSTRATION OF HYBRID STANDING IN A SUBJECT WITH SCI**

Subject with SCI A4 performed 4 trials of hybrid sitting to standing with motors and FES knee actuation: 3 trials with an FES amplitude of 40mA and 1 trials with an FES amplitude of 50mA. Three of the trials yielded usable data, but trial 2 did not since the FSM never successfully transitioned from state 2 to state 3. The experiment needed to be ended early due to torsional bending in the left shank frame. Minor discomfort was reported by the user during standing when the neuroprosthesis hip brace rubbed against the back of the subject, however this only caused a minor skin abrasion. Another major issue observed in the trials is that the user was leaning backward during sitting to standing, which negatively affected the performance results.

Figure 33 shows the knee angles versus time in trial 3 during standing. The graph shows that the left knee joint angle follows the right knee joint angle, with some noticeable joint angle differences between the two legs. Both knees lock at nearly 75 degrees, the knee angle set to trigger the transition into state 3 of the FSM, when the VC engages. However, the knees do not lock at the same angles, and the right knee appears to lock a few degrees past 75 degrees.

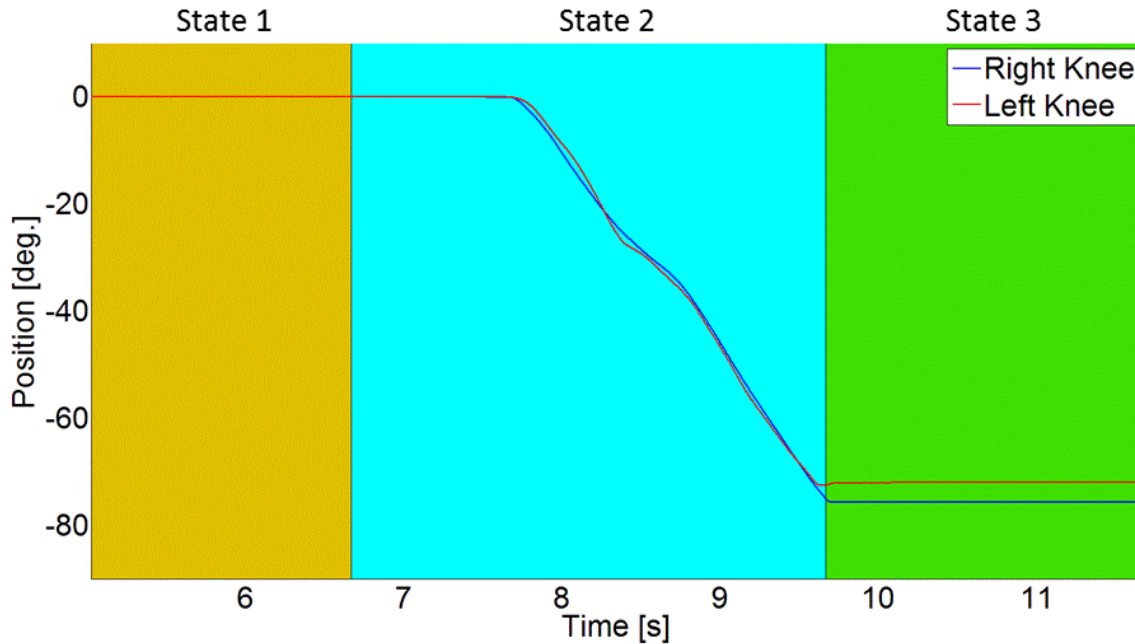


**Figure 33.** Knee angles versus time for trial 3 of the hybrid standing experiment

The graph of the knee synch error versus time in Figure 34 shows that the knee synch error, and the error is held below an absolute maximum of 2.50 degrees during sitting to standing with an RMS error of 1.08 degrees. These results show the worst overall synch controller performance, as compared to the 3 other experiments. The synch error approaches a very high value towards the end of state 2. Since the FSM only switches into state 3 once both knees have exceeded 75 degrees, this error will propagate into state 3 when the VC is turned on.

A graph of the calculated EE trajectory during the experiment is shown in Figure 35. The EE tracking only partially guides the position of the EE along the predefined linear trajectory specified in the controls. The hips first lean the torso forward by 15 degrees and then adjust to keep the EE along the desired trajectory, however the EE soon drifts to a low y-position, and it does not end in the desired position. The main cause for this error is the fact that the subject had poor footing and leaned back too far during standing. This phenomenon creates undesired HMI

which forces the hip motor joint angles into positions lower than they should be. This also indicates that the torque supplied to the user's hip is insufficient to guide the EE in a backward leaning stance.

Furthermore, the graph of the hip error, shown in Figure 36, shows relatively small state 1 absolute maximum hip errors of 0.26 degrees and 0.33 degrees for the right hip and the left hip, respectively. The RMS error for state 1 is 0.63 degrees and 1.90 degrees for the right hip and the left hip, respectively.

For state 2 there are absolute maximum hip errors of 9.52 degrees and 11.41 degrees for the right hip and the left hip, respectively. The RMS error for state 2 is 5.79 degrees and 6.03 degrees for the right hip and the left hip, respectively.

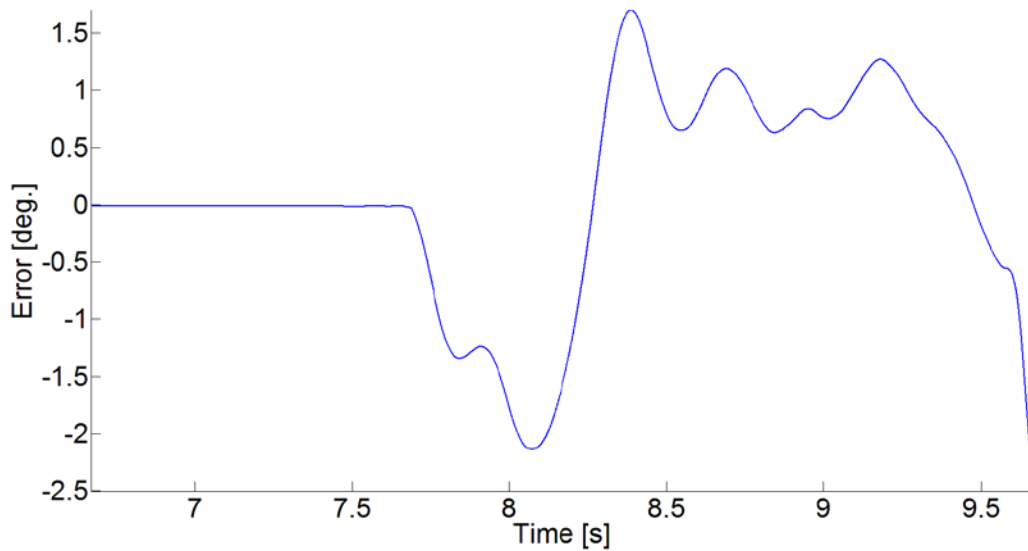


**Figure 34.** Left knee motor synchronization error versus time in state 2 for trial 3 of the hybrid standing experiment

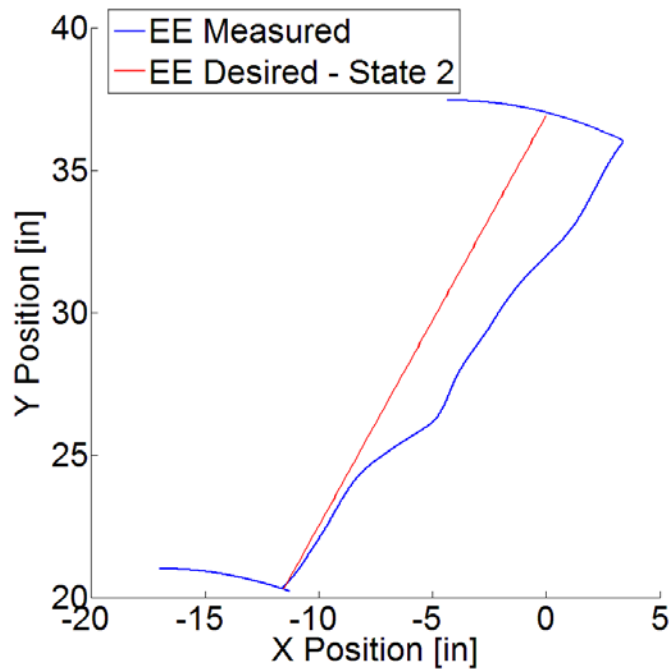


**Figure 35.** The measured end effector trajectory and the desired end effector trajectory of the subject in X and Y for trial 3 of the hybrid standing experiment

For state 3 there are very large hip error spikes after the initiation of the VC. There are absolute maximum hip errors of 12.13 degrees and 12.29 degrees for the right hip and the left hip, respectively. The RMS error for state 3 is 4.97 degrees and 5.74 degrees for the right hip and the left hip, respectively. Overall, the errors for the hips during sitting to standing are much higher than the previous 3 experiments and are high in an absolute sense.

The walker handle forces are analyzed to determine weight distribution of the subject's body during sitting to standing. The graph of the walker handle forces versus time are shown in Figure 37. The graph shows that the user's hand weight distribution is almost completely located at the back FSR's of the walker handles and that the total loading of both handles peaks at approximately 85 lbf at state 2, after the user begins controlled standing in state 2. The user leans more to the right-side walker handle in state 2 and this may be due to the user's right-handed

bias. The subject with SCI relies less on the walker to support their weight in trial 3 of this experiment than in trial 2 of experiment 3. The subject with SCI applies approximately 35 lbf of combined walker handle support forces in upright standing.

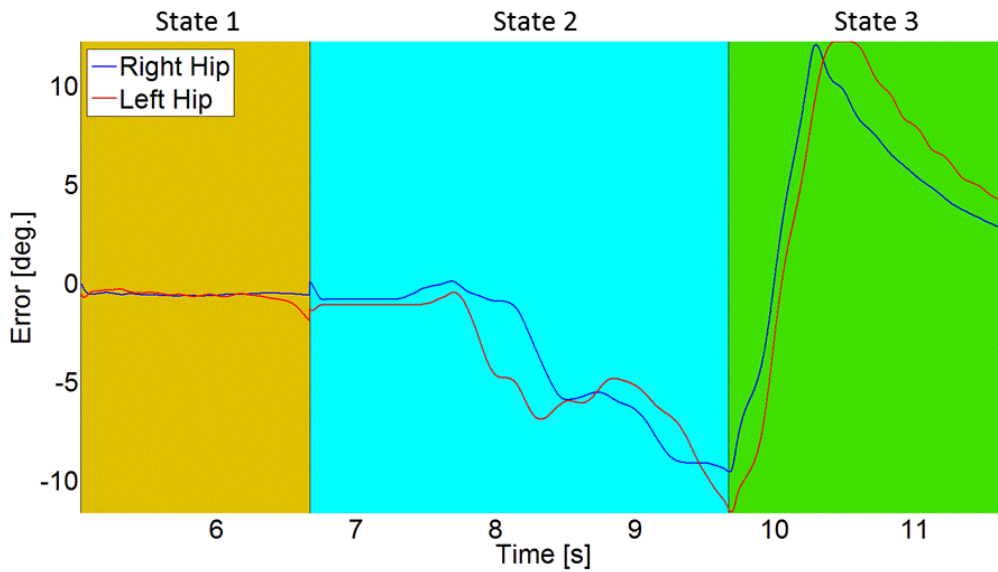


**Figure 36.** The hip error versus time for trial 3 of the hybrid standing experiment

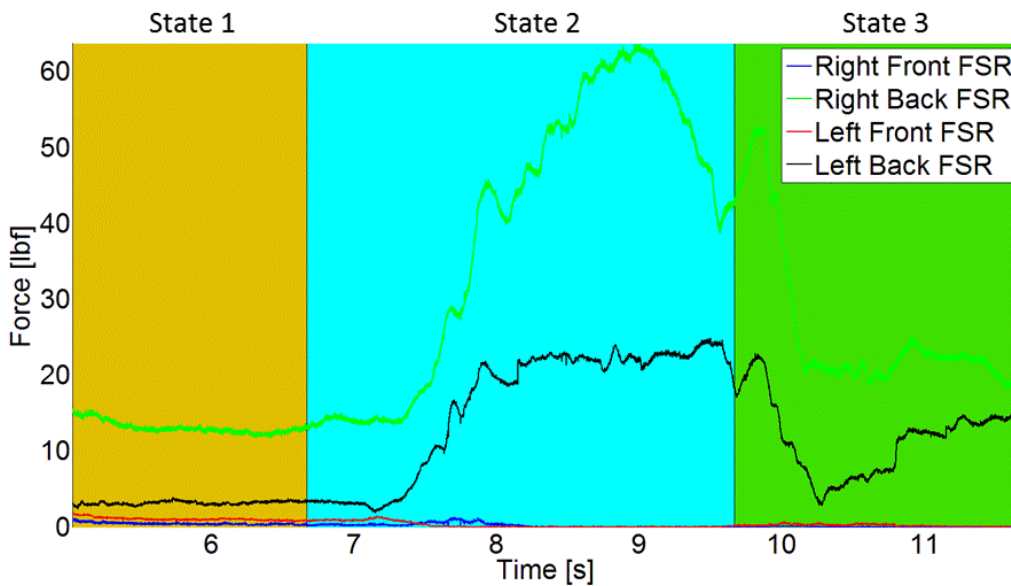


**Figure 37.** The walker handle forces versus time for trial 3 of the hybrid standing experiment

Although trial 3 successfully performed standing, it showed poor overall EE tracking and hip error. These results are most likely caused by the user leaning back during standing caused by their poor footing at the beginning of the experiment. These results also may indicate that the torque settings for the hip motors may be insufficient to guide the user's EE, especially in the case of poor footing.

Another issue observed was that the VC locking was jerkier with hybrid actuation, and this was also the case with the able-bodied subject in experiment 2. It appears that the higher overall torque at the knee and the speed of standing produces a high load on the VC when it is required to lock the knees at the beginning of state 3.

## **5.6 CONTROL SYSTEM PERFORMANCE DISCUSSION**

Compared to the preliminary standing experiment, described in Section 1.2.1, this control system was successful in enabling safe assisted standing in an able-bodied subject and a subject with SCI. These experiments showed that the slower sitting to standing speed in experiment 2 produced similar error results to the experiment 1 in the presence of greater disturbance in the form of FES. This suggests that the slower standing speed in this experiment is more desirable for control system performance.

In the four experiments performed, four main problems in the control performance were identified, and the solutions to these problems are also listed below:

- 1) State 1 Hip Jerk – The state 1 controller did not perform correctly in Experiment 1 because it jerked forwards or backwards when the subject initiated state 1 with the walker

handles. This error was caused by a combination of the nature of the incremental encoders, which always start state 0 at zero degrees, and the control programming. Since the subject sometimes subconsciously moved their torso before state 1, the state 1 tracking controller would see an initial error and jerk the user into the tracked angle. This problem was solved by retroactively changing the desired hip angle to equal the starting hip angle at the beginning of state 1. In addition, the maximum allowable hip torque was reduced to decrease jerk, however, it seems likely that the torque reduction implemented was overconservative. The jerking error was subsequently minimized in Experiments 2-4.

- 2) Large Experiment 4 Errors Caused by Poor Footing – Experiment 4 had very large hip tracking errors due to the undesirable HMI caused by backward leaning during standing. This error was not caused by controller maleficence, but was caused by the subject's torso pushing back against the hip motors. This also explains why the subject had rubbing abrasions on their lower back during standing. It was also observed in several unsuccessful trials that the subject with SCI had difficulty establishing footing to begin the experiment. This phenomenon was observed to a lesser extent with the able-bodied subject, presumably because they had better control and spatial perception of their lower legs. Furthermore, the sitting to standing posture taken at the start of state 2 in the experiments, where the knees are locked at 90 degrees, does not appear to be a natural posture for standing. A more natural posture begins standing with the knees flexed past 90 degrees by a small angle, as observed in the stroboscopic records of able-bodied standing created by Bajd et al<sup>[4]</sup>. With this posture, knee movement into extension will not be able to lift the feet up off the ground, since the feet will be pushed into the ground.

No programming changes are needed to solve this problem. In future experiments, the user will be instructed to start standing with their knees at approximately a 70 to 80 degree angle. This ankle angle would need to be corrected in the first two steps of an assisted gait control.

- 3) Torsional Shank Frame Bending – Unexpectedly high torsional loads were present on the neuroprosthesis shank frames. These loads were caused by a mechanical conflict between the user’s knee joint dynamics and the dynamics of the neuroprosthesis knee<sup>[75]</sup>. Additionally, the torsional bending may have caused energy inefficiencies in experiment 3 and 4. The shank frames were designed to resist bending in the sagittal plane, but not torsion. This torsion caused experiment 4 to be stopped prematurely and future frame designs will need to resist torsional bending.
- 4) Rubbing at the back of the user’s torso in Experiment 4 – This problem was caused by a combination of poor HMI during backward leaning standing and neuroprosthesis connection at the hip. This problem will be solved by a new hip design with better padding and beginning standing with the user’s shanks angled backwards.

## **5.7 POWER AND ENERGY ANALYSIS DURING STANDING EXPERIMENTS**

One of the main motivations of using FES stimulation in a hybrid neuroprosthesis is reducing energy requirements<sup>[33,34,70]</sup>, therefore it is important to analyze the power and energy data during experiments 1-4. Energy consumption for hybrid standing is compared with motor-only standing. Additionally, the quantification of the power and energy requirements during standing is an

important statistic for the design of a mobile hybrid neuroprosthesis. Energy consumption statistics can be used to evaluate the efficacy of a battery or other mobile power source.

Multiple neuroprosthesis components are powered: the knee motors, the hip motors, all four incremental encoders, the walker joystick, the walker FSR's, and the FES stimulator. However, it is assumed that the electric motors will consume the largest amount of energy during standing. Furthermore, the highest power requirements are at the knees, and therefore the power and energy analyses are performed on the knees only.

### 5.7.1 Power and Energy Measurement Methodology

The instantaneous power for the knees is evaluated at the input to the knee controllers because this correlates to the output of a mobile power source. In order to measure the instantaneous power at the input to the knee motor controllers, the knee controller analog outputs are used to collect performance statistics of the knee motors. Knee controller output 1 collects the knee motor input amperage and knee controller output 2 collects the knee motor angular speed in RPM. It was observed that both knee controller outputs have noisy signals, so these inputs were passed through low pass filters with frequency cutoffs of 20hz. This power measurement method neglects power losses associated with the EC motor.

The voltage going into each EC motor is directly proportional to the RPM in the motor through the motor speed constant. This speed constant is equal to 88 RPM per volt for the EC90 knee motors. The instantaneous power input into the knee motor controllers is represented by the electric power equation below:

$$P_{km,c} = \frac{I_{km} V_{km}}{\mathcal{E}_c}$$

where  $I_{km}$  is the amperage at the input of the knee motor,  $V_{km}$  is the voltage at the input of the knee motor, and  $\varepsilon_c$  is the efficiency of the ESCON 50/5 knee motor controllers, which is equal to 95% per the information provided by Maxon Motors. This calculation is performed in the SIMULINK control program for the right and left motors during all operation of the neuroprosthesis. The energy consumption is also calculated by integrating the absolute value of the power signal over time.

The equation above assumes that there is no energy consumption in the motors when the knees are locked in position with the VC during full standing in state 3 of the FSM. This is not precisely correct due to energy losses in the circuitry, but it is assumed that the energy consumption of the motors during VC engagement is negligible.

### **5.7.2 Power Analysis**

Power usage is compared in the right knee motors for the trials analyzed in the controls performance section. Figure 38 shows the power consumption of the right knee motor, at the input to the driver, in trial 5 of experiment 1. The power curve shows a high-power demand during the beginning of standing and liftoff, as expected, with a maximum power of 36.3 watts. The power then gradually decreases until knee braking with the VC in state 3. The left knee power, which is not shown in figures of this section, was typically higher than the right knee motor due to internal mechanical inefficiencies in the left gearmotor. Since the EC90 motor has a rated power output of 90 watts, the power requirements are less than half of what the motors can produce. A power spike of over 10 watts is seen at the beginning of braking in state 3.

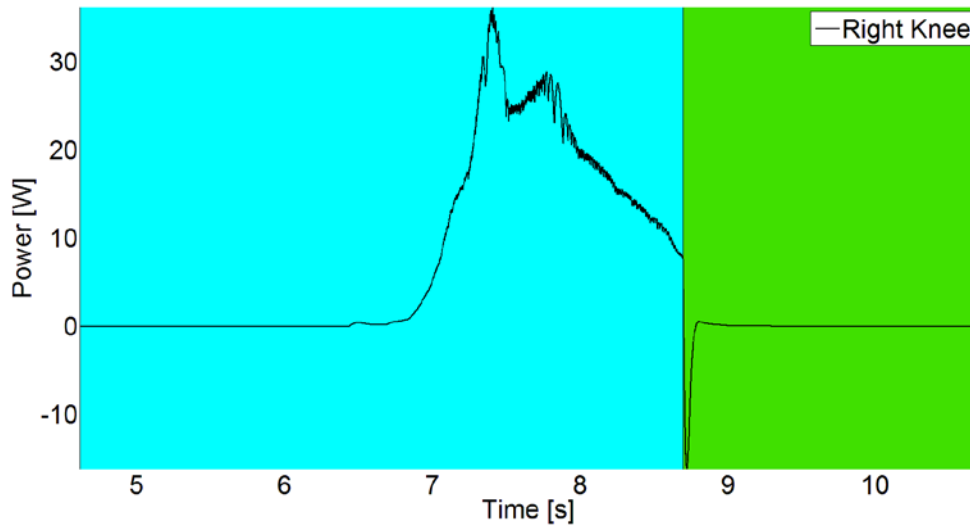


**Figure 38.** The right knee motor power for trial 5 of experiment 1

Figure 39 shows the absolute values of the power consumption of the right knee motor, at the input to the driver, in trial 2 of experiment 2. These power results seem unusual, since they are much lower than the powers measured in experiment 1. However, these lower power requirements can be attributed to two factors: a much lower standing speed and the presence of FES in hybrid standing. The standing in trial 2 of experiment 2 took nearly 5 seconds, as compared to under 2 seconds in trial 5 of experiment 1. Furthermore, able-bodied subject B1 has an advanced level of muscular development and they perform regular weightlifting at the gym in their free time, and they could produce high forces through FES with extensive FES training.

A maximum knee motor power of 6.3 watts occurs shortly after standing, with a braking spike of over 4 watts. This dramatic power reduction is partially caused by lowered acceleration during standing, with most of the power being used to overcome gravity instead of accelerating the user upwards. Thus, the combination of slower standing and high muscular output through FES achieved a high required knee power reduction of over 80%. Experiment 2 had a power

measurement malfunction for the powers in the left knee motors. The measurement malfunction was not found in any other experiments and the exact cause of this malfunction is unknown.

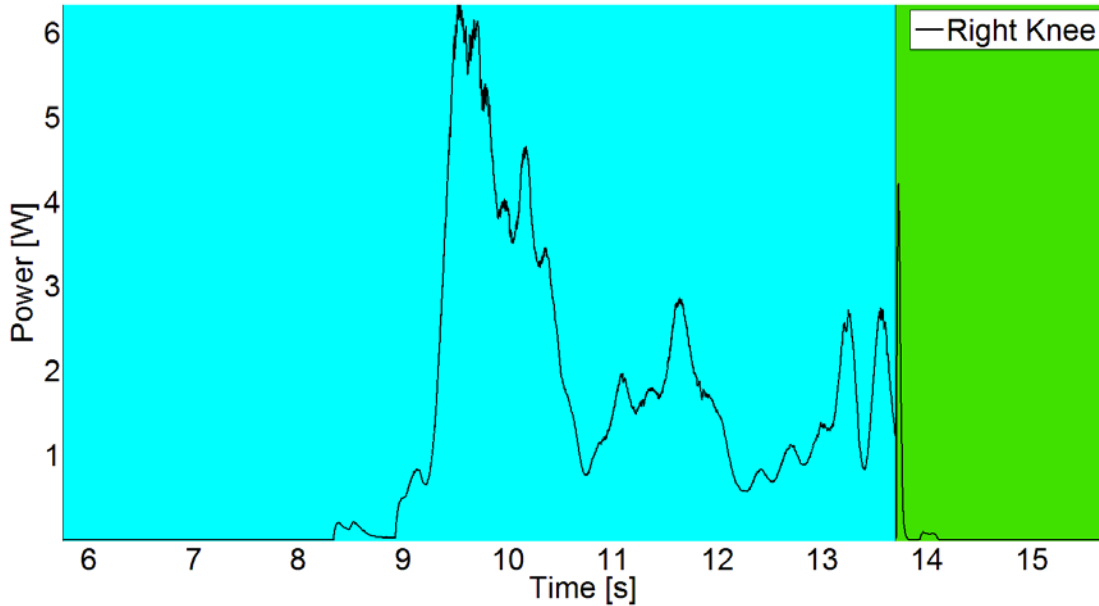


**Figure 39.** The absolute values of the right knee motor power for trial 2 of experiment 2

Figure 40 shows the absolute values of the power consumption of the right knee motor, at the input to the driver in trial 2 of experiment 3 with subject with SCI A4. The power curve shows a high-power demand during the beginning of standing and liftoff, as expected, with a maximum torque of 39.8 watts. A power spike of nearly 15 watts is seen in the braking in state 3. The torque then gradually decreases until knee braking with the VC in state 3. Sitting to standing occurs in nearly the same overall time as in trial 5 of experiment 1. The user A4 reportedly weights slightly more than subject B1, so it is expected that the power usage is slightly higher.

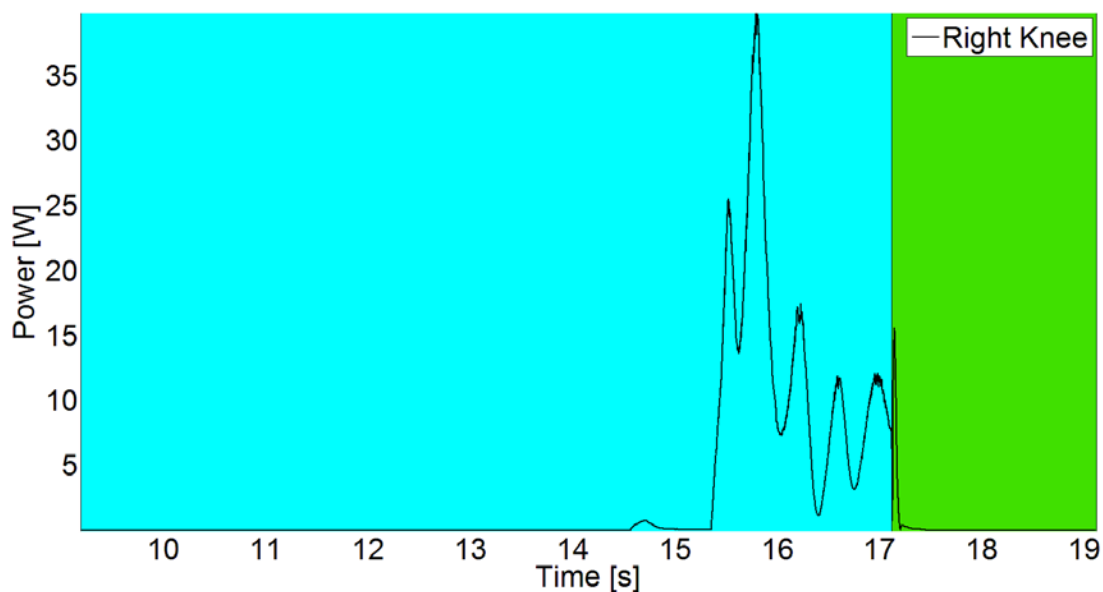


**Figure 40.** The absolute values of the right knee motor power for trial 2 of experiment 3

Figure 41 shows the absolute values of the power consumption of the right knee motor, at the input to the driver, in trial 3 of experiment 4, with subject with SCI A4. The power curve shows a high-power demand during the beginning of standing and liftoff, as expected, with a maximum torque of 40.3 watts. A small power spike is seen in the braking in state 3. The torque then gradually decreases until knee braking with the VC in state 3. Sitting to standing occurs in nearly the same time as in trial 5 of experiment 1.

These results show that the knee motor have nearly the same maximum power requirements in motors only standing and hybrid standing for the subject with SCI. This result is undesirable, and it can be attributed to two factors: a low FES output for the subject with SCI and a fast standing speed. Subject with SCI A4 had virtually no experience with FES training before experiments 3 and 4 were performed and is not expected to have a high muscular output for FES, especially in comparison with subject B1. Furthermore, it is possible that the fast standing speed in experiments 3 and 4 created a situation where the movement was dominated by

knee motors as opposed to FES, and it is possible that with this quick acceleration there was undesirable HMI. Also, it is possible that the combination of the knee joint angles and knee joint angular speed at the beginning of standing were not ideal for FES stimulation. The power requirements were not shown to drop for the subject with SCI with hybrid standing in trial 3 of experiment 4.

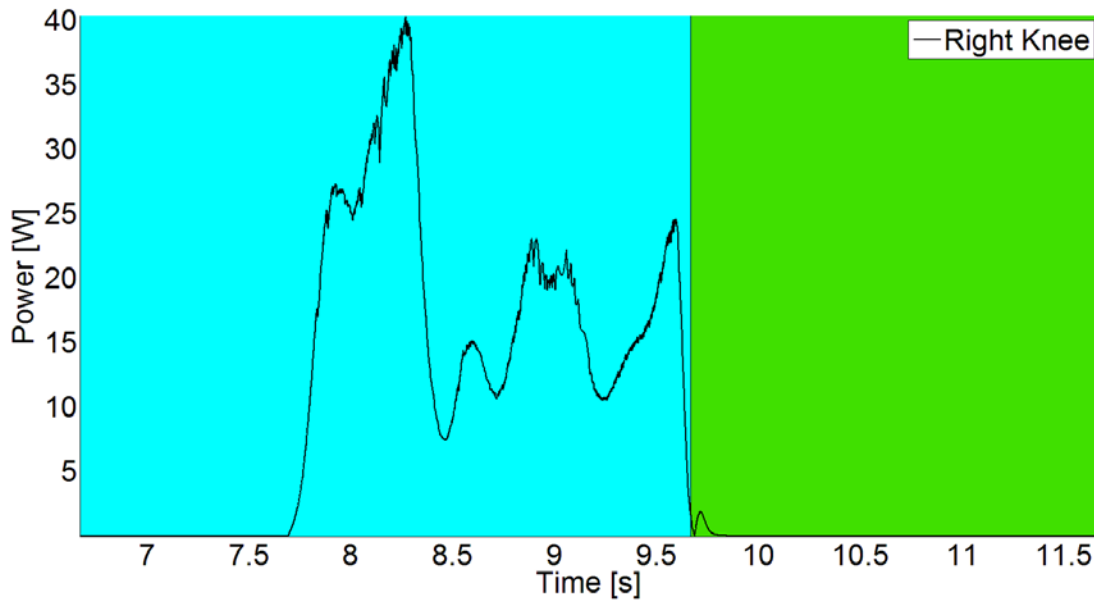


**Figure 41.** The absolute values of the right knee motor power for trial 3 of experiment 4

### 5.7.3 Energy Consumption Analysis

Table 2, Table 3, Table 4, and Table 5 show the energy consumption for the knee motors during sitting to standing in experiments 1-4, respectively. These tables also show the maximum total FSW support force, or the maximum of the net sum of all FSR forces, for all standing trials to show the amount of support effort exerted by the subject. As mentioned earlier, a data recording malfunction caused only the right knee power to record correctly for experiment 2 due to an

unknown error. All energy consumption values shown are the motor controller input level, or the output of the power source.

The results show that the average energy consumption for both knees in experiment 1 was 88.4 joules. The average energy consumption for the right knee in experiment 1 was 38.9 joules. The average energy consumption for the right knee in experiment 2 was 10.1 joules. The average energy consumption for the both knee motors in experiment 3 was 65.6 joules. The average energy consumption for the both knee motors in experiment 4 was 56.5 joules.

**Table 2.** Energy consumption for all trials in experiment 1

Trial	Max FSW Force (lbf)	FES (mA)	Energy- Right Knee (j)	Energy- Left Knee (j)	Energy- Both Knees (j)
1	115.6	0	34.2	59.0	93.2
2	91.2	0	33.8	42.1	75.9
3	101.7	0	46.0	53.8	99.8
4	97.1	0	46.3	43.8	90.1
5	102.4	0	34.0	48.8	82.8

**Table 3.** Energy consumption for all trials in experiment 2

Trial	Max FSW Force (lbf)	FES (mA)	Energy- Right Knee (j)
1	93.5	25	4.1
2	89.1	25	10.4
3	92.0	25	9.2
4	102.4	30	14.0
5	96.6	30	11.4
6	79.9	30	11.8

**Table 4.** Energy consumption for all trials in experiment 3

Trial	Max FSW Force (lbf)	FES (mA)	Energy- Right Knee (j)	Energy- Left Knee (j)	Energy- Both Knees (j)
1	125.0	0	50.5	67.7	118.2
2	173.3	0	23.3	36.8	60.1
3	187.0	0	26.5	14.1	40.6
4	177.9	0	20.7	22.6	43.3

**Table 5.** Energy consumption for all trials in experiment 4

Trial	Max FSW Force (lbf)	FES (mA)	Energy- Right Knee (j)	Energy- Left Knee (j)	Energy- Both Knees (j)
1	85.5	40	30.6	18.9	49.5
3	93.8	40	36.6	26.0	62.6
4	103.5	50	37.6	19.7	57.3

The results show a relatively high data outlier of 118 joules consumed in trial 1 of experiment 3. The exact cause of this high energy usage is unknown; however, it could be due to twisting in the neuroprosthesis shank frames during standing. The motors work efficiently in the plane of the output face, however twisting of the shank frames can cause load misalignment, which might result in high friction and energy inefficiencies. This problem could be greatly mitigated by a structurally improved neuroprosthesis frame.

The results from the energy analysis shows that the right knee motor achieved a dramatic 74% decrease in the average energy consumption in experiment 2. A sizable portion of the energy decrease most likely comes from the reduction of standing speed and standing acceleration seen in experiment 2, since the motors were limited to a lower overall speed. However, since the speed was only decreased by 50%, it appears plausible that some of this energy reduction was the result of using FES in hybrid standing. It is also possible that these ideal results were caused by a better controller performance and better HMI in slow sitting to standing. It seems likely that the slower standing speed allowed the FES to operate more efficiently.

However, it must be noted due to the small number of trials in all experiments that these experimental demonstrations of standing results do not yield statistical significance. Furthermore, the user-controlled nature of this control system and the dangers associated with

running a high number of standing trials with SCI users make it relatively impractical to standardize these experiments in a way that would produce statistically meaningful results for energy consumption. Even if accurate and statistically significant energy consumption results were obtained, this data would be heavily dependent on the state of the neuroprosthesis hardware, the coincidental nature of the user-controlled input, and the exact standing dynamics of the user<sup>[4]</sup>.

The results for standing in the subject with SCI show a less dramatic energy reduction between experiments 3 and 4. Experiments 3 and 4 were run at roughly the same standing speeds, equivalent to the speed in experiment 1. The total energy consumption in experiment 4 shows a modest energy reduction of 15%, although this reduction does not appear significant due to the small number of trials in experiment 4, which was caused by the frame torsional bending. It appears that the subject with SCI had a low level of lower leg muscular development and had virtually no lower leg FES training, which may have contributed to the poor energy reduction results in experiment 4. Furthermore, it was observed from the video of standing in experiment 4 that the backwards leaning of the subject was prevalent across multiple trials. This backwards leaning caused controller inefficiency, which may have propagated into energy inefficiency. From these results, it seems reasonable to conclude that a subject with SCI with poor training will not achieve a substantial reduction in total energy consumption during standing. Whereas, as seen in able-bodied subject B1, who had high muscular development, the possibility of energy reduction through hybrid standing appears to be much higher. Additionally, the control method for FES in hybrid standing was a relatively simplistic open-loop design, so it is likely that a more advanced hybrid standing control could achieve better energy reductions in the knee motors with an untrained person with SCI.

As an unexpected result, the knee motor energy consumption for the able-bodied subject in experiment 1 is higher than the knee motor energy consumption for the subject with SCI in experiment 3. This could be caused by an increase in upper body effort by the subject with SCI. The subject with SCI applied very high FSW support forces in experiment 3. In some cases, the support force almost equaled the subject's weight. This high support force could be due to user inexperience and lack of confidence in the control system, since this experiment was the first time that subject A4 used the control system. It is also possible that these high force readings could have been due to FSR measurement errors due to an incidental poor distribution of the subject's weight on the FSW FSR's. Subject with SCI A4 decreased their support force considerably in experiment 4.

These energy consumption results also showed the overall power requirements for standing. These power requirements can be used to size a mobile battery or other power source and can be used to determine how much mobile neuroprosthesis operation could be achieved. The highest energy consumption was found in experiment 1, with an average total energy consumption of 88.4 joules. Table 6 shows the energy capacity of several types of batteries. It will be assumed that, due to weight constraints, the battery for a mobile exoskeleton will be constrained to 0.5 kg. Table 6 shows the estimated motors only operational capacity, or the standing cycles, from sitting to standing, that could be achieved in one battery life, for each of the several common types of batteries<sup>[68]</sup>.

**Table 6.** Motors only energy capacity and operational range of several types of potential mobile neuroprosthesis batteries

Battery Type	Theor. Specific Energy*	Est. Capacity - 0.5 kg Battery
Units:	KJ/kg	Standing Cycles
Alkaline MnO <sub>2</sub>	522	2952
Lead-Acid	126	712
Lithium-Ion	540	3054
Lithium-Thionyl Chloride	2124	12013
Nickel-Cadmium	126	712
Nickel-Metal Hydride	270	1527
Zinc-Air	1332	7533

\*This value is based on single cell battery performance only, and does not factor in battery design

## APPENDIX A

### THE EARLY HISTORY OF ELECTRICAL STIMULATION

The use of electrical stimulation as a medical treatment predates modern history, in which ancient physicians would use animals that can produce electricity, such as electric eels, to treat health disorders<sup>[62,67]</sup>. Scientific inquiries into the effects of electrical stimulation on human beings began with Kruger in 1744, who observed that electrical stimulation could “restore sensation and re-establish the power of motion”<sup>[67]</sup>. Following this, in 1746 Kratzenstein, who was both a physicist and a physician (and who is hypothesized by some to be Mary Shelley’s inspiration for Dr. Frankenstein), identified that static electricity could be used to produce contraction in the muscles of his patients<sup>[6,62,67]</sup>. Another tremendously influential development came in 1791 when Luigi Galvani published “The Effects of Electricity on Muscular Motion,” which detailed experiments where he stimulated movement in frog legs by applying the electricity generated from a Leyden jar to the nerves<sup>[29,30,67]</sup>. A diagram of Galvani’s experimental setup is shown in Figure 42 below. Despite these early scientific developments, which would eventually beget FES, the underlying physics and biology of electrical stimulation were not well understood until the 19th century<sup>[67]</sup>.

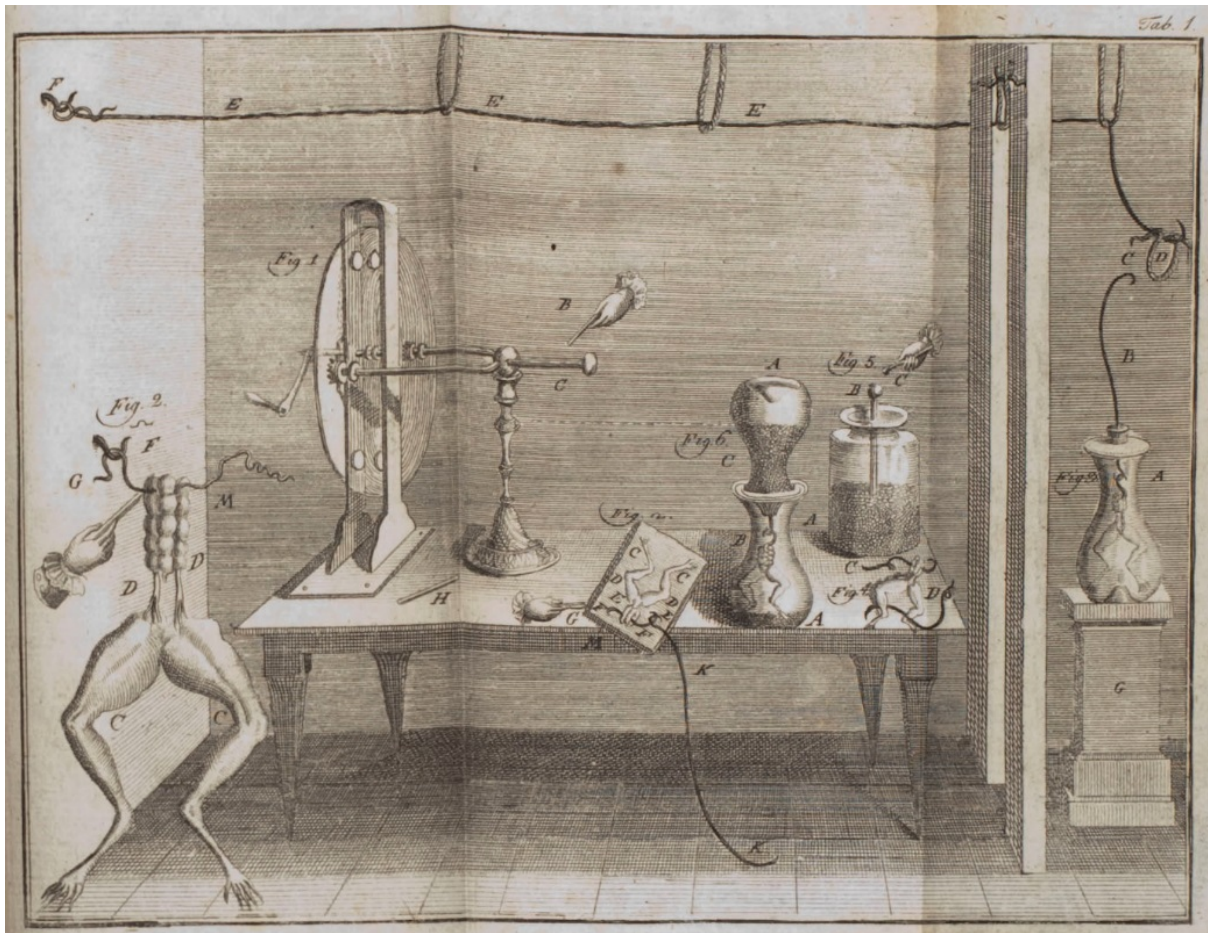


Figure 42. Luigi Galvani's experimental setup in his work "The Effect of Electricity on Muscular Motion"<sup>[29]</sup>

## APPENDIX B

### FES FUNCTIONALITY IN SKELETAL MUSCLES

FES works by applying short electrical pulses to generate muscular contraction<sup>[57]</sup>. In skeletal muscles, electrochemical signals in the brain are transmitted to the nervous system through motor neurons<sup>[35,57,62]</sup>. Muscle groups are grouped into motor units which are recruited to varying degrees based on the type of movement the muscles are performing<sup>[57]</sup>. However, one impulse by a motor neuron only produces a short jolt from the muscle, and therefore sustained muscular effort requires a train of neural impulses, wherein the frequency of the impulses controls the contraction intensity<sup>[57]</sup>. Contraction is also spread across multiple motor units so that fatigue occurs slower<sup>[57]</sup>.

Muscle is broken into two types, fast twitch, which responds quickly to impulses but fatigues quickly, and slow twitch, which responds slowly but also fatigues slowly<sup>[57]</sup>. When a person's muscles have atrophied over time, such as in people with SCI, they develop a higher proportion of fast twitch muscle as compared to healthy people<sup>[57,64]</sup>. Thus, the muscles of SCI users can fatigue quickly, however it has typically been found that the muscles can be retrained with FES to achieve better performance and a slower onset of fatigue<sup>[57,74]</sup>.

In order to actuate the muscles, FES applies a series of electrical stimulations to induce current in motor neurons<sup>[57]</sup>. Four types of physical application of FES are available: transcutaneous, or applying stimulation to the skin surface, percutaneous, or within the muscle body, epimysial, or applied to the muscle surface, and cuff, or attached to the muscle nerve<sup>[57,74]</sup>. The joint torque produced by FES can be adjusted by changing the pulse amplitude, pulse duration, and frequency of the amplitude, although frequency is not usually changed in most FES systems. FES is typically run at 20-40hz as compared to 6-8hz in a natural muscle contraction<sup>[57]</sup>.

In comparison to natural muscle recruitment, FES applies stimulation to all muscle fibers continuously, without alternating muscle activation to decrease fatigue<sup>[57]</sup>. It is a combination of the increased stimulation frequency and the continuous nature of FES stimulation that causes accelerated muscle fatigue in users as compared with natural stimulation<sup>[57]</sup>. Additionally, FES recruits fast twitch fibers before slow twitch fibers, which aggravates the problem of fatigue<sup>[57]</sup>. One of the only methodologies known to increase a user's muscular stamina is to introduce them to a regular FES training regimen<sup>[18,57,69]</sup>.

## BIBLIOGRAPHY

- [1] Alibeji, N. A., Kirsch, N. A., & Sharma, N. (2015). A muscle synergy-inspired adaptive control scheme for a hybrid walking neuroprosthesis. *Frontiers in bioengineering and biotechnology*, 3.
- [2] Amdur, R. J., & Bankert, E. A. (2010). *Institutional review board: member handbook*: Jones & Bartlett Publishers.
- [3] Bajd, T., Kralj, A., Krajnik, J., Turk, R., Benko, H., & Segal, J. (1984). *Standing by FES in paraplegic patients*. Paper presented at the Proc. 8th Int. Symposium on ECHE, Dubrovnik.
- [4] Bajd, T., Kralj, A., & Turk, R. (1982). Standing-up of a healthy subject and a paraplegic patient. *Journal of biomechanics*, 15(1), 1-10.
- [5] Bajd, T., Kralj, A., Turk, R., Benko, H., & Šega, J. (1983). The use of a four-channel electrical stimulator as an ambulatory aid for paraplegic patients. *Physical Therapy*, 63(7), 1116-1120.
- [6] Baker, L. L., Wederich, C., McNeal, D. R., Newsam, C. J., & Waters, R. L. (2000). *Neuro muscular electrical stimulation: a practical guide*: Los Amigos Research & Education Institute.
- [7] Bélanger, M., Stein, R. B., Wheeler, G. D., Gordon, T., & Leduc, B. (2000). Electrical stimulation: can it increase muscle strength and reverse osteopenia in spinal cord injured individuals? *Archives of physical medicine and rehabilitation*, 81(8), 1090-1098.
- [8] Blaya, J. A., & Herr, H. (2004). Adaptive control of a variable-impedance ankle-foot orthosis to assist drop-foot gait. *IEEE Transactions on Neural Systems and Rehabilitation Engineering*, 12(1), 24-31.
- [9] Bogue, R. (2009). Exoskeletons and robotic prosthetics: a review of recent developments. *Industrial Robot: An International Journal*, 36(5), 421-427.

- [10] Brown-Triolo, D. L., Roach, M. J., Nelson, K., & Triolo, R. J. (2002). Consumer perspectives on mobility: implications for neuroprosthesis design. *Journal of rehabilitation research and development*, 39(6), 659.
- [11] Carey, N. (2005). Establishing pedestrian walking speeds. *Karen Aspelin, Portland State University*, 1(01).
- [12] Chen, S.-C., Lai, C.-H., Chan, W. P., Huang, M.-H., Tsai, H.-W., & Chen, J.-J. J. (2005). Increases in bone mineral density after functional electrical stimulation cycling exercises in spinal cord injured patients. *Disability and Rehabilitation*, 27(22), 1337-1341.
- [13] Chu, A., Kazerooni, H., & Zoss, A. (2005). *On the biomimetic design of the berkeley lower extremity exoskeleton (BLEEX)*. Paper presented at the Robotics and Automation, 2005. ICRA 2005. Proceedings of the 2005 IEEE International Conference on.
- [14] Contreras-Vidal, J. L., Bhagat, N. A., Brantley, J., Cruz-Garza, J. G., He, Y., Manley, Q., . . . Zhu, F. (2016). Powered exoskeletons for bipedal locomotion after spinal cord injury. *Journal of neural engineering*, 13(3), 031001.
- [15] Contreras-Vidal, J. L., & Grossman, R. G. (2013). *NeuroRex: A clinical neural interface roadmap for EEG-based brain machine interfaces to a lower body robotic exoskeleton*. Paper presented at the Engineering in medicine and biology society (EMBC), 2013 35th Annual international conference of the IEEE.
- [16] Crewe, N. M., & Krause, J. S. (2009). Spinal cord injury. *Medical, psychosocial and vocational aspects of disability*. Athens: Elliott and Fitzpatrick, 289-304.
- [17] Cruciger, O., Schildhauer, T. A., Meindl, R. C., Tegenthoff, M., Schwenkreis, P., Citak, M., & Aach, M. (2016). Impact of locomotion training with a neurologic controlled hybrid assistive limb (HAL) exoskeleton on neuropathic pain and health related quality of life (HRQoL) in chronic SCI: a case study. *Disability and Rehabilitation: Assistive Technology*, 11(6), 529-534.
- [18] Daly, J. J., Marsolais, E. B., Mendell, L. M., Rymer, W. Z., & Stefanovska, A. (1996). Therapeutic neural effects of electrical stimulation. *IEEE Transactions on Rehabilitation Engineering*, 4(4), 218-230.
- [19] del-Ama, A. J., Gil-Agudo, Á., Pons, J. L., & Moreno, J. C. (2014). Hybrid FES-robot cooperative control of ambulatory gait rehabilitation exoskeleton. *Journal of neuroengineering and rehabilitation*, 11(1), 27.

- [20] Dodson, A., Alibeji, N., & Sharma, N. (2017). *Experimental demonstration of a delay compensating controller in a hybrid walking neuroprosthesis*. Paper presented at the 2017 8th International IEEE/EMBS Conference on Neural Engineering (NER).
- [21] Dollar, A. M., & Herr, H. (2008). Lower extremity exoskeletons and active orthoses: challenges and state-of-the-art. *IEEE Transactions on robotics*, 24(1), 144-158.
- [22] Donaldson, N., & Yu, C.-H. (1998). A strategy used by paraplegics to stand up using FES. *IEEE Transactions on Rehabilitation Engineering*, 6(2), 162-167.
- [23] Donaldson, N. d. N., & Yu, C.-N. (1996). FES standing: Control by handle reactions of leg muscle stimulation (CHRELMS). *IEEE Transactions on Rehabilitation Engineering*, 4(4), 280-284.
- [24] Duschau-Wicke, A., Brunsch, T., Lunenburger, L., & Riener, R. (2008). *Adaptive support for patient-cooperative gait rehabilitation with the lokomat*. Paper presented at the Intelligent Robots and Systems, 2008. IROS 2008. IEEE/RSJ International Conference on.
- [25] Ellis, M., Seedhom, B., Amis, A., Dowson, D., & Wright, V. (1979). Forces in the knee joint whilst rising from normal and motorized chairs. *Engineering in Medicine*, 8(1), 33-40.
- [26] Esquenazi, A., Talaty, M., Packel, A., & Saulino, M. (2012). The ReWalk powered exoskeleton to restore ambulatory function to individuals with thoracic-level motor-complete spinal cord injury. *American journal of physical medicine & rehabilitation*, 91(11), 911-921.
- [27] Fick, B., & Makinson, J. (1971). Final report on Hardiman I prototype for machine augmentation of human strength and endurance. *United States Army Project No. IM62410105072, General Electr. Co., New York, DTIC Accession Number: AD0739735*.
- [28] Franceschini, M., Baratta, S., Zampolini, M., Loria, D., & Lotta, S. (1997). Reciprocating gait orthoses: a multicenter study of their use by spinal cord injured patients. *Archives of physical medicine and rehabilitation*, 78(6), 582-586.
- [29] Galvani, L., Carminati, B., Licht, S., & Pupilli, G. C. (1953). *A Translation of Luigi Galvani's De Viribus Electricitatis in Motu Musculari Commentarius, Commentary on the Effect of Electricity on Muscular Motion, by Robert Montraville Green,...[Preface by Sidney Licht. Introduction by Giulio C. Pupilli. Dissertation of Giovanni Aldini. Letter from Bassano Carminati.]*: E. Licht.

- [30] Galvani, L., & Roller, D. H. (1954). Commentary on the effect of electricity on muscular motion. *American Journal of Physics*, 22(1), 40-40.
- [31] Grobelnik, S., & Kralj, A. (1973). Functional electrical stimulation—a new hope for paraplegic patients. *Bull. Prosthet. Res*, 20, 75-102.
- [32] Guizzo, E., & Goldstein, H. (2005). The rise of the body bots [robotic exoskeletons]. *IEEE spectrum*, 42(10), 50-56.
- [33] Ha, K. H., Murray, S. A., & Goldfarb, M. (2016). An approach for the cooperative control of FES with a powered exoskeleton during level walking for persons with paraplegia. *IEEE Transactions on Neural Systems and Rehabilitation Engineering*, 24(4), 455-466.
- [34] Ha, K. H., Quintero, H. A., Farris, R. J., & Goldfarb, M. (2012). *Enhancing stance phase propulsion during level walking by combining FES with a powered exoskeleton for persons with paraplegia*. Paper presented at the Engineering in medicine and biology society (EMBC), 2012 annual international conference of the IEEE.
- [35] Hall, J. E. (2015). *Guyton and Hall Textbook of Medical Physiology E-Book*: Elsevier Health Sciences.
- [36] Harmonic Gear Strain Wave Gear Principle. Harmonic Drive (2017). Retrieved from <http://www.harmonicdrive.net/technology>
- [37] Hartrick, C. T., Kovan, J. P., & Shapiro, S. (2003). The numeric rating scale for clinical pain measurement: a ratio measure? *Pain Practice*, 3(4), 310-316.
- [38] Hristic, D., Vukobratovic, M., & Timotijevic, M. (1981). *New model of autonomous' active suit'for dystrophic patients*. Paper presented at the Proceedings of the International Symposium on External Control of Human Extremities.
- [39] Hsia, L.-M. (1988). *The analysis and design of harmonic gear drives*. Paper presented at the Systems, Man, and Cybernetics, 1988. Proceedings of the 1988 IEEE International Conference on.
- [40] Huo, W., Mohammed, S., Moreno, J. C., & Amirat, Y. (2016). Lower limb wearable robots for assistance and rehabilitation: A state of the art. *IEEE systems Journal*, 10(3), 1068-1081.

- [41] Jatsun, S., Savin, S., Yatsun, A., & Malchikov, A. (2016). Study of controlled motion of exoskeleton moving from sitting to standing position *Advances in Robot Design and Intelligent Control* (pp. 165-172): Springer.
- [42] Kantrowitz, A. (1960). Electronic physiologic aids. *Report of the Maimonides Hospital*, 4-5.
- [43] Kawamoto, H., Kanbe, S., & Sankai, Y. (2003). *Power assist method for HAL-3 estimating operator's intention based on motion information*. Paper presented at the Robot and human interactive communication, 2003. proceedings. ROMAN 2003. The 12th IEEE international workshop on.
- [44] Kazerooni, H., Racine, J.-L., Huang, L., & Steger, R. (2005). *On the control of the berkeley lower extremity exoskeleton (BLEEX)*. Paper presented at the Robotics and automation, 2005. ICRA 2005. Proceedings of the 2005 IEEE international conference on.
- [45] Kirsch, N., Alibeji, N., Fisher, L., Gregory, C., & Sharma, N. (2014). *A semi-active hybrid neuroprosthesis for restoring lower limb function in paraplegics*. Paper presented at the Engineering in Medicine and Biology Society (EMBC), 2014 36th Annual International Conference of the IEEE.
- [46] Kirsch, N. A. (2016). *Control methods for compensation and inhibition of muscle fatigue in neuroprosthetic devices*. University of Pittsburgh.
- [47] Kirsch, N. A., Alibeji, N. A., Redfern, M., & Sharma, N. (2017). Dynamic Optimization of a Hybrid Gait Neuroprosthesis to Improve Efficiency and Walking Duration: A Simulation Study *Converging Clinical and Engineering Research on Neurorehabilitation II* (pp. 687-691): Springer.
- [48] Kiryu, Y. (1986). *Harmonic gear apparatus*: Google Patents.
- [49] Kobetic, R., To, C. S., Schnellenberger, J. R., Bulea, T. C., CO, R. G., & Pinault, G. (2009). Development of hybrid orthosis for standing, walking, and stair climbing after spinal cord injury. *Journal of rehabilitation research and development*, 46(3), 447.
- [50] Kolakowsky-Hayner, S. A., Crew, J., Moran, S., & Shah, A. (2013). Safety and feasibility of using the Ekso™ bionic exoskeleton to aid ambulation after spinal cord injury. *J Spine*, 4, 003.

- [51] Kong, K., & Jeon, D. (2006). Design and control of an exoskeleton for the elderly and patients. *IEEE/ASME Transactions On Mechatronics*, 11(4), 428-432.
- [52] Kralj, A. R., & Bajd, T. (1989). *Functional electrical stimulation: standing and walking after spinal cord injury*: CRC press.
- [53] Krause, P., Szecsi, J., & Straube, A. (2008). Changes in spastic muscle tone increase in patients with spinal cord injury using functional electrical stimulation and passive leg movements. *Clinical rehabilitation*, 22(7), 627-634.
- [54] Liberson, W. (1961). Functional electrotherapy: stimulation of the peroneal nerve synchronized with the swing phase of the gait of hemiplegic patients. *Arch Phys Med Rehabil*, 42, 101.
- [55] Lichy, A. M. (2012). Asymmetric lower-limb bone loss after spinal cord injury: case report. *Journal of rehabilitation research and development*, 49(2), 221.
- [56] Low, K. (2011). *Robot-assisted gait rehabilitation: From exoskeletons to gait systems*. Paper presented at the Defense Science Research Conference and Expo (DSR), 2011.
- [57] Lynch, C. L., & Popovic, M. R. (2008). Functional electrical stimulation. *IEEE control systems*, 28(2), 40-50.
- [58] Makinson, B. J. (1971). *Research and development prototype for machine augmentation of human strength and endurance. hardiman i project*. Retrieved from
- [59] Marsolais, E., & Kobetic, R. (1987). Functional electrical stimulation for walking in paraplegia. *JBJS*, 69(5), 728-733.
- [60] McDonald, J. W., & Sadowsky, C. (2002). Spinal-cord injury. *The Lancet*, 359(9304), 417-425.
- [61] McHorney, C., Ware Jr, J., & Raczek, A. (1993). Psychometric and Clinical Tests of Validity in Measuring Physical and Mental Health Constructs. The MOS 36-Item Short-Form Health Survey (SF-36): II. Psychometric and clinical tests of validity in measuring physical and mental health constructs. *Med Care*, 31(3), 247-263.

- [62] Mecheroui, C. A. (2012). *Development of a wireless ditributed three channel stimulator used for automatic triggering of stimulation to enable co-ordinated task execution of stroke patients*. Bournemouth University.
- [63] Mohammed, S., & Amirat, Y. (2009). *Towards intelligent lower limb wearable robots: Challenges and perspectives-State of the art*. Paper presented at the Robotics and Biomimetics, 2008. ROBIO 2008. IEEE International Conference on.
- [64] Mortimer, J. T. (1981). Motor prostheses. *Comprehensive Physiology*.
- [65] Niku, S. B. (2001). *Introduction to Robotics: Analysis, Systems, Applications.*: Prentice Hall.
- [66] Peckham, P. H., & Knutson, J. S. (2005). Functional electrical stimulation for neuromuscular applications. *Annu. Rev. Biomed. Eng.*, 7, 327-360.
- [67] Petrofsky, J. S. (1988). Functional Electrical Stimulation and Its Application in the Rehabilitation of Neurologically Injured Individuals *Brain Injury and Recovery* (pp. 273-305): Springer.
- [68] Pistoia, G. (2005). *Batteries for portable devices*: Elsevier.
- [69] Popovic, M. R., Thrasher, T. A., Adams, M., Takes, V., Zivanovic, V., & Tonack, M. I. (2006). Functional electrical therapy: retraining grasping in spinal cord injury. *Spinal cord*, 44(3), 143.
- [70] Quintero, H. A., Farris, R. J., Ha, K., & Goldfarb, M. (2012). *Preliminary assessment of the efficacy of supplementing knee extension capability in a lower limb exoskeleton with FES*. Paper presented at the Engineering in Medicine and Biology Society (EMBC), 2012 Annual International Conference of the IEEE.
- [71] Raab, K., Krakow, K., Tripp, F., & Jung, M. (2016). Effects of training with the ReWalk exoskeleton on quality of life in incomplete spinal cord injury: a single case study. *Spinal cord series and cases*, 2, 15025.
- [72] Riener, R., Ferrarin, M., Pavan, E. E., & Frigo, C. A. (2000). Patient-driven control of FES-supported standing up and sitting down: experimental results. *IEEE Transactions on Rehabilitation Engineering*, 8(4), 523-529.

- [73] Riener, R., & Fuhr, T. (1998). Patient-driven control of FES-supported standing up: a simulation study. *IEEE Transactions on Rehabilitation Engineering*, 6(2), 113-124.
- [74] Rigelsford, J. (2001). Control of Movement for the Physically Disabled. *Industrial Robot: An International Journal*, 28(5).
- [75] Schiele, A., & van der Helm, F. C. (2006). Kinematic design to improve ergonomics in human machine interaction. *IEEE Transactions on Neural Systems and Rehabilitation Engineering*, 14(4), 456-469.
- [76] Sekhon, L. H., & Fehlings, M. G. (2001). Epidemiology, demographics, and pathophysiology of acute spinal cord injury. *Spine*, 26(24S), S2-S12.
- [77] Sharma, N., & Dani, A. (2014). *Nonlinear estimation of gait kinematics during functional electrical stimulation and orthosis-based walking*. Paper presented at the American Control Conference (ACC), 2014.
- [78] Sharma, N., Mushahwar, V., & Stein, R. (2014). Dynamic optimization of FES and orthosis-based walking using simple models. *IEEE Transactions on Neural Systems and Rehabilitation Engineering*, 22(1), 114-126.
- [79] Sharma, N., Stegath, K., Gregory, C. M., & Dixon, W. E. (2009). Nonlinear neuromuscular electrical stimulation tracking control of a human limb. *IEEE Transactions on Neural Systems and Rehabilitation Engineering*, 17(6), 576-584.
- [80] Simpson, L. A., Eng, J. J., Hsieh, J. T., Wolfe, & the Spinal Cord Injury Rehabilitation Evidence Research Team, D. L. (2012). The health and life priorities of individuals with spinal cord injury: a systematic review. *Journal of neurotrauma*, 29(8), 1548-1555.
- [81] Singer, B. (1987). Functional electrical stimulation of the extremities in the neurological patient: a review. *Australian Journal of Physiotherapy*, 33(1), 33-42.
- [82] Tator, C. (1995). Epidemiology and general characteristics of the spinal cord injury patient. *Contemporary Management of Spinal Cord Injury. Neurosurgical Topics. Park Ridge, IL: American Association of Neurological Surgeons*, 9-13.
- [83] Tsukahara, A., Hasegawa, Y., & Sankai, Y. (2009). *Standing-up motion support for paraplegic patient with Robot Suit HAL*. Paper presented at the Rehabilitation Robotics, 2009. ICORR 2009. IEEE International Conference on.

- [84] Virgala, I., Gmitterko, A., Surovec, R., Vacková, M., Prada, E., & Kenderová, M. (2012). Manipulator end-effector position control. *Procedia Engineering*, 48, 684-692.
- [85] Viteckova, S., Kutilek, P., & Jirina, M. (2013). Wearable lower limb robotics: A review. *Biocybernetics and Biomedical Engineering*, 33(2), 96-105.
- [86] Walsh, C. J., Endo, K., & Herr, H. (2007). A quasi-passive leg exoskeleton for load-carrying augmentation. *International Journal of Humanoid Robotics*, 4(03), 487-506.
- [87] White, N. H., & Black, N. H. (2016). *Spinal cord injury (SCI) facts and figures at a glance*.
- [88] Winter, D. A. (2009). *Biomechanics and motor control of human movement*: John Wiley & Sons.
- [89] Yaniger, S. (1991). *Force sensing resistors: A review of the technology*. Paper presented at the Electro International, 1991.
- [90] Young, A. J., & Ferris, D. P. (2017). State of the Art and Future Directions for Lower Limb Robotic Exoskeletons. *IEEE Transactions on Neural Systems and Rehabilitation Engineering*, 25(2), 171-182.
- [91] Zeilig, G., Weingarden, H., Zwecker, M., Dudkiewicz, I., Bloch, A., & Esquenazi, A. (2012). Safety and tolerance of the ReWalk™ exoskeleton suit for ambulation by people with complete spinal cord injury: A pilot study. *The journal of spinal cord medicine*, 35(2), 96-101.
- [92] Zoss, A. B., Kazerooni, H., & Chu, A. (2006). Biomechanical design of the Berkeley lower extremity exoskeleton (BLEEX). *IEEE/ASME Transactions On Mechatronics*, 11(2), 128-138.